7-2016

Development and evaluation of custom prosthetic devices for a companion animal utilizing additive manufacturing.

Benjamin Joseph Cahill

DEVELOPMENT AND EVALUATION OF CUSTOM PROSTHETIC DEVICES FOR
A COMPANION ANIMAL UTILIZING ADDITIVE MANUFACTURING

By

Benjamin Joseph Cahill
B.S., University of Louisville, 2014

A Thesis
Submitted to the Faculty of the
University of Louisville
J.B. Speed School of Engineering
as Partial Fulfillment of the Requirements
for the Professional Degree

MASTER OF ENGINEERING

Department of Bioengineering

July 2016

i

DEVELOPMENT AND EVALUATION OF CUSTOM PROSTHETIC DEVICES FOR A COMPANION ANIMAL UTILIZING ADDITIVE MANUFACTURING

Submitted by: _____

Benjamin Cahill

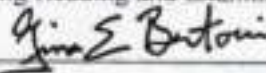A Thesis Approved On

Nov 21, 2016

(Date)

by the Following Reading and Examination Committee:

_____
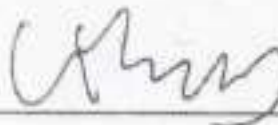
Dr. Gina Bertocci, Thesis Director

_____

Dr. Nathan Brown

_____

Dr. Hermann Frieboes

_____

Dr. Li Yang

i

Table of Contents

Acknowledgements

To my mother who supported me through this process, and my father who showed me the value of a strong work ethic, I cannot thank you enough.

Abstract

BACKGROUND AND SIGINIFICANCE: Few options exist for companion animals in need of prosthetic devices. With the rise of rapid prototyping technology, the availability and customization of prosthetic devices for individual companion animals is now a viable and cost effective alternative to the current options of a peg leg prosthetic, or wheel-assisted prosthetic device. The goals of this study were to describe the (1) specific needs and (2) biomechanics of a feline with bilateral thoracic limb amputation, (3) develop custom prosthetic devices utilizing rapid prototyping technology, and (4) describe the biomechanics of a feline with bilateral thoracic limb amputation using the custom prosthetic devices. The feline being studied in this project is a 2 year old Maine Coon feline weighing 9 lbs. She was a stray that was found with severe frostbite on her thoracic limbs. These sections of her thoracic limbs were amputated to remove the necrotic tissue.

SPECIFIC AIMS: The goals of this study is to describe the (1) specific needs and (2) biomechanics of feline with bilateral thoracic limb amputation, (3) develop custom prosthetic devices utilizing rapid prototyping technology, and (4) describe the biomechanics of a feline with bilateral thoracic limb amputation with the use of the custom prosthetic devices.

MATERIALS & METHODS: Fused Deposition Modeling (FDM) technology was utilized to fabricate the prosthetic devices that were designed and put through a Finite Element Analysis to simulate static loading and fatigue testing during various stages of the gait cycle. The devices were mechanically tested to ensure device failure did not occur during static loading, as well as fatigue tested to resemble continued use.

Kinematic gait analysis was performed prior to and after use of the prosthetic devices, and outcomes were compared between the scenarios. Gait data was also compared to published feline gait data to determine any effects to the feline's gait resulting from the amputation, and if this effect was corrected through the use of the prosthetic devices.

RESULTS: FDM was a cost effective way to fabricate strong, durable prosthetic devices designed specifically for a companion animal with dual thoracic limb amputation. Mechanical testing ensured that the prosthetic devices can survive over 10,000 loading cycles at 6 N, and 3000 N of vertical force. The gait analysis performed without the use of the prosthetic devices show increased flexion of the elbows, stifle, and tarsus joint during ambulation. Gait analysis during the use of the prosthetic devices removes this additional flexion.

CONCLUSION: Use of prosthetic devices can have a positive influence in the gait of companion animals with amputations. The comparison between the two data sets shows removal of the additional flexion found in the thoracic limbs when the prosthetic devices are used. This project showcases the feasibility of using additive manufacturing to create cost effect and durable prosthetic devices for use in companion animals.

List of Tables

List of Figures

SPECIFIC AIMS

1.   The need for a companion animal prosthetic device can stem from any number of indicators that an animal may exhibit. These indicators range from incomplete limb formation associated with congenital limb deformity, traumatic incident that resulted in amputation, or surgical amputation to remove necrotic tissue (Marcellin-Little 2015). This research shows the benefits of designing, fabricating and using custom fit prosthetic devices in a feline companion animal with bilateral thoracic limb necrotic tissue surgical amputations. The design of these prosthetic devices uses the latest 3D printing technology to provide strength, flexibility, and support to the individual. These 3D printed devices are more cost and time effective than the current industry standard.

A long-term goal of this research is to provide the industry with an animal model showing the feasibility of rapid prototyping a custom prosthetic foot and a prosthetic socket. Through this process, a companion animal is provided functional mobility that reduces the potential for secondary complications stemming from this condition (Thrall 2007). This provides evidence to support the development of 3D printed custom load-bearing prosthetic devices, componentry, and sockets to improve the quality of life of amputees. In addition to this long-term goal, another potential outcome from this project could be the foundation for an e-Nable equivalent community for companion animals with amputations.

<div align="center">Specific Aims</div>

1) Describe specific needs of a feline with bilateral thoracic limb amputation.

2) Describe biomechanics of a feline with bilateral thoracic limb amputation during ambulation.

3) Develop custom feline thoracic limbs prosthetic devices using rapid prototyping technology.

4) Describe biomechanics of a feline with bilateral thoracic limb amputation using custom prosthetic devices during ambulation.

Hypothesis

1) Biomechanics of a feline with bilateral thoracic limb amputations will be improved through the use of prosthetic devices.

Objectives

1) Determine patient specific need for prosthetic devices.

2) Design, develop, fabricate, and analyze custom prosthetic devices.

3) Analyze the subject's gait prior to and following use of the prosthetic devices.

Design Goals

1) Improve dorsal-ventral spinal alignment to provide a level topline.

2) Correct for bilateral shoulder height discrepancy.

3) Distribute subject weight uniformly throughout the prosthetic socket.

4) Design device to withstand daily use of the end user.

5) Design device to optimize 3D fabrication.

6) Design device to minimize cost and weight.

BACKGROUND AND SIGNIFICANCE

2.

The field of rehabilitation and assistive devices for companion animals is a niche, yet expensive market. With rapid prototyping becoming available to the general population, custom prototypes that would normally cost thousands of dollars to create can be made for a fraction of the cost. The significance of this project is to produce a functional product that reduces the cost and increases the availability of these devices to the public. A goal of this project is to design, develop, fabricate, and test custom prosthetic devices for a feline companion animal with bilateral thoracic limb amputation. The design, development and analysis of the devices is done using 3D computer aided drawing (CAD) and finite element analysis (FEA) software, fabrication utilizes a fused deposition modeling printer, and efficacy is analyzed using gait analysis prior-to and following use of the prosthetic devices. All of these aspects are performed in a manner that minimizes overall prosthetic device cost.

2.1 Introduction

Limb amputation in companion animals may occur in animals with traumatic, neoplastic, neurological, congenital, and chronic infectious diseases of the appendicular system. (Goldner 2015) Loss of limbs in companion animals increases the potential for a number of health complications. These complications include hip dysplasia, osteoarthritis, spina bifida, and hemiverterbra and associated spinal curvature among others. (Thrall 2007) The occurrence of these complications can be reduced through the use of orthotic and prosthetic devices. (Adamson 2005)

In veterinary practices, the traditional level of thoracic and pelvic limb amputation occurs at the shoulder and hip, respectively. In contrast, surgical amputation in humans

typically occurs at 10 different levels depending on the severity and location of injury. (Shurr 2001) These amputation locations include shoulder disarticulation, above elbow amputation, elbow disarticulation, below elbow amputation, wrist disarticulation, hip disarticulation, above knee amputation, knee disarticulation, below knee amputation, and Syme's amputation. (Shurr 2001) Syme's amputation refers to ankle disarticulation. Today, Syme's amputation is still used for traumatic, congenital, and some vascular conditions (Shurr 2001). The wide range of amputation sites for humans has led to an increase in the technological range of prosthetic devices that enable enhanced function in the affected limb, regardless of the amputation site. In the past, this technology was not available for companion animals, and risk of injury to the residual limb outweighed functionality (Farrell 2014). Therefore, it was deemed best to remove the entire limb. However, with the emergence of veterinary orthotic and prosthetic devices, the traditional approach of total limb amputation has been reduced, and amputation levels for companion animals are similar to amputation levels for humans. (Adamson 2005)

Current technology for animal prosthetic devices either incorporates a peg-leg system, or consists of a sling and wheels. (Orthopets, Denver, CO) The peg-leg system is typically used for single limb amputation, while the sling is utilized when bilateral limbs are either amputated or are not functional. The decision of which prosthetic device system to use for a specific companion animal is the responsibility of the veterinary team and companion animal's owner.

The techniques used by a veterinarian and supporting staff mimic those used by a certified human prosthetist and include casting the residual limb to create a negative mold of the limb that is then sent off to be turned into a positive model to create a nearly

identical model of the individual's residual limb. The prosthetic or orthotic device is then created by a prosthetist using this model to develop an individual-specific device.

With the introduction of 3-D printing, the means of manufacturing single lot, unique designs of products have greatly increased. Now, conceptual drawings can quickly be turned into tangible prototypes in a matter of hours rather than days; the same is true for fabrication techniques (Gibson 2015). The additive properties and techniques of 3-D printing allow for geometric designs that would be nearly impossible to fabricate using traditional techniques. (Campbell 2012)

2.2 Role of Orthotic and Prosthetic Devices

Human and animal orthotic and prosthetic devices are used to attain an improved level of ambulation following a traumatic injury or physical disability. The severity of injury and individual condition determine whether an orthotic or prosthetic device is needed. Orthotic devices are used when a full limb is present, but a device is needed to aid in achieving full use of the limb. Orthotic devices are designed to brace the limb. These devices adjust the alignment of a complete limb back to its natural state. A prosthetic device is used when a residual limb is present and a device is needed to replace the missing portion of the limb in order to achieve useful function. These devices are attached directly to the residual limb, either through the use of a socket, or by integrating directly into the bone and skin. (Farrell 2014)

Animal prosthetic and orthotic devices are typically available in two variations, depending on the amputation level of the user. These devices are either a wheel-assisted prosthetic, or prosthetic socket and peg leg device. If a residual limb is deemed long

FIGURE 1- Peg-Leg Style Companion Animal Prosthetic Device. (OrthoPets, Denver, Co.)

enough by a veterinarian, a prosthetic socket and peg leg style device is implemented. An example of this system can be seen in Figure 1. These devices use a strap system to secure the device to the user, and provide no energy absorption during the gait cycle. Should a companion animal have multiple missing or deformed limbs, a wheel-assisted prosthetic is implemented (Figure 2). These devices require a harness to secure the

FIGURE 2- Wheel-Assisted Prosthetic Companion Animal Device. (OrthoPets, Denver, Co.)

device to the user, and provide limited mobility to the animal. Great strides have recently

been taken to create an osseointegrated prosthetic device for humans, and companion

FIGURE 3- Osseointegrated Companion Animal Prosthetic Device. (Farrell, B.J., et al. 2014)

animals are being used as a scaled down model to show efficacy (Figure 3) (Farrell, 2014). There have been promising results using this technology, but practical use is still far off in the future due to high cost and risk of infection at the insertion site. Human prosthetic systems are more complex and end users have a wider selection of technology to choose from than their animal counterparts.

An entire human prosthetic leg system (Figure 4) is made up of modular

components. In general, the system includes a socket, a spacer or pylon, a prosthetic
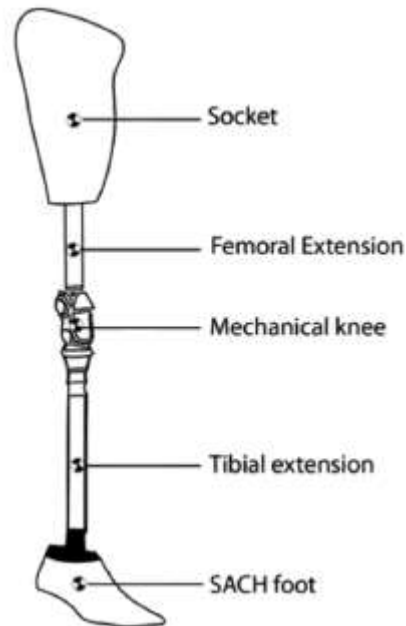
FIGURE 4-Human Above-Knee Prosthetic System. (Ramirez J. 2012)

foot, and a securement system. (Shurr 2001) For humans, the foot, spacer, and

securement system are manufactured independently by prosthetic companies. The socket

and assembly of the prosthetic leg system is performed by a Certified Prosthetist (CP) at

a privately owned clinic or a prosthetic device company. Multiple designs are available

for the prosthetic foot depending on the expected activity level of the end user. These

designs include the solid ankle-cushion heel (SACH), solid ankle-flexible endoskeleton

(SAFE), single-axis foot, multi-axis foot, and dynamic-response foot.

The Solid Ankle Cushioned Heel (SACH) foot (Figure 5) consists of a rigid keel, and a rubber heel. The density of the rubber heel is selected based on the weight of the end user. Mechanically, the SACH foot is completely static. The lack of moving parts
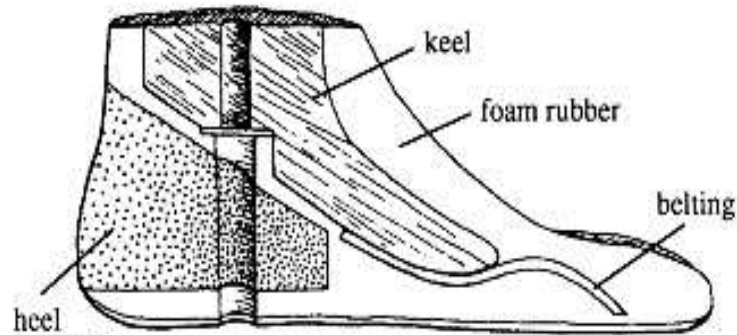
FIGURE 5- Components Of A Solid Ankle Cushioned Heel Foot.
(Edelstein 1988)

means that very little maintenance is required. However, a major complaint with this static design has an increased "dead spot" which refers to the point in the stride where two points of contact in the foot bear weight. (Shurr 2001) Having two points of contact reduces the smooth motion during weight transfer from the heel to the toes. (Agrawal 2012) The priority of this concern to the end user increases as activity level increases.

The SAFE foot (Figure 6) was created in an attempt to address this concern. The SAFE foot functions in a similar fashion as the SACH foot, with the major difference being the flexible keel that was implemented to reduce the physical size of the "dead spot". The flexible keel attempts to replicate plantar flexion, allowing the user to ambulate over uneven terrain. Similar to the SACH foot, the lack of moving parts in the SAFE foot requires very little maintenance.
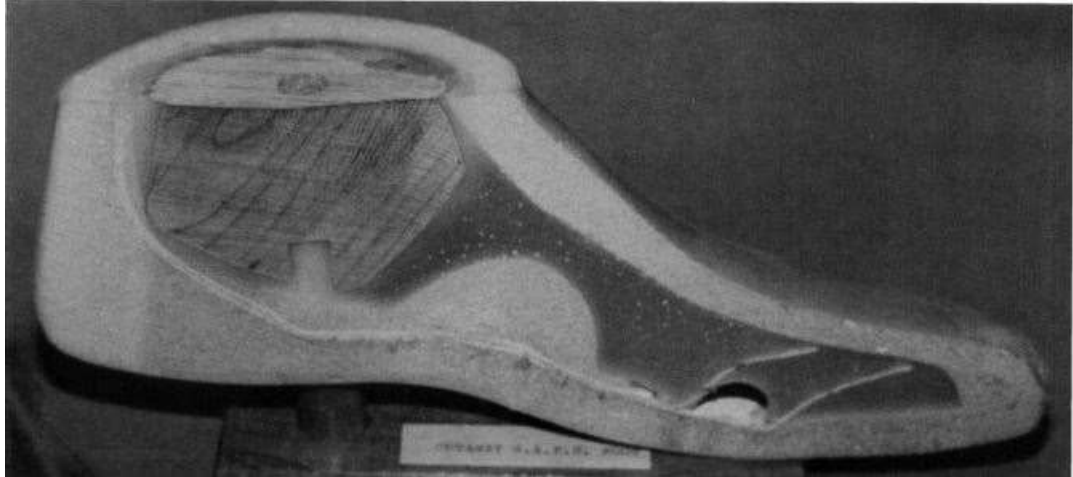
FIGURE 6- Components Of A Solid Ankle Flexible Endoskeleton (SAFE) Foot. . (Edelstein 1988.)

To represent the ankle joint, a single axis of movement was implemented (Figure 7). This new prosthetic foot has an axis that allows dorsiflexion and plantar flexion of the ankle joint, increasing the range of motion. Rubber blocks are placed within the foot
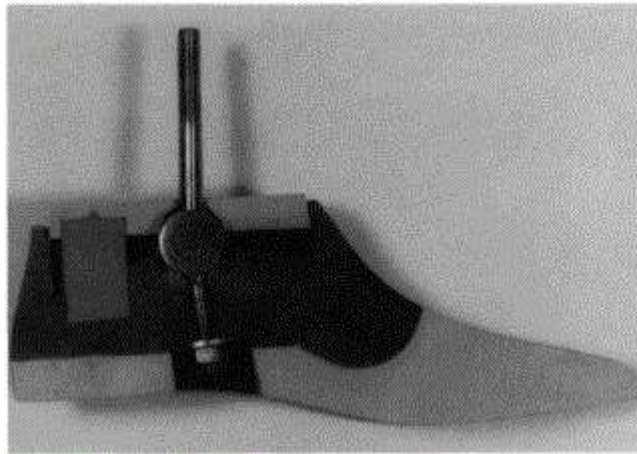
FIGURE 7- Components Of A Single-Axis Foot-Ankle Assembly. (Edelstein 1988)

proximal and distal to this axis to provide stops for flexion-extension ankle movement. These blocks are made of hard rubber and can vary in height to minimize or maximize the allowed range of motion. (Shurr 2001) The "dead spot" was still present in this design, but the range of motion was drastically increased.

The next iteration of prosthetic foot design added multiple axes of rotation (Figure 8). This type of prosthetic foot is commonly referred to as a multi-axis foot. This design is similar to the single-axis foot in terms of weight, maintenance requirement, and cost, but this design allows for three axes of rotation, pitch, roll, and yaw. These three axes of
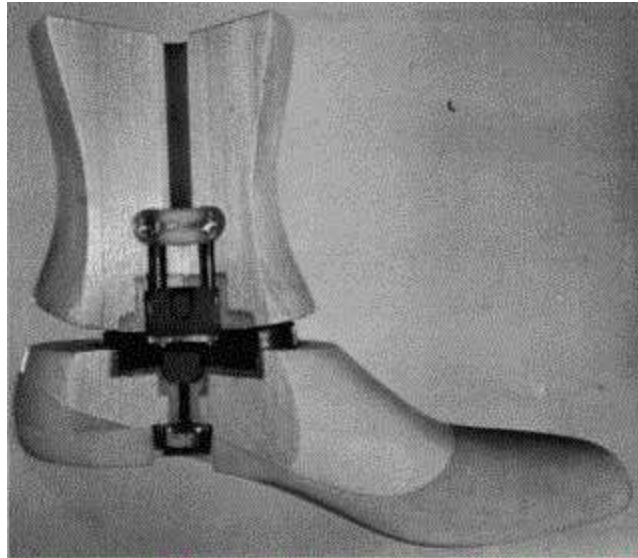
FIGURE 8- Components Of A Multi-Axis Foot-Ankle Assembly. (Edelstein 1988)

rotation allow for plantar and dorsiflexion, foot eversion and inversion, and toe-in or toe-out of the foot.

The SACH foot, SAFE foot, single-axis foot, and multi-axis foot are used by individuals desiring to achieve moderate activity levels. To accommodate individuals with a desire for even higher levels of activity, the dynamic-response foot was designed. The design and material used for this type of foot stores energy during heel strike and returns stored energy to the user during push-off. This energy is stored in the elastic properties of the material used, and returns the energy when the material returns to its natural conformation. The dynamic-response foot provides a more normal range of motion and a balanced gait as compared to a multi-axis foot. (Agrawal 2012) To help

increase stability of the foot during increased activity, most dynamic-response feet have a

split toe design. The split toe feature enables the toes to apply a uniform force to an

uneven surface without rotating the heel. This is particularly critical when ambulating

over rough or uneven terrain, such as sand or grass. The design of this "blade" type foot

FIGURE 9- Example Of A Dynamic-Response Foot. (Ability Dynamics, Tempe, Arizona)

(Figure 9) further reduces the size of the "dead spot" so that most individuals experience

a smooth motion from heel strike to push-off. This design is currently the closest

biomechanical representation of a natural foot. (Agrawal 2012)

Most recently, to represent the function of the gastrocnemius, a microprocessor-

controlled ankle (MPA) was created. This foot has sensors in the heel and toes that sense

when bodyweight has shifted forward, and push-off is about to occur. At the instant of

FIGURE 10- Example Of A Microprocessor-Controlled Ankle. (Össur, Foothill Ranch, California)

push-off, the MPA initiates active plantarflexion to propel the leg forward. Following

push-off, the MPA brings the foot back into dorsiflexion. This movement helps prevent

interference of the foot with the ground, minimizing the risk of the individual tripping and falling. However, this foot requires a significant amount of maintenance, is very costly, heavy, and limits the selection of securement technique of the prosthetic system onto the residual limb or prosthetic limb. (Agrawal 2012)

Choosing a category of prosthetic device, based on the individual's characteristics and needs, is the first of a multi-step process to develop a patient-specific prosthetic system. The main consideration when prescribing a prosthetic device to an individual is to identify the individual's activity level. These levels range from level 0 through level 4.

As defined by the Anthem clinical user manual guidelines, Level 0 is defined as an individual who does not have the ability, or shows the potential to ambulate or safely transfer (Anthem, Inc., Indianapolis, IN). This refers to the ability to move from a wheelchair to a bed, or a bed to a chair. These individuals also cannot transfer with or without help from others, and the prosthetic device does not enhance quality of life.

The next level of activity, level 1, refers to an individual who has the ability, or potential for the ability, to use the prosthetic device to safely transfer, or ambulate on level surfaces. This ambulation is at a fixed cadence. The population in this category is often referred to as the household ambulator. This means that these individuals can safely maneuver through their homes or hospitals, but cannot navigate outside.

Level 2 prosthetic device users are classified as having the ability, or potential for the ability to ambulate or traverse low-level environmental barriers such as curbs, stairs, or uneven surfaces. This classification is typical of an individual that is referred to as a limited community ambulator.

An individual who has the ability or potential to ambulate with a varying cadence is classified as Level 3. This is typical of a community ambulatory who has the ability or potential to have the ability to maneuver most environmental barriers. These individuals may have vocational, therapeutic, or exercise activities that demand utilization of prosthetic devices that go beyond simple ambulation.

The highest classification of prosthetic device users, Level 4, includes individuals who have the ability or potential for ambulation with prosthetic devices that exceed basic ambulation skills. These devices must withstand high impact and stresses and have the capability of storing high amounts of energy. This classification is typical of the needs of children, active adults, or athletes that require the use of a prosthetic device. Prosthetic devices are designed around the amputee's level of activity.

After a prosthetic device is chosen based on the requirements of the user, the attachment to the end user must be as biomechanically sound as possible. (Shurr 2001) The most critical aspect to attain proper fit stems from casting and measuring the residual limb. Traditionally, a plaster cast is made by a prosthetist who emphasizes areas of support and anatomical features. This is done to provide relief to bony prominences, and apply pressure to the softer tissues of the limb that are capable of bearing weight. Applying pressure to selected areas of the limb limits the likelihood of pressure ulcers developing. (Shurr 2001) The plaster cast is then filled with plaster of paris and modified to emphasize the areas of interest the prosthetist discerned during casting. The modification of the plaster model includes the addition or removal of plaster in various locations of the plaster model (Figure 11). Plaster is added to areas of the model that

represent bony prominences of the individual's residual limb. Additionally, some plaster

is removed in areas of softer tissue to increase contact area on the residual limb so the

prosthetic socket fits better. If the socket does not fit the individual well enough, several
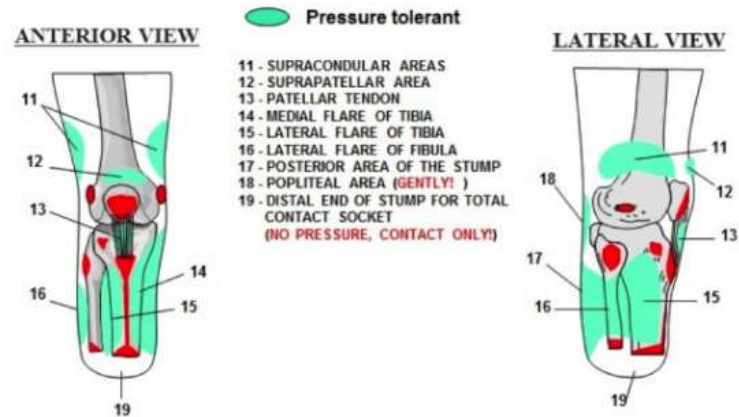
FIGURE 11- Diagram Of Pressure Tolerant (Green) And Pressure
Intolerant (Red) Regions Of The Typical, Below-Knee Amputation.

complications can occur including volume fluctuation, pistoning of the residual limb

inside the socket, reduced tissue health, and poor gait. (Hayden, M. 2015. Personal

Communication.) There are 4 socket designs that are commonly used throughout the

prosthetic industry. These include use of a pin system, vacuum or suctioning, a ratchet

system, or a suspension belt.

The pin system (Figure 12) utilizes a thick compressive liner that is worn with the

prosthetic socket. The liner has a pin attached to the distal end which fits securely into a

lock that is anchored to the prosthetic socket.   The nature of the pin and lock system

FIGURE 12- Diagram Of Prosthetic Socket Pin Anchoring
System.

allows the user to don the socket and remain anchored until the release is activated. This

type of anchoring system is not a total surface bearing system and mitigates issues that

arise due to limb volume fluctuation throughout the day.

A vacuum or suctioning securement system (Figure 13) uses a total surface bearing

concept. A one way valve provides negative air pressure that anchors the prosthetic

device to the individual's residual limb.   This systems requires lubrication to insert the

FIGURE 13- Examples Of Vacuum Systems Used In Prosthetic
Sockets. Shown Here Are Ohio WilloWood's (Mt. Sterling, OH)
LimbLogic On The Left, And Ottobock's (Dunderstadt, DE)
Harmony vacuum System On The Right.

residual limb completely into the prosthetic with an air tight fit. Volume fluctuation of

the residual limb occurs during the day, so a near perfect fit of the prosthetic socket must

be maintained. Some individuals may require a new prosthetic socket to be fabricated if

their residual limb fluctuates enough. A liner or flexible interface can be used depending on the individual's preference to mitigate these volume changes.

A ratcheting system is an additional securement method that builds on a vacuum securement system (Figure 14). A plastic flexible interface is created from the positive mold of the individual's residual limb, and a hard outer shell is laminated over the flexible interface. During the lamination layup, tubing is wound around the model and laminated with the carbon fiber and a dummy ratcheting housing. After the resin cures,

FIGURE 14- Diagram Of Prosthetic Socket Ratcheting System. (Click Medical, Steamboat Springs, CO)

portions of the carbon fiber outer shell are removed and the dummy housing is replaced with an actual ratcheting mechanism. Nylon is then fed through the tubing and anchored into the ratcheting mechanism, which allows the individual to select the amount of compression the socket applies to the residual limb. A similar concept is utilized in this project.

The least common securement method is use of a suspension belt (Figure 15). This is typically used when an individual has a very short residual limb, or the other securement methods are inadequate. The suspension belt supports the weight of the prosthetic device, and transfers the load onto the hips using a heavy duty belt that is

attached to the prosthetic socket, and wrapped around the individual's waist.   This

FIGURE 15- Diagram Of Prosthetic Socket Suspension Belt System. (Knit-Rite, Miamisburg, OH)

securement method is used on less active individuals. However, it is a very durable

method to anchor the prosthetic device to the individual.

Regardless of securement method chosen, a check socket needs to be fabricated in

order to ensure that the individual is comfortable with the fit before a final socket is

made. Check sockets are created from heated thermoplastics that are draped over the

positive model and form-fitted using a vacuum system. The socket is then attached to the

system detailed in Figure 4. Once the individual and prosthetist are satisfied with the fit

of the check socket, a final carbon fiber socket is created using similar techniques.

Layers of carbon fiber are draped over the positive model and vacuum suction pulls resin

into the weaves of fiber. This provides a sturdier socket than the thermoplastic version

while retaining the same fit.

Once the prosthetic system is fitted, it is aligned to provide stability and support to

the end user. This is done first on the bench to obtain a static alignment that enables the

user to stand with the system. Once the user dons the system and takes initial steps,

dynamic alignment can occur. This process adjusts the yaw of the foot to create a toe-out

or toe-in stance, the roll to have the inside, outside, or flat of the foot on the ground

during stance, and the pitch to induce plantar or dorsiflexion. Typical settings attempt to

resemble the natural gait of the contralateral leg. (Shurr 2001) All of these steps are

done through an active conversation between the prosthetist and user. Following

dynamic alignment, the prosthetic system is ready for use by the individual. The typical

methods for prosthetic adjustment do not work for this thesis project, since the anatomy

of the feline subject differs greatly from that of a human.

2.3 Feline Anatomy

    The feline anatomy is designed for speed, agility, and strength. The specialized

design of the thoracic limbs (Figure 16) contributes to these attributes. At the distal end

of the limb, the paws are orientated in a way so that only the toes make contact with the

ground during a full stride. This is referred to as digitigrade posture, as opposed to the

plantigrade posture in humans, and is the most efficient type of movement for a

quadrupedal predator.   (Wright 1980) Locomotion using this technique combines speed
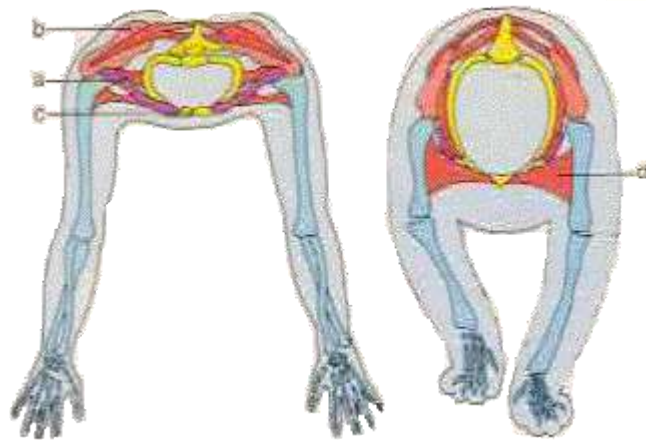
FIGURE 16- The Thoracic Limbs Of Humans (Left) And Felines (right). The
Collarbone Of The Human, A, Are Rigid Struts Between The Scapula, B, And
The Sternum, C. In The Feline Anatomy, Muscles, D, Connect The Thoracic
Limbs To The Sternum. (M. Wright 1980)

with stability. Since only a small area of the paw contacts the ground, it can be moved on

quickly to the next step. Also, by using only the most distal portion of the limb to exert

forces on the ground, the overall length of the limb, and therefore the stride, is increased. (Wright 1980) This technique is mimicked by human sprinters to maximize speed and stride length while minimizing ground contact time. (Gillinov 2015)

Another aspect of the feline anatomy that plays a significant role in locomotion is the division of roles between thoracic and pelvic limbs. The thoracic limbs of a cat resemble those of a human with a few differences. One of these differences is the presence and functionality of the clavicle. (Wright 1980) In humans, the clavicle serves as a rigid structure connecting the scapula and the sternum and provides the ability to exert large amounts of force. In felines, as seen in Figure 17, the clavicle bones are either lacking or they are vestigial. Therefore, the limbs are connected to the breastbone by muscles alone. This greatly increases the control and flexibility of the thoracic limbs. (Wright 1980) The pelvic limbs of the feline anatomy have sacrificed mobility for power because the larger surface area of the pelvis allows for more muscle attachment. This
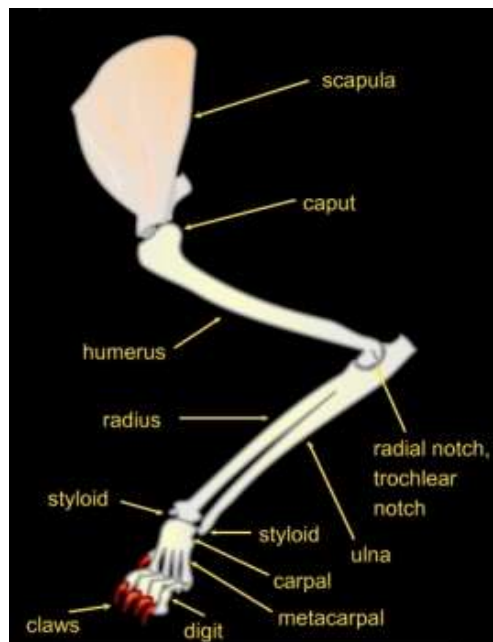
FIGURE 17- Feline Thoracic Limb. (Katzenzeitung 2008)

translates to more muscle mass in a concentrated volume and therefore more localized

power. Forward thrust is produced from the pelvic limbs and the ability to control that

thrust in a deliberate direction is achieved by the thoracic limbs. The flexibility, range of

motion, and control of the thoracic limbs are essential for jumping, balancing, and

graceful landings.

2.4 Methods for Establishing Design Criteria

2.4.1. Quality Function Deployment

A Quality Function Deployment (QFD) is a systematic approach to enable a design

team to clearly identify the customer's wants and needs and to assign a priority level to

each identified design feature. (Cohen 1995) The purpose of a QFD is to decrease cost

of production, prioritize customer needs, increase revenue, and reduce the time it takes to
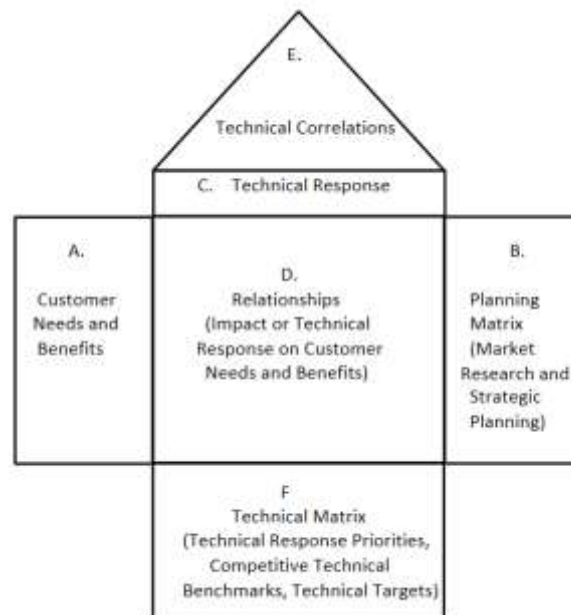
FIGURE 18- Schematic Of A Quality Function Deployment System

plan, produce, and sell a new product. Utilization of a QFD typically gives an advantage

to a company over its competition. A hasty product development timeline typically

results in unforeseen obstacles such as poor understanding of customer needs and failure to strategically prioritize goals. The QFD process addresses these obstacles, allowing the design team to produce a reliable and effective product. Performing a QFD requires dedicated time and proactive work. Due to this required time, many projects proceed without performing a proper QFD. However, the time gained from avoiding complications due to poor planning justifies the time it takes to perform a proper QFD. (Cohen 1995) The QFD consists of multiple matrices displaying the customer's needs and wants and the design team's interpretations of these requests. These matrices are interrelated to determine which priority level to assign each characteristic. Typically the customer's needs described in Section A (Figure 18) are determined by performing qualitative market research such as focus groups or customer interviews. Section B (Figure 18) contains quantitative market data, and computations for determining ranking order of the customer's needs and wants. Section C (Figure 18) stores the technical response. This refers to the high level description using technical language of the product being developed that is generated using the customer's wants and needs from Section A. Section D (Figure 18) portrays the strength of the interactions between the technical response and the customer's needs and wants. Section E (Figure 18) consists of the Technical Correlations which refers to the design team's assessment of the relationships found within Section C. Section F (Figure 18) is the Technical Matrix and contains the computed rank ordering of the technical responses based on the customer wants and needs from Section B and the relationships found within Section D. Section F also provides comparative information on the competition's technical performance, as well as technical performance targets.

<u>2.4.2. 4-D Development Method</u>

The development process utilized throughout the prosthetic industry is adapted from a development model used in the information technology and computer engineering industry. This method is the 4-D Development Method which refers to the basic four stages of a project's timeline. These stages include Define, Design, Develop, and Deploy (Advanced Information Management, Schenectady, NY). The terms used in different companies may vary, but the general concept of the 4-D Development Method remains the same.

The first step of this process is the Define stage. This stage focuses mainly on background research and establishing a team that is involved with the product for the entirety of the project. The team defined the goals, objectives, and scope of the project. Client interaction is crucial during this stage of the process to make sure the design criteria of the project matches the needs and requirements of the client. Total clarity and understanding between the two parties at this stage of the project alleviates potential future complications. Once all parties are in agreement, the project moves on to the second stage, Design.

The Design stage of the 4-D Development Method incorporates the technical and client needs defined in the Define stage. These include functional, technical, and aesthetic requirements that the final device must fulfill. This process involves multiple iterations to generate a design for the final device to ensure all requirements are met. Computer evaluation of the design model determined whether or not a prototype should be created using this design. The evaluation performed includes stress and fatigue analysis, to comply with the International Organization for Standardization (ISO)

standards or equivalent standards for the device. After a design passes these computational evaluations, a prototype was generated. This prototype underwent physical testing before large scale production. This testing begins the third step in the 4-D Development Method, Develop.

The Develop stage deals with the logistical and quality concerns a company has during new device generation. To alleviate the logistical concerns to manufacture a new product, the infrastructure surrounding the fabrication process is refined and streamlined to create an efficient method to produce quality products. To ensure high product quality, rigorous testing is performed on a number of manufactured products. These tests must comply with the ISO or equivalent standards that relate to product development. A dedicated testing team constantly monitors the testing process and ensures quality does not diminish over time. After quality can be guaranteed for the efficient manufacturing process, the product is distributed to market. This is the beginning of the Deploy stage of the 4-D Development model.

The Deploy stage refers to the post-production support of the product, success analysis of the project, and an ongoing review of failed devices. Once a product is delivered to the end user, questions on use will arise, and a support department is responsible for ensuring the customer uses the product as designed and to its full intent. This support is made available for the entirety of production and life expectancy of the product. Testing of random samples within production lots provides statistical evidence that the products deployed to the market maintain the company's standards. Unfortunately, there is no feasible method to ensure 100% of all products sent to market never fail. To better the overall quality of the finished products, devices that have failed

and returned to the company will be evaluated and the source of the failure identified and analyzed. By learning how these devices failed, the next iteration of products can be designed to address these failures. This process is then repeated for subsequent iterations of products.

2.5 Prototyping Options

2.5.1 Additive Manufacturing

Additive manufacturing (AM), commonly referred to as 3-D printing, is used when a very specific, unique devices need to be created with high precision. Additive manufacturing is the process of creating an object by adding material to a base. The subtractive manufacturing process starts with a block of material, and sections of this material are removed to produce the desired shape. This method produces both the desired object and a large amount of waste material. (Wong 2012) In some forms of additive manufacturing, there is either no waste material, or the waste material is completely recyclable. There are several types of additive manufacturing currently available in the general categories of vat photopolymerization process, material jetting, binder jetting, material extrusion, powder bed fusion, sheet lamination, and directed energy deposition. (Gibson 2015)

The first additive manufacturing technique is a type of vat photopolymerization called stereo-lithography (3D Systems Inc, Valencia, CA) and is still the most widely used technique. (Wong 2012) 3D Systems Inc created a type of CAD file that would be used by their machine as a template to create the object. This file was called a stereo-lithography (STL) file and is the standard file format used for all additive manufacturing devices. An STL file essentially divides a 3-D digital model into multiple layers. The greater the number of digital slices, the greater the number of layers of material created, the greater the resolution, and the longer the build time. The STL device (Figure 19) consists of a build plate, vat of photopolymer resin, and UV laser. The laser moves along
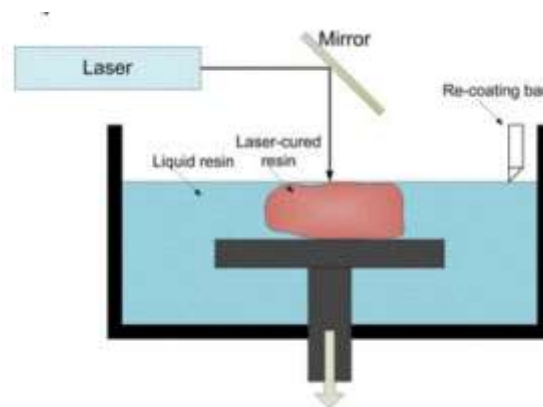
FIGURE 19- Diagram Of A Stereo-Lithography
Setup. (Torabi K., Farjood E. et al. 2015)

the x and y axis, while the build plate moves along the z axis. Currently, the highest resolution achievable using STL is 10µm. (Wong 2012) Unfortunately, the surface of the object needs to be sanded by hand, and the resin is still very expensive, costing approximately $80-$200/liter. (Wong 2012) Also, if the object being created has multiple materials in the design, the entire vat of resin needs to be drained and replaced with the new desired material. This process needs to be repeated any time the design indicates a material change within a layer.

Another additive manufacturing technique is Fused Deposition Modeling (FDM) and is the basis of 3-D printing. FDM resembles a traditional inkjet printer, but instead of ink, the device uses a thin filament of plastic. The printer head then melts the filament and extrudes it onto the build plate (Figure 20). Similar to STL, the printer head, like the UV laser, moves in the x-y axis while the build plate travels along the z axis. The
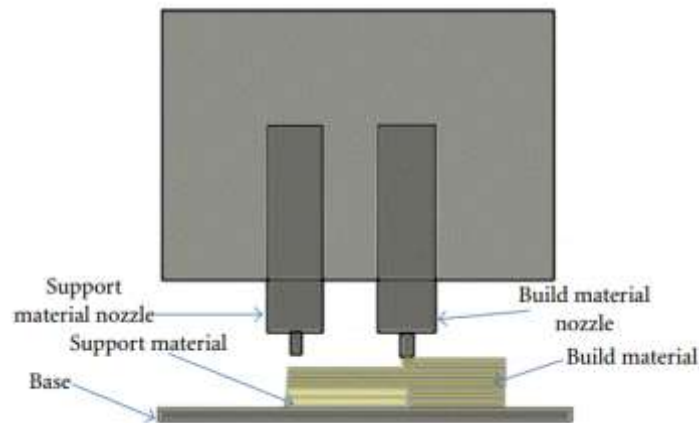
FIGURE 20- Diagram Of A Fused Deposition Modeling Device. (Wong K. and A. 2012)

resolution of this technique depends on the thickness of the filament but is typically 0.25 mm. The lower resolution also requires hand sanding the surface to post-process. The FDM printing process requires the use of a support material printed along with the actual build material that washes away in a water bath. Therefore, no chemicals are required post-process. The machine and material of this technique are relatively inexpensive; machines sell for around $2800.00, while the material sells for roughly $100.00 per Kilogram. (3D Systems, Rock Hill, SC) The printing heads used in FDM have become more complex which enables multiple materials to be used simultaneously without requiring changing of filament material or additional time.

Selective laser sintering (SLS) is a powder bed fusion technique that is similar to the STL technique, but instead of a build plate that moves down into a vat of resin, the build plate moves down and a new layer of powder is rolled on top of the current object and is sintered to the prior layer. An example of this setup can be seen in Figure 21. Adding material in this manner takes away the need for a support material. The powder that is
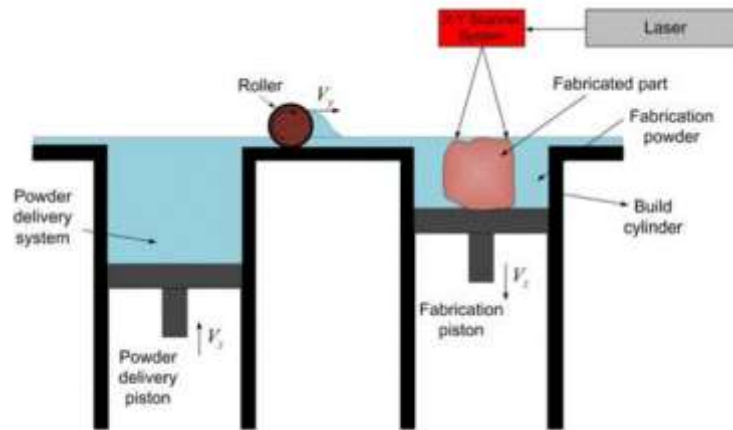
FIGURE 21- Diagram Of A Selective Laser Sintering Device. (Torabi K., Farjood E. et al. 2015)

not sintered together becomes the support material as the build plate moves down. After the entire object is created, the excess support material can be recycled for the next part, creating zero waste. The resolution of this technique depends on the size of the powder particles being sintered, with a maximum resolution of 0.004 in. (ProtoLabs, Maple Plain, Minnesota) Since the build material is in a powder form, a wide range of materials including plastics and titanium are available. This has huge implications for creating tools or molds because traditional manufacturing techniques often generate more waste material than is present in the finished part. (Wong 2012)

2.5.2 Materials

Materials selection for prosthetic and orthotic devices has traditionally focused on 6 characteristics including yield strength, stiffness, durability, density, corrosion resistance,

and ease of fabrication. (Shurr 2001) Yield strength refers to the maximum stress a

material can withstand before permanent deformation occurs, which is very important in

a load-bearing prosthetic device. Not only does the device need to withstand the

individual's bodyweight, but also the increased forces during walking, running, and

jumping.

Another characteristic related to strength is the stiffness of the material. Stiffness

refers to the stress-to-strain (or Young's Modulus) ratio. A material will stretch or
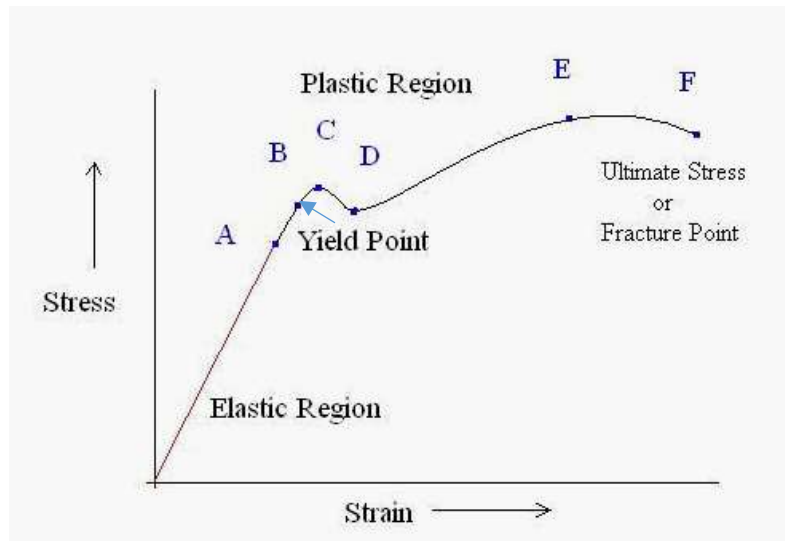
FIGURE 22- Diagram Of A Stress-Strain Curve

compress a certain distance whenever a force is applied. The ultimate strain of a material

refers to the amount of bending deformation, compression, or elongation a material

exhibits before failure. The compressive stress applied to a material refers to the applied

load that acts to reduce the length of the material in along the axis through which it was

applied. Shear stress refers to the stress state resulting from the combined energy of

opposing forces acting along parallel lines of action. Tensile stress refers to the stress

state resulting from applied loads that elongate the material along the axis through which

the force is applied. Figure 22 represents the stress-strain plot for a plastic material. In

this figure, the region from the origin to point A is the elastic region in which Hooke's Law is followed. Hooke's Law is a concept that the force required to displace a spring by a distance, is proportional to that distance. From this curve, we see that for a small Δx the force exerted by a spring is approximately proportional to Δx. Due to Hooke's Law, this elastic region maintains a linear relationship between stress and strain until point B, yield stress, is reached. This point is also called the elastic point or yield point because at this point, the relationship between ultimate stress and strain moves away from being linear as the strain increases at a faster rate than the stress at all points on the curve beyond point B. Point C refers to when the material's cross-sectional area begins to decrease which is material "necking". The initial point of necking is the location of the material's ultimate failure. At point D, the material changes length with no or little increase in stress. This characteristic remains true until point E. The portion between points D and E is commonly referred to as yielding of the material at constant stress. From point E to point F, the material's ultimate strength actually increases and requires more stress for deformation to occur. Point F is the point of ultimate stress or the fracture point where the material completely fails.

In order to have a fully supporting prosthetic device, a high-stiffness material is desired. However, a high-stiffness material may reduce the amount of flexibility and comfort the socket provides the individual. The device needs to provide sufficient stiffness to withstand day to day activities, yet be comfortable enough so that the individual chooses to use the device. The relationship between stiffness and comfort comes from the material or materials used, and the design of the prosthetic device and socket.

The durability of the device refers to the ability of the selected materials to withstand repeated force loading and unloading while maintaining material integrity. Many materials degrade or become fatigued after repeated exposure to loading and unloading. Once a material is fatigued, the force required to reach failure is reduced. Since a prosthetic device is loaded and unloaded with every step, repeated hundreds to thousands of times per day, fatigue strength is an important material characteristic in prosthetics.

The density, or mass per unit of volume, is a concern for all prosthetic users because a low density reduces the overall device weight. Decreasing the weight of the prosthetic system or increasing the device's energy storage and return minimizes the metabolic energy required to ambulate, allowing increased mobility.

Corrosion resistance and ease of fabrication are important characteristics pertaining to the life cycle and fabrication of the device. Additional characteristics to consider are material costs and availability. Consideration of all of these characteristics guides material selection. (Shurr 2001)

Another measure of a materials ability to withstand a load is the factor of safety. Factor of safety is a ratio used in structural applications to determine the ratio of the maximum working stress to the maximum stress the material can withstand. The factor of safety for components that are to be subjected to repeated impact loading, as expected in a cat jumping from a height, should be no less than 10. The final design is the product of numerous design and testing iterations until a finalized product with a sufficient life expectancy is created.

Traditionally, prosthetic and orthotic materials commonly used were wood, leather, and fabric. Fabrication technology has increased over the past several decades to increase this materials list. Now prosthetic and orthotic devices can be made using pre-impregnated carbon fiber, rubber, steel, aluminum, titanium, thermoplastics, and thermosets.

The main appeal of FDM, aside from the resolution of the device, is the wide selection of materials available that can be printed simultaneously and fused together during fabrication that do not require post-production modification. Therefore, a rubber-like material can be used adjacently and even fused to a rigid material to supply a combination of support and cushion. Currently, FDM printers have the ability to use over 140 materials with unique material properties. For this project, the most common material for FDM printers, acrylonitrile butadiene styrene, ABS plastic, is utilized.

2.5.3 Applications

Rapid prototyping has been used in the medical community for approximately twenty years. Some early applications of rapid prototyping include surgical planning, medical education, customized dental implants, prosthetics, and orthotics. (Negi 2014) Some complications during surgery can be avoided with proper preparation. Having a physical model of the organ or bone during surgical planning allows the surgical team to formulate a plan to minimize potential complications. (Negi 2014) With the help of rapid prototyping, a surgical team now has the ability to hold a replica of the organ in their hands and plan how to best perform a surgery and avoid potential complications. Furthermore, physical models of human anatomy can provide an alternative form of education for medical students. These prototypes can be used to study and evaluate

certain surgical methods without the need of live or cadaveric subjects. Finally, rapid prototyping has revolutionized orthodontics. Instead of metal wire being directly attached to each individual tooth to gradually adjust the alignment, an x-ray taken by an orthodontist can be used to fabricate a clear, form fitting mouth piece. This mouth piece performs in the same manner as traditional braces but without the social stigma of wearing traditional braces. (Negi 2014)

More recently, rapid prototyping has been used by the prosthetic and orthopedic fields. Attempts have been made to create prosthetic sockets using additive manufacturing techniques. (Rogers 2001, Ng 2002, Hsu 2010) These studies have used various techniques, ranging between selective laser sintering and fused deposition modeling. These devices used 2 mm thick polycarbonate for selective laser sintering (Hsu 2010) and 4 mm thick of polypropylene for fused deposition modeling (Ng 2002). One of the studies experienced a catastrophic failure of the prosthetic socket, resulting from an area of high stress shown by finite element analysis. (Rogers 2001) Other studies showed promising results, indicating feasibility of using additive manufacturing techniques to create patient specific prosthetic sockets. However, none of these studies incorporate prosthetic devices into their additive manufacturing designs. These studies focus only on the prosthetic socket, and use the prosthetic foot or knee unit the individual already has. One study included a resin layer over top of the 3D printed device post-production to increase the strength and durability of the device (Hsu 2010) but required several additional hours for fabrication.

2.6 Finite Element Analysis

Finite element analysis is a computational tool that allows for displacement and stresses to be calculated for a complex shape. (Brauer 1993) This technique creates a finite element, or mesh where the individual elements can vary in size and shape. An FEA model contains information regarding the complex shape's geometry, material properties assigned to the shape, magnitude and direction of forces being applied to the shape, and constraints or fixtures of the complex shape. This information is needed to determine the displacement and stresses that occur when external forces are applied to the complex shape. The nodes of the elements found within the mesh represent the corners of the finite elements. Each of these nodes in a structural problem exhibits 6 degrees of freedom, translations in three directions and rotations about these three directions. Most nodes in the mesh are unconstrained, with the fixtures of the shape being the only elements that are constrained. These fixtures are known as the boundary conditions. The finite element analysis software then solves for all of the unknown nodes.

A simplified model of this method can be represented by a spring. Two nodes are represented by the ends of the springs, and the material properties are related to the stiffness of the spring. A force acting on either of the two nodes creates a displacement, which relate to a stress and strain on the element in question. This process generates two equations and two unknowns. The matrix for these equations is shown below. The "k" refers to the stiffness of the spring, "u" is the variable representing the displacement, and "f" being the known force. Once the boundary conditions are known, "u_1" goes to zero, and this system can be solved. The resulting answer of this system becomes the reaction

that is applied to the next set of springs, and this process continues until all unknowns are solved for.

$$\begin{bmatrix} k^a & -k^a & 0 \\ -k^a & (k^a + k^b) & -k^b \\ 0 & -k^b & k^b \end{bmatrix} \begin{Bmatrix} u_1 = u_{given} \\ u_2 \\ u_3 \end{Bmatrix} = \begin{Bmatrix} f_1^a \\ f_2^a + f_1^b \\ f_2^b \end{Bmatrix} = \begin{Bmatrix} R \\ 0 \\ F \end{Bmatrix}.$$

When this general concept is adapted for three-dimensional analysis, the method remains the same but increases in complexity. Since designs created by engineers are typically three-dimensional, a three-dimensional finite element is utilized.

A three-dimensional finite element consists of at least four nodes which do not lie in the same plane. The three possible finite elements in a three-dimensional analysis are the tetrahedron, pentahedron, and hexahedron. When hundreds or thousands of these finite elements are required to represent complex shapes, hundreds or thousands of unknowns and equations are created. Computer finite element software arranges these unknowns and equations into a matrix, and perform the iterative process of solving for the unknowns to determine the displacements at every node in the complex shape. Relationships between displacement, stress, and strain can be used to determine the stress and strain at the various nodes.

2.7 Gait Analysis

Physical examinations of animals may not reveal signs of lameness during ambulation. (Stadig 2014) Therefore, gait analysis is often performed to determine if lameness or hindrance exists during ambulation. Even though the type of locomotion may differ between species of mammals, the core principles of kinematic gait analysis are similar. (Lacquaniti 1999) Numerous systems exist to capture and process kinematic

data, but most utilize video or infrared cameras to capture motion. Gait analysis can be

performed using a kinematic motion tracking system that uses reflective spheres attached
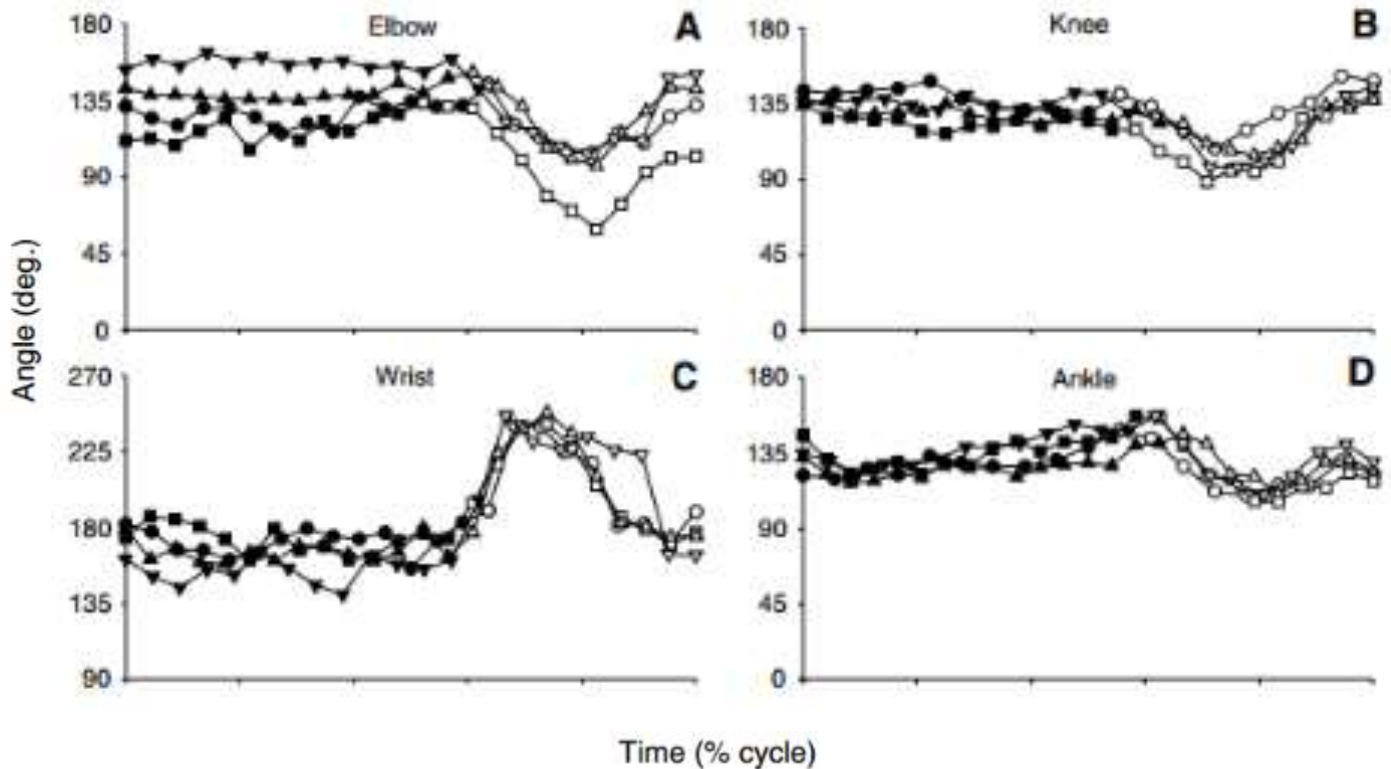
FIGURE 23- Feline Joint angles with respect to time. (Day 2006)

to the subject to represent the location of significant anatomical features, such as the knee

joint, shoulder joint, etc. This method was utilized to capture gait data for the distal

joints of various species of feline (Day 2006). These species include the domestic cat,

ocelot, cheetah, and the tiger. The data was reported in comparison to one another, so a

chart of isolated domestic cat gait data does not exist. Multiple trials were performed in

order to obtain multiple trials of similar speed. The average speed of all trials across all

species was 93.11cm/sec, with a standard deviation of 29 cm/sec. It is interesting to note

that there is no significant difference in joint angles during a gait cycle with increased

relative limb length. (Day 2006)

Motion capture data can be analyzed to determine joint angles and spinal curvature. Differences in kinematics and/or kinetics between the thoracic or pelvic limbs may indicate compensation and increased biomechanical loading. (Fuchs 2014) Prosthetic devices help alleviate this increased loading on the remaining limbs, by applying the loads to the pressure tolerant areas of the residual limb. Changes in kinematics and/or kinetics are important to physicians and caregivers and provide a better understanding of the biomechanical consequences following a serious injury or surgery. (Goldner 2015) The Goldner (2015) study simulated an amputation in a single dog by tying one pelvic leg to the body, and assessed ambulation on three limbs. The Fuchs study, a companion study to the Goldner study, used the same companion animal and methods to simulate pelvic-limb amputation on a single canine. This approach removed variability associated with using multiple test subjects, simulated amputation, and analyzed the changes in certain kinematic measurements. The Fuchs study concluded that kinetic changes in the canine's gait indicated a compensatory mechanism in which the unaffected diagonal limb pair is involved. The proposed study compared kinematic measurements prior to and following prosthetic device use in a feline bilateral thoracic limb amputee to quantify gait changes attributed to the use of the devices.

2.7 Prior Work

The proposed thesis project expanded upon a Rehabilitation Engineering (BE 658) course group project offered in the fall semester of 2014. The class project developed a general concept and proof of concept. The goal of the proposed project is to 1) develop a prosthetic device that is designed for a specific feline subject, 2) perform gait analysis to demonstrate improved individual ambulation, and 3) provide the individual with an

effective prosthetic device solution. The devices in the proposed project expand upon the

general concepts produced in the Rehabilitation Engineering class of 2014. The devices

created in the proposed project are used during gait analysis of the subject to determine if

the prosthetic devices have a significant impact upon the walking capabilities of a

companion animal with a bilateral thoracic limb amputation.

In the class group project, the subject was sedated, fur on her thoracic limbs was

trimmed, and the limbs were wrapped in fiber glass casting material. Once the material

FIGURE 24- Prior Work Proof Of Concept.

dried and hardened, it was removed and used to develop a mold from plaster of paris. The

mold of each limb was scanned using a portable 3D scanner (Desktop 3D Scanner,

NextEngine, Inc., Santa Monica, CA). The point cloud created from this scanning

process was then manipulated to create a solid body model using SolidWorks (Dassault

Systèmes, Waltham, MA). The detailed model shows key anatomical features that are essential for design consideration in order to ensure a proper fit is maintained on the prosthetic socket. A proof of concept design was fabricated using a SLS machine (Figure 24).

Since this cast was taken in 2014, the subject may have grown or changed shape since the initial casting. Changes could be due to either skeletal maturity or hypertrophy or atrophy of soft tissue. Soft tissue measurements should be taken every six months as the subject grows, to assure the prosthetic socket fits as effectively as possible.

Materials & Methods

Anatomical information for a dual thoracic limb feline amputee are used to develop

and fabricate custom prosthetic devices using the computer aided design software

3.   SolidWorks (Dassault Systèmes, Waltham, MA). The design of the prosthetic devices

incorporate a custom fit prosthetic socket attached to a custom designed prosthetic foot

that borrows design concepts from both the animal and human prosthetic industry. The

prosthetic devices are created using Additive Manufacturing (AM) techniques, more

commonly referred to as 3-D printing. The feline subject undergoes gait analysis under

two conditions. First, the subject walked as she currently does with no external support

to document her current ambulation technique. Second, the subject walked using the

prosthetic devices. Elbow, shoulder, and stifle joint angles and spinal curvature across

the gait cycles, are compared between the two scenarios, to determine the influence of the

prosthetic devices.

3.1 Feline Subject

Elsa is a Maine Coon feline that weighs 9 lbs. She is 2 years old, and was found by

a University of Louisville faculty member during the winter of 2014.   She exhibited

severe frostbite in the distal end of her thoracic limbs, resulting in amputation to remove

the necrotic tissue. This surgery removed phalange and carpal bones on which to walk.

She currently walks on the distal end of her radius and ulna on her left limb and residual

metacarpal bones on the right limb. The amputation of her limbs also did not occur at the

same anatomical level. This results in an uneven gait that has the potential to develop
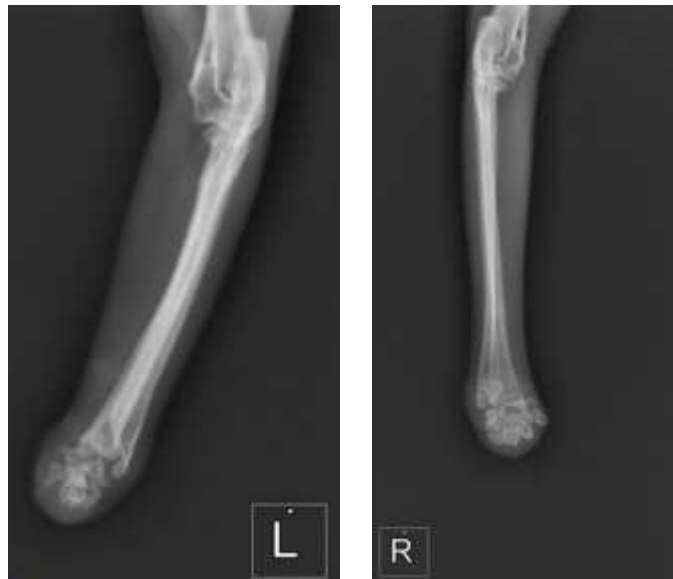
FIGURE 25- Radiograph Of Residual Limbs (not to scale).

into secondary complications. (Thrall 2007)

3.2 QFD

The QFD assembled for this project was evaluated by the designer, thesis advisor,

and caretaker of the companion animal. The QFD is comprised of the technical

requirements and the customer needs and benefits. The technical requirements were split

between device efficacy and individual comfort. Efficacy of the device is defined as

whether or not the device aligns with the caudal aspect of the limb, medial-lateral

shoulder alignment, and retention of the device during use. The prosthetic foot also

needs to prevent slipping or skidding during use. User comfort is defined by the

technical team as localized pressure reduction of the residual limb, shock absorption of

the prosthetic foot, and material at the user device interface that prevents tissue

breakdown. The customer needs are comprised of three categories, including

performance of the device, device durability, and needs of the caretaker. The

performance of the device is defined by the user as ensuring a normalized feline line from

the head to pelvis, level shoulders, even weight distribution between the two limbs, shock

absorption, user comfort, and ability for the user to walk without sliding. The concerns

of the caretaker in the durability category include replaceable securement straps,

durability of the prosthetic leg, and prosthetic device retention. The specific needs of the

caretaker include ease of putting on and taking the prosthetic device off, keeping the cost

below $200, and keeping the aesthetic value of the device in mind during design. The

caretaker, thesis advisor, and technical team completed this evaluation, and the factors

with the highest weights are implemented in the design process. The final prosthetic

device was evaluated using the same criteria to ensure all technical requirements were

met.

3.3 Device Development

3.3.1 Residual Limb Model

In order to create a model of the residual limb, methods established in the human

prosthetic community are applied to the companion animal. This method begins with

preparation of the residual limb, which includes trimming of the fur. This is done to

provide the closest possible interface to the companion animal's skin when the cast is taken. Once the limb is prepared, plaster wrap is tightly wrapped around the residual limb to obtain topical features of the limb. This fiberglass wrap is allowed to dry on the residual limb and then removed. The fiberglass cast is then filled with plaster of paris, creating an exact positive model of the residual limb.

Since this prior work was performed nearly 16 months before this researcher was able to meet with the subject, the model of the residual limbs are altered to account for any soft tissue atrophy that has occurred in this region. A new cast is not necessary to determine the physical changes, but measurements of the current condition of the residual limbs are essential to develop an accurate model of the prosthetic socket. A standard method for assessing measurements is based on human and animal residual limb measuring techniques adapted from Kentucky Prosthetics & Orthotics, (Louisville, Kentucky) and OrthoPets (Denver, Colorado). The outcome measurements assessed can be found in the Appendix on the Right Limb Measurement Form. Once these measurements are recorded, the 3D solid model created in the prior work was modified to resemble the limb's current conformation, and the prosthetic socket was designed using the new 3D model.

3.3.2 Prosthetic Socket Design

The prosthetic socket was designed around the residual limb model described in section 3.2.1. The prosthetic socket was created using the shell feature in SolidWorks (Dassault Systèmes, Waltham, MA) to create a negative socket surrounding the residual limb model. After the shell is created, the solid body resembling the residual limb is suppressed, leaving the prosthetic socket. An adapter is created on the bottom of this

43

socket so that the prosthetic foot component of this system attached through the use of four set screws. The function of these four set screws adjust the alignment of the prosthetic foot in relation to the socket, allowing for inversion or eversion as needed.

This technique is modeled after the fabrication process of a prosthetic socket for a human individual. With the attachment of the prosthetic device to the socket accomplished, the next challenge is to securely attach the prosthetic socket to the residual limb of the individual. The prosthetic socket is split into two sections, a caudal portion and a cranial portion, so that the subject's caregiver could easily attach and remove the prosthetic system from the subject. The caudal piece attached to the rest of the socket, fully encapsulating the residual limb. The cranial and caudal portions of the socket are secured together around the limb using Velcro straps on either side of the separation line.

3.3.3 Prosthetic Foot Development

The prosthetic foot was designed using computer aided design software SolidWorks (Dassault Systèmes, Waltham, Massachusetts). The initial concept was to mimic aspects of a human prosthetic foot design specifically for walking. The individual's center of gravity was maintained over the center of the foot, and the interface to the ground is curved to assist in the transition from heel strike to toe-off. Similar to Össur's Flex-Run foot (Reykjavik, Iceland), tread was added to the bottom of the device to give the user extra traction when traversing various surfaces.

An integral component to the prosthetic foot design is the prosthetic alignment pyramid. This pyramid acts as an interface between the prosthetic food and the pylon of the prosthetic socket. Manipulating the set screws that connect the alignment pyramid and pylon adjusts the alignment of the prosthetic foot. Varying the depth of any of the

four set screws can adjust the pitch and roll of the prosthetic foot. The dynamic alignment of the prosthetic foot solely depends on the presence of the prosthetic alignment pyramid.

3.4 Device Evaluation

3.4.1 Computer Modeling

The developmental software used to create these prosthetic devices also has the capability to represent forces applied by the subject to the device and to perform stress analyses. Only the beta and final prototype designs were subjected to evaluation. The proof of concept and alpha designs were used as presentation aids to determine efficacy of this project. A fatigue and static analysis was applied using this software. The forces in both of these studies resembled the vertical forces experienced during gait. A vertical force of 23N was used in the stress analysis, since this was the maximum force recorded from cats jumping from a height of 1m. (Corbee, 2014) To replicate the ground reaction forces from this type of movement, the proximal end of the prosthetic pyramid was treated as a fixed entity, and forces perpendicular to the distal face of the tread depict the ground reaction forces. The simulation software, SolidWorks Simulation (Dassault Systèmes, Waltham, MA), was used to perform fatigue analysis on the device, and test cyclic loading and unloading with 23N until device failure. This approximated how many cycles the device can withstand and when a replacement device may be required. Should the stresses calculated during the simulation approach the yield strength of the material, the design is altered to mitigate the risk of failure and tested again to achieve a design that is durable enough for daily use with a reasonable life. The benchmark for the durability of this device reflects the standards used within the prosthetic device industry.

Several prosthetic device companies were consulted and it was determined that a

prosthetic foot should withstand over 2 million steps in its lifetime. However, prosthetic

device companies are not limited to 3D printing and incorporate a wide range of

advanced materials that can serve to increase fatigue life. Given that this project was

limited to the materials suitable for use with a 3D Systems Cube Pro FDM printer, 50,000

steps was used as the target benchmark.

3.4.1.1 Static Analysis

A static analysis was performed to determine the maximum stress, strain,

displacement, and factor of safety for each design under a specified load. Finite element

analysis was used to statically analyze three scenarios using SolidWorks Simulation. A

standard trapezoidal mesh tool was utilized, and 14273 elements were defined. The

material properties applied to this study were standard ABS plastic material properties

listed in the materials library of SolidWorks. Each scenario resembled the phases of the

gait cycle, all with the maximum possible force exerted by a feline of Elsa's size, 23 N.

The scenarios include a heel strike, mid-stance phase, and toe-off simulation. All

analysis performed through SolidWorks Simulation have the same fixed constraints

across all three scenarios. The static analyses for these scenarios were performed for the

beta and final designs of the prosthetic foot. Maximum stress, strain, displacement, and

minimum factor of safety were determined from these tests.

3.4.1.1.1 Beta Prototype Design

Three computer simulations were conducted for the beta design to determine the

performance of the prosthetic foot during the three main phases of a gait cycle. These
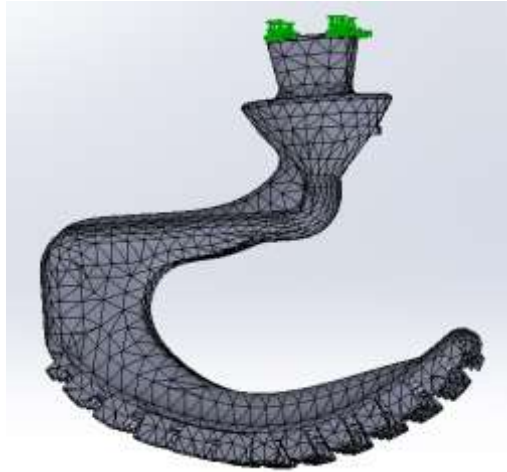
FIGURE 26- Beta Prototype Design Fixed Geometry And Finite Element Mesh In Static Simulation.

simulated scenarios consisted of the heel strike, stance phase, and toe-off. All three

scenarios shared the same fixed geometry on the most proximal face of the prosthetic

foot, with forces applied to different portions of the most distal aspect. The mesh used in

finite element analysis calculation was the same across all three gait phase simulations.

The mesh type was solid, with an element size of 0.113 inches. A mesh with 25,049

nodes and 14,340 total elements was used.

3.4.1.1.1.1 Heel Strike

To simulate the first of the three gait phases, ground reaction forces are applied to the three most caudal treads. A total ground reaction force of 23 N is applied over all 12

FIGURE 27- Beta Prototype Design Heel Strike Fixed Geometry And Finite Element Mesh In Static Simulation.

faces of the caudal treads.

3.4.1.1.1.2 Stance Phase

To simulate the second of the three gait phases, ground reaction forces are applied to the three most central treads. A total ground reaction force of 23 N is applied over all 12

FIGURE 28- Beta Prototype Design Stance Phase Fixed Geometry And Finite Element Mesh In Static Simulation.

faces of the central treads.

3.4.1.1.1.3 Toe-Off

To simulate the last of the three gait phases, ground reaction forces are applied to the

three most cranial treads. A total ground reaction force of 23 N is applied over all 12

FIGURE 29- Beta Prototype Design Toe-Off Phase Fixed Geometry And Finite Element Mesh In Static Simulation.

faces of the caudal treads.

3.4.1.1.2 Final Prototype Design

Three computer simulations were conducted for the final prototype design to

determine the performance of the final prototype design during the three main phases of a

FIGURE 30- Final Prototype Design Fixed Geometry And Finite Element Mesh In Static Simulation.

gait cycle. These phases consist of the heel strike, stance phase, and toe-off. All three

scenarios shared the same fixed geometry on the most proximal face of the prosthetic

foot, with forces applied to different portions of the most distal face. The mesh used in

finite element analysis calculation was the same across all three gait phase simulations. The mesh type was solid, with an element size of 0.0905 inches. A mesh with 23,323 nodes and 14,273 total elements was used.

3.4.1.1.2.1 Heel Strike

To simulate the first of the three gait phases, ground reaction forces are applied to the three most caudal treads. A total ground reaction force of 23 N is applied over all 12
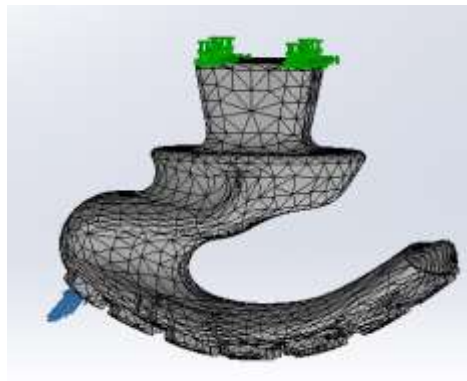
FIGURE 31- Final Prototype Design Heel Strike Fixed Geometry And Finite Element Mesh In Static Simulation.

faces of the caudal treads.

3.4.1.1.2.2 Stance Phase

To simulate the second of the three gait phases, ground reaction forces are applied to the three most central treads. A total ground reaction force of 23 N is applied over all 12

FIGURE 32- Final Prototype Design Stance Phase Fixed Geometry And Finite Element Mesh In Static Simulation.

faces of the central treads.

3.4.1.1.2.3 Toe-Off

To simulate the last of the three gait phases, ground reaction forces are applied to the three most cranial treads. A total ground reaction force of 23 N is applied over all 12
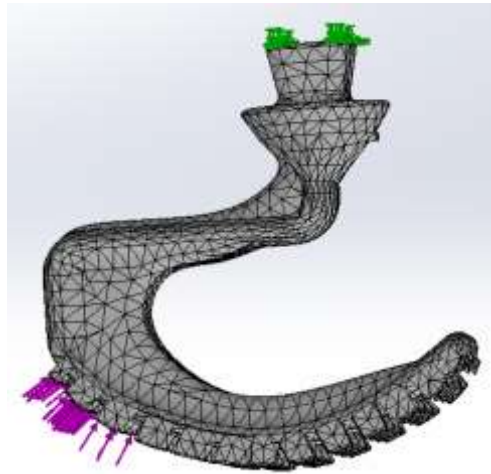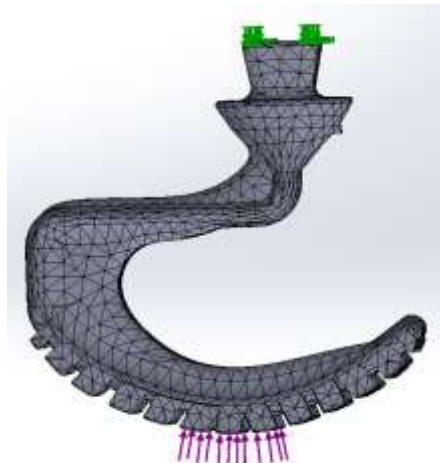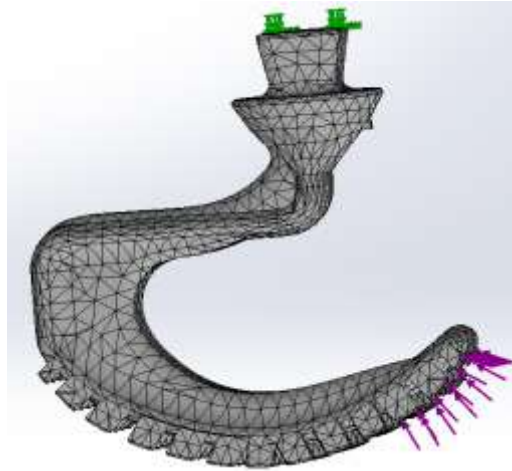

FIGURE 33- Final Prototype Design Toe-Off Phase Fixed Geometry And Finite Element Mesh In Static Simulation.

faces of the caudal treads.

3.4.1.2 Fatigue Analysis

A fatigue analysis is performed to determine the expected lifespan of a device under cyclic loading and unloading of a specified magnitude. The fatigue simulation and analysis determined the number of cycles of loading and unloading that is required for failure of the device to occur. Three scenarios were tested using SolidWorks Simulation. These scenarios resembled the phases of the gait cycle, all with the average force a feline exerts during a normal gait cycle. The force applied to the proximal end of the prosthetic end of the foot was 1.4 times the feline's bodyweight. In the fatigue test, the force that is applied to the prosthetic foot is 6 N. The loading condition was zero based, meaning 6 N was loaded, unloaded to 0 N, and loaded again. (Demes et al., 1994) The loading frequency was kept at the default 100 Hz. The scenarios included a heel strike, stance phase, and toe-off simulation. All analysis performed through SolidWorks Simulation have the same fixed constraints across all three scenarios. The fatigue analyses for these scenarios were performed for the beta and final prototype designs of the prosthetic foot.

3.4.1.2.1 Beta Prototype Design

Three computer simulations were conducted for the beta design to determine the performance of the prosthetic foot during the three main phases of a gait cycle. These
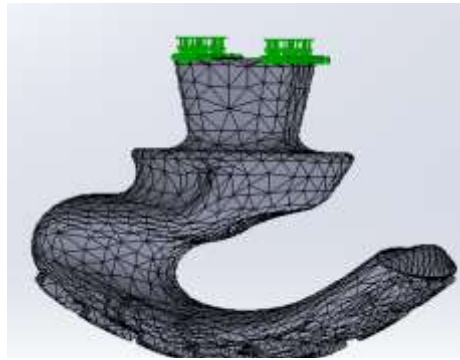

FIGURE 34- Beta Prototype Design Fixed Geometry And Finite Element Mesh In Fatigue Analysis Simulation.

phases consist of the heel strike, stance phase, and toe-off. All three scenarios shared the same fixed geometry on the most proximal face of the prosthetic foot, with forces applied to different portions of the most distal face.   The mesh used in finite element analysis calculation was the same across all three gait phase simulations. The mesh type was solid, with an element size of 0.113 inches. A mesh with 25,049 nodes and 14,340 total elements was used.

3.4.1.2.1.1 Heel Strike

To simulate the first of the three gait phases, ground reaction forces are applied to the three most caudal treads. A total ground reaction force of 6 N is applied over all 12
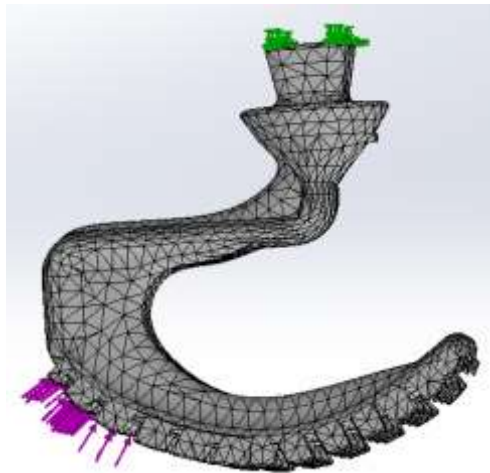
FIGURE 35- Beta Prototype Design Heel Strike Fixed Geometry And Finite Element Mesh In Fatigue Analysis Simulation.

faces of the caudal treads.

3.4.1.2.1.2 Stance Phase

53

To simulate the second of the three gait phases, ground reaction forces are applied to the three most central treads. A total ground reaction force of 6 N is applied over all 12
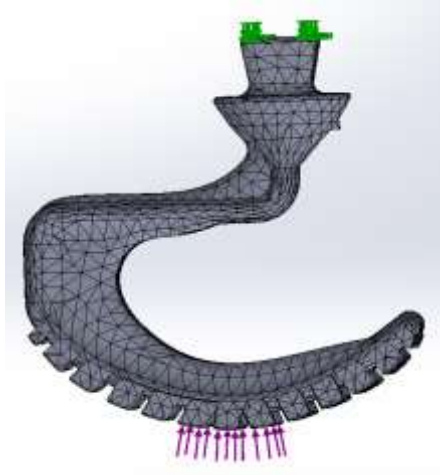
FIGURE 36- Beta Prototype Design Stance Phase Fixed Geometry And Finite Element Mesh In Fatigue Analysis Simulation.

faces of the central treads.

3.4.1.2.1.3 Toe-Off

To simulate the last of the three gait phases, ground reaction forces are applied to the three most cranial treads. A total ground reaction force of 6 N is applied over all 12 faces
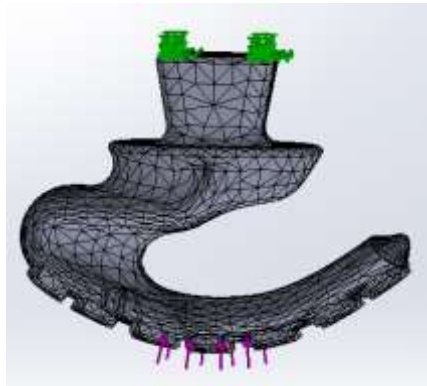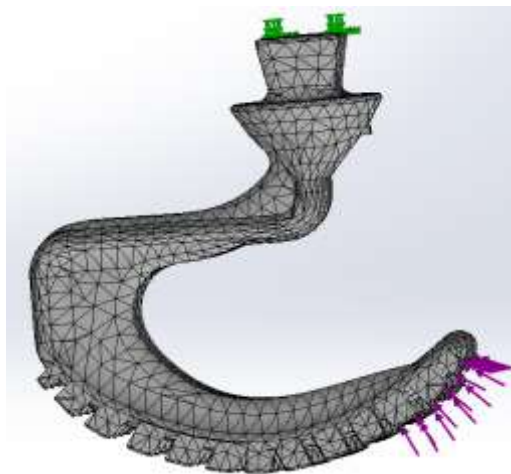

FIGURE 37- Beta Prototype Design Toe-Off Phase Fixed Geometry And Finite Element Mesh In Fatigue Analysis Simulation.

of the caudal treads.

54

<u>3.4.1.2.2 Final Prototype Design</u>

　　　Three computer simulations were conducted for the beta design to determine the

performance of the prosthetic foot during the three main phases of a gait cycle.　These

phases consist of the heel strike, stance phase, and toe-off.　All three scenarios shared the
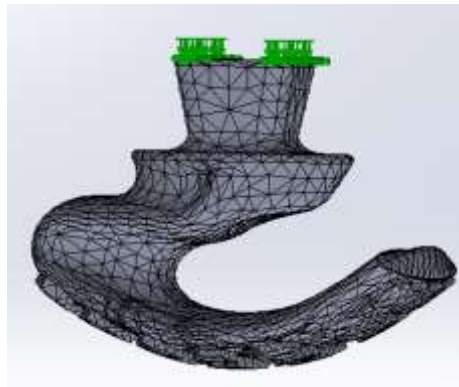
FIGURE 38- Final Prototype Design Fixed Geometry And Finite Element Mesh In Fatigue Analysis
Simulation.

same fixed constraint on the most proximal face of the prosthetic foot, with forces

applied to different portions of the most distal face.　The mesh used in finite element

analysis calculation was the same across all three gait phase simulations.　The mesh type

was triangular, with an element size of 0.0905 inches.　A mesh with 23,323 nodes and

14,273 total elements was used.

<u>3.4.1.2.2.1 Heel Strike</u>

To simulate the first of the three gait phases, ground reaction forces are applied to the three most caudal treads. A total ground reaction force of 6 N is applied over all 12
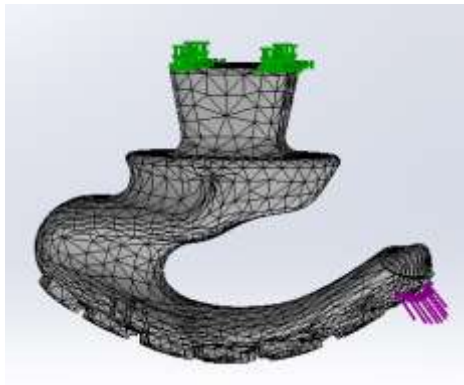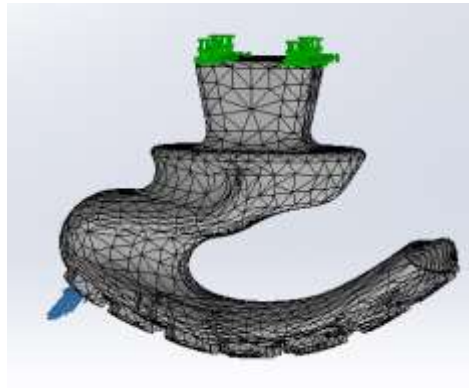

FIGURE 39- Final Prototype Design Heel Strike Fixed Geometry And Finite Element Mesh In Fatigue Analysis Simulation.

faces of the caudal treads.

3.4.1.2.2.2 Stance Phase

To simulate the second of the three gait phases, ground reaction forces are applied to the three most central treads. A total ground reaction force of 6 N is applied over all 12
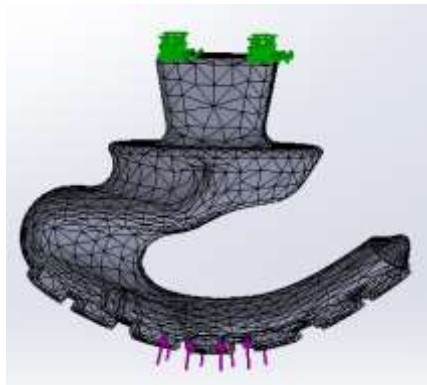
FIGURE 40- Final Prototype Design Stance Phase Fixed Geometry And Finite Element Mesh In Fatigue Analysis Simulation.

faces of the central treads.

3.4.1.2.2.3 Toe-Off

To simulate the last of the three gait phases, ground reaction forces are applied to the three most cranial treads. A total ground reaction force of 6 N is applied over all 12 faces of the cranial treads.
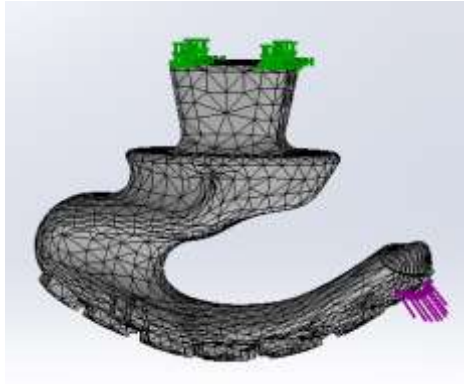
3.4.2 Mechanical Testing of Final Prototype Design

Mechanical testing is performed to test the strength and durability of the final design of the prosthetic foot. The static testing consisted of a downward force applied at the three most central treads to simulate a feline landing on its thoracic limbs from a 3 foot jump. This testing was performed with forces that exceed typical feline forces, to ensure device efficacy. An ADMET eXpert 2611 (ADMET, Inc. Norwood, MA) mechanical testing machine was used to apply compressive loading and unloading. The alignment pyramid of the prosthetic foot was mounted to the mechanical press. A force of 25 N was applied to the distal end of the prosthetic foot. This applied vertical force is slightly higher than the documented 23 N force feline jumping recorded from the Corbee study (Corbee, 2014). The 25 N was selected to build in extra confidence that the device does not fail during use: it represents 4.15 times the anticipated feline ground reaction force associated with gait. The MTEST Quattro Materials Testing System software provided by ADMET was utilized to set all the parameters of the test, and also serve as the data

acquisition for this experiment. The testing parameters for the static test included setting a fixed upper limit of 25 N, with a rate of 2 mm/sec vertical compressive force. The deformation curve of the prosthetic foot was recorded at 100 Hz and compared to the displacement values obtained through the simulation testing.

The MTEST software and ADMET machine were also used to perform a fatigue analysis. The repeated loading followed a saw-tooth pattern allowing the prosthetic foot to be loaded and unloaded. The load was applied at 2 mm/sec, and unloaded at 4 mm/sec. This speed is selected to represent gradual loading of the prosthetic foot at mid-stance, and the sudden push off seen during toe-off of the gait cycle. The testing machine used in this experiment is belt driven, rather than hydraulically powered. Belt driven testing machines may not provide exact upper force limits set within the software. The use of the belt reduced the response time of the mechanical press. To correct for this, a displacement value was selected that produced an average value of 25 N. A limit of 0.15 mm was determined through trial and error. Due to the limited speed of the ADMET machine, 10,000 cycles was selected in order to complete the study within one day. When a higher speed was selected, the accuracy of the machine decreases and the applied forces were 375 N over the 25 N limit. Force-deformation data was collected and recorded at 100 Hz and compared to the simulated fatigue analysis.

The prosthetic foot was anchored to the machine using a vice anchors on the alignment pyramid and force was applied to the mid-stance portion of the foot. This setup replicates the testing scenario and fixture locations defined in the computer simulation. An aluminum block was fixed in a vice attached to the mobile portion of the mechanical press to provide a flat, uniform surface through which forces were applied to

58

the prosthetic foot. The vice holding this aluminum block was attached to the mechanical press with a loose fitting pin.

Once the static and fatigue tests were complete, an ultimate failure test was performed on the prosthetic foot. The prosthetic foot was secured into the mechanical testing machine using the same method described above, but the parameters set in the software were set with the intent to cause failure. The limit for displacement was set to 7 mm, the load was applied at 2 mm/sec, and the deformation curve was obtained during this test. The point of failure from this experiment was compared to the results of the computer simulation.

3.5 Device Fabrication

The devices for this project were created using a 3D Systems (Rock Hill, SC) CubePro printer. This device is a FDM rapid prototype machine with build area dimensions of 10.75 x 10.75x 9.5 inches. The printer has a build resolution of 70 microns. During the build process, support structures were needed to support areas of overhang. Without these supports, the build will fail and the print job will need to be repeated. After the print job is complete, these support structures are removed. These supports are constructed in a manner that allows for them to break away with little effort. Some areas may require use of a knife to be used to separate the support structure from the designed part. Once the supports are removed, the residual structure is sanded smooth. In order to achieve a smooth and uniform finish, the designed parts are placed into an acetone vapor bath for 3 hours. The acetone vapor slowly dissolved the outermost layer of ABS plastic, creating a smooth finish. This bath is performed by placing paper towels soaked in acetone in the bottom of a sealable glass container, which are then

soaked in acetone. A piece of aluminum foil is then gently placed on top of the acetone

soaked paper towels, and the designed pieces are positioned on top of the foil. The

aluminum foil serves as a physical barrier between the liquid acetone and the designed

parts. If this barrier were not present, the piece of the designed part that would be in

contact with the liquid acetone would dissolve at a faster rate than the rest of the designed

part. The container is then sealed, and left undisturbed for 3 hours. After 3 hours, the

designed parts are removed and rinsed with water to remove any residual acetone vapor

that still clings to the part. Following the smoothing process, four holes are drilled and

tapped on the prosthetic socket to hold the set screws that interact with the alignment

pyramid on the prosthetic foot. Velcro straps and a silicone liner are installed for

retention purposes.

3.5.1   Proof of Concept

A proof of concept was generated using 3-D Computer Aided Design software

SolidWorks. (Dassault Systèmes, Waltham, MA) The design for the prosthetic foot was

modeled after several human prosthetic feet used for amputees with high activity levels.

The goal of the proof of concept is to develop two prosthetic devices that alleviated the

height difference that results from an uneven level of amputation across the subject's left

and right thoracic limbs. The proof of concept was not evaluated using either computer

simulation or mechanical testing.

3.5.2 Alpha Prototype

The alpha prototype built upon the ideas brought forward in the proof of concept.

The goals for the alpha prototype include testing 3D printer settings and determining the

proper orientation of the designed parts to be fabricated. The prosthetic socket and foot

were printed separately, and joined using an acetone-ABS slurry that acted as a glue once dried. Since this device was not evaluated on the feline subject, the computer simulation was not performed on this design.

3.5.3 Beta Prototype

A goal of fabrication of the beta prototype included the evaluation of the prosthetic alignment pyramid. This feature resembles components found on human prosthetic systems that enables the adjustment of the prosthetic foot. The beta prototype also explored the infill possibilities. Various infill settings were used to minimize building material and fabrication time. In addition to manipulating the conformation of the infill, the support structures can also be added or removed, saving on material and speeding up the print job. The connection between the prosthetic socket and prosthetic foot consist of four set screws that also have the ability to adjust the alignment of the prosthetic foot. The areas of the prosthetic socket housing the set screws were set to 100% infill. This was done to facilitate tapping of the holes. The rest of the prosthetic socket was printed at 75% infill. This prototype was worn by the feline subject, so computer simulation was performed with this design. A method for applying a tread to the distal end of the prosthetic foot was explored, adding traction to avoid slipping during device use.

3.5.4 Final Prototype

The design of the final prototype alleviated any limitations found in the beta prototype, specifically in the height of the prosthetic foot. The prosthetic sockets adjusted for the discrepancy in the amputation levels, but the height of the beta prototype was too drastic for the subject to confidently walk. This design was analyzed using computer simulation and mechanical material testing. The ultimate goal of this prototype

is to create a device that the feline subject felt comfortable and confident enough in to take a few steps and allow capture of a valid gait trial to analyze.

3.6 Gait Analysis

3.6.1Subject Testing

Once the final prototype prosthetic system was thoroughly evaluated through computer simulation and benchtop physical testing, it was introduced to the feline subject. The devices were secured to the residual limbs, and the individual was allowed time to acclimate to the devices. This acclimation process consisted of several visits with the individual, attaching the prosthetic devices to the residual limb, encouraging weight bearing on the prostheses before steps were attempted. These visits were kept short, around 40 minutes, so as to not introduce fear or anxiety associated with either the researchers or the prosthetic devices. Once acclimated, a testing area was set up following the Gait Analysis Protocol found in Appendix B and following procedures set forth in section 3.5. This protocol dictated how to set up the testing area and also how to perform the gait analysis that evaluated the influence of the prosthetic devices on the subject's gait.

3.6.2 Marker Set

Reflective markers were placed on the subject's body and prosthetic devices corresponding to anatomical landmarks. There are a total of 24 markers placed on the subject. These markers include 10 anatomical features of the limbs on both left and right side of the body, as well as 4 markers placed along the spine (locations can be found in

TABLE I:

MARKER LOCATIONS

A: Dorsal aspect of thoracic paw	H: Sacrum
B: Styloid process of the radius	I: Greater trochanter of the femur
C: Olecranon	J: Lateral Femoral condyle
D: Lateral epicondyle	K: Lateral tibial condyle
E: Greater tuberosity	L: Lateral malleolus of the fibula
F: T1 vertebrae	M: Dorsal aspect of the pelvic paw
G: L1 vertebrae	

Table I). The subject's fur was trimmed overlying bony prominences where markers are positioned. The markers were adhered to the subject's skin using 3M Clear #1522 toupee tape. (St Paul, MN)
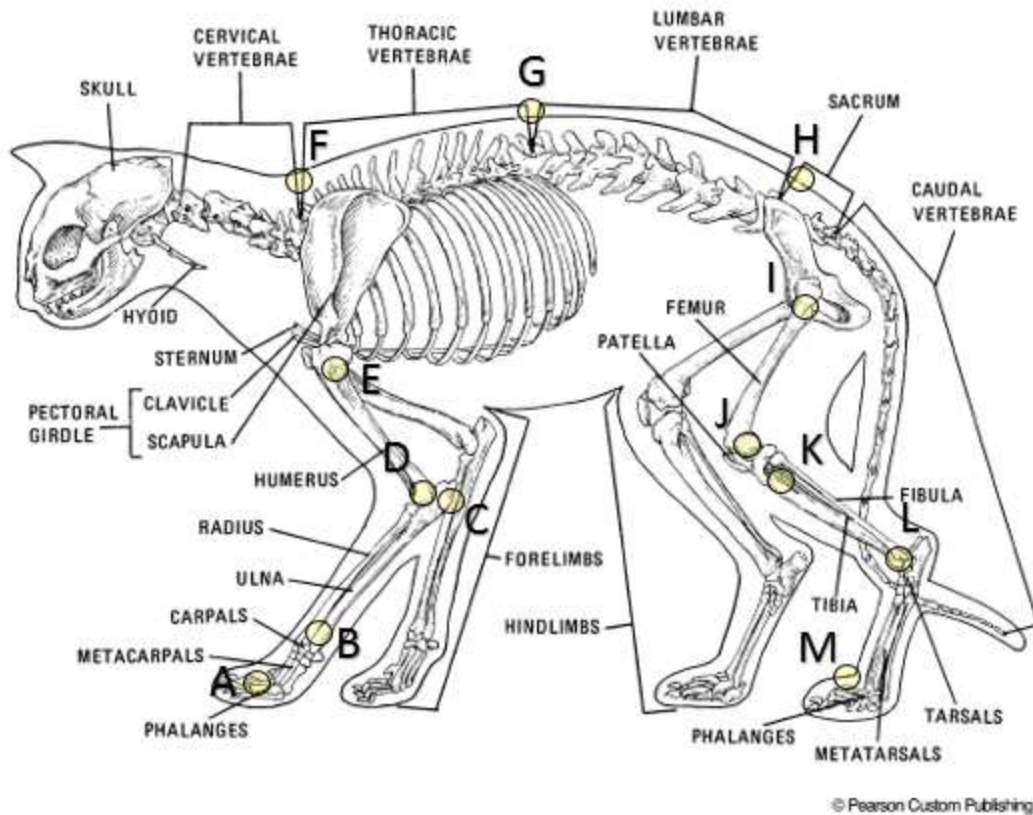
FIGURE 42- Anatomical Positions Of Reflective Markers, Marker A Was Placed On The Prosthetic Foot.

3.6.3 Data Collection

Data was planned to be collected using reflective markers found in the anatomical

positions described in Figure 42 and Feline Gait Analysis Protocol. Subject right and left

sagittal plane motion was captured during each trial using one camera on each side of the

subject. To allow for portability and assessment of subject motion within the home

environment, two iPhone 6 (Apple, Cupertino, California) smartphone cameras were

utilized. These cameras record video in 1080p at 60 frames per second. These cameras

were mounted on tripods and set to a height of 8 inches from camera lens location to the

floor. Each camera was placed perpendicular to and 3 feet from the designated walkway

to maintain acceptable video image resolution. Yardsticks were incorporated within the camera view to ensure reference measurements can be made throughout the entire trial. Seven successful walking trials with a minimum of 3 gait cycles were collected.

Data collection was conducted twice. The first instance of data collection occurs with the feline subject in her natural state (no prosthetic devices). The gait data was collected while the subject ambulates on the distal ends of her residual limbs to establish a gait baseline. This baseline was compared to the second instance of data collection, when the individual is using the custom made prosthetic devices. The independent variables across data collection instances were the presence of the prosthetic devices and the speed of the feline subject. Filming location was changed during the second data collection to better aid the companion animal in donning the prosthetic devices. Due to this location change, data from the companion animal's right side was unable to be collected.

3.6.4 Data Interpretation and Analysis

Joint angles and spinal curvature were determined. The joints of interest for this study include the elbow, shoulder, hip, stifle, and ankle. The spinal curvature refers to the angle between the three markers centered around the L1 vertebrae (markers F, G, and H). Outcome measures were compared across data collection instances to determine the influence of the prosthetic devices on spine alignment and gait pattern. A gait cycle is defined as when one foot strikes the ground, to the next time that same foot strikes the ground. Data was interpreted from the video files captured in section 3.6.2, using a motion capture and analysis software (MaxTraq, Innovision Systems inc., Columbianville, Michigan) Coordinate data was filtered using a 2-pass 60 Hz

Butterworth-filter. Data was resampled to represent angles in percent gait cycle and the gait cycle was delineated into stance and swing phase.

The video files taken during the preliminary gait analysis were converted from mp4 files to avi, and then imported into the MaxTraq (Innovision Systems inc., Columbiaville, MI) software for analysis. Joint angles were determined and exported to Excel, where the values from individual frames were compiled into graphs during each phase of the gait cycle. The gait cycles were calculated so that 0% of the gait cycle is the initial heel strike, and 100% of the gait cycle is at the subsequent heel strike of the same extremity. Since speed could not be controlled during the experiment, the data was resampled between each trial to normalize to one complete gait cycle. All of the normalized gait cycles at a particular joint or bony prominence was then plotted on the same graph. This allowed comparison of all viable trials from the left side to the right side. Comparing the angles across left and right sides depicted which effects, if any, are present due to the uneven amputation levels across her residual limbs when not using the prostheses. The spinal curvature angles should mirror one another from the right side and left side, and should not have significant variance.

3.7 Device Evaluation

The trials from the two gait collection instances were compared (pre-prosthetic and post-prosthetic), and substantial differences were recorded. These differences were evaluated by determining if they meet the top five priorities set by the QFD. If the differences from the pre and post prosthetic gait analysis, along with results from computer simulation and benchtop testing, pass the QFD requirements, then the prosthetic device's design was considered successful.

Results

4.1 Feline Subject

Elsa is a 2 year old (4kg) Maine Coon cat with dual thoracic limb amputation that

was performed in the winter of 2014 to remove necrotic tissue. The formation of the

necrotic tissue was the result of severe frostbite to her paws. The amputation was not

done at the same anatomical level, resulting in uneven residual limbs. In the right

thoracic limb, several metacarpal bones remain. In the left thoracic limb the metacarpals

were removed. Since the subject continues to ambulate on the distal ends of her residual

limbs, lameness has developed resulting in a minor limp, as well as tenderness at the

most distal portion of the left thoracic limb. In addition to lameness, the presence of the

metacarpals also creates a bulge at the most distal region of her right residual limb, which

created complications during the application and removal of the prosthetic devices.

4.2 QFD

The design group, thesis advisor, and subject caretaker were involved in determining

importance of each customer needs by weighting each need using a scale ranging from 1

to 5 where 1 indicates highest priority and 5 indicates lowest priority. As seen in Figure

43, the breakdown of importance is translated into technical priority of inclusion in the

design. The five highest priority categories include shock absorption, device material,

pressure reduction, retention of device during use, and cost. These factors were
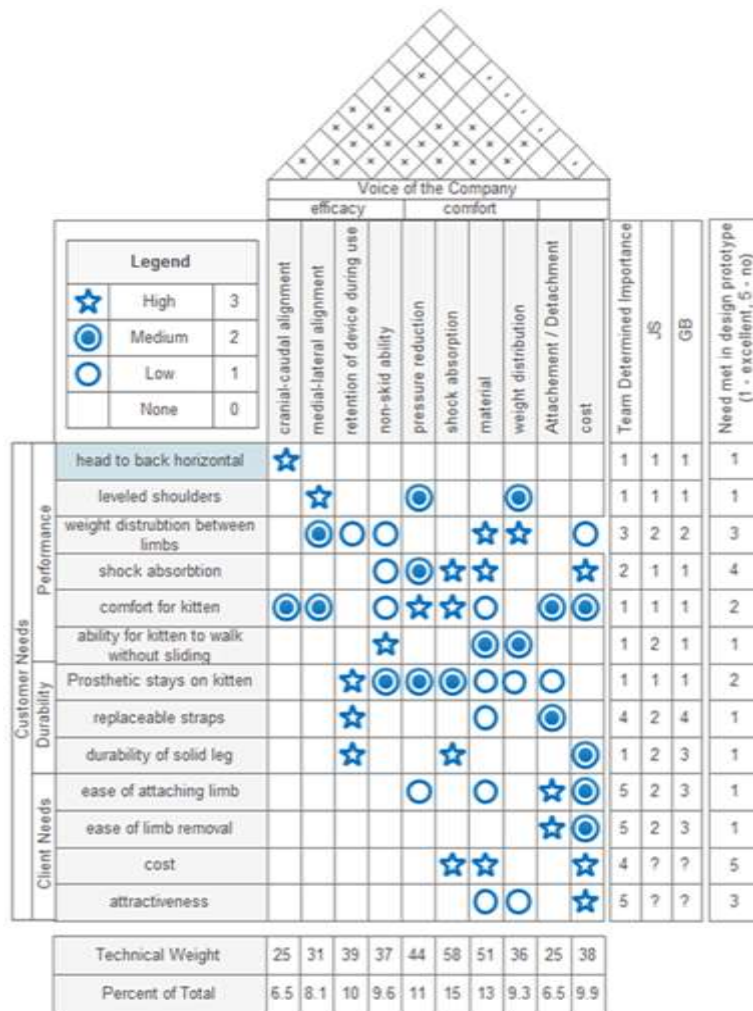
FIGURE 43- Results Of QFD.

prioritized during the development of the device design.

4.3 Device Development

4.3.1 Residual Limb Model

Measurements were taken of the subject's residual limbs and recorded (Table II). Using this information, the residual limb 3D models developed during the prior work were modified to reflect these measurements (Figure 44).

RESIDUAL LIMB MEASUREMENTS

Distance from Left Distal End (in)	Circumference (in)		Distance from Distal End (in) Right	Circumference (in)
0.00	2.75		0.00	2.25
0.50	2.25		0.50	2.25
1.00	2.25		1.00	2.25
1.50	2.31		1.50	2.25
2.00	2.50		2.00	2.50
2.50	2.50		2.50	2.50
3.00	2.50		3.00	2.50

	Left Limb	Right Limb
Elbow to Distal End of Limb (in)	5.33	4.00
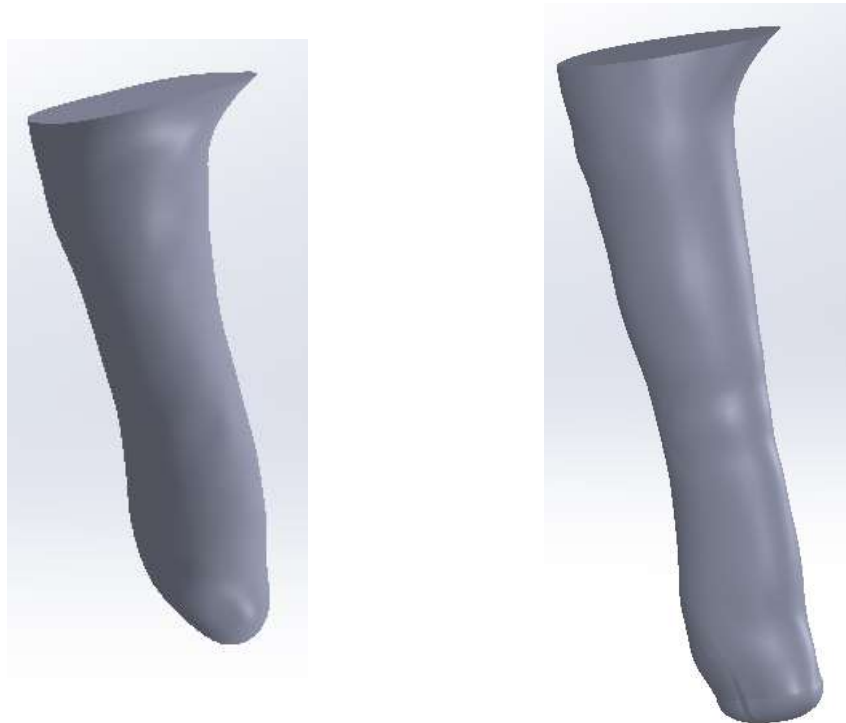
FIGURE 44- Left and Right Residual Limb 3-D CAD Models.

4.3.2 Prosthetic Socket Design

69

The prosthetic socket was designed using the modified positive residual limb model

described in section 4.3.1. (Figure 44) Since the amputation was performed without the
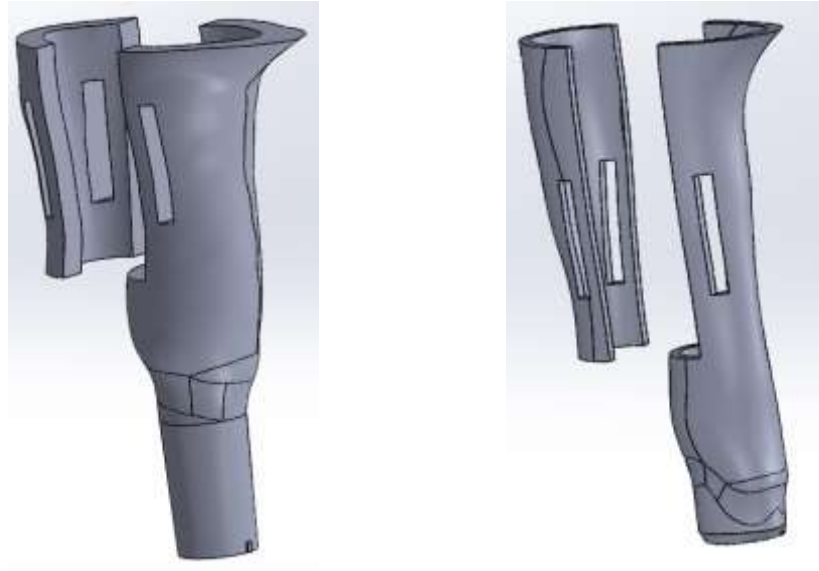
FIGURE 45- Left And Right Prosthetic Socket 3-D Cad Models. (not to scale)

intent of using a prosthetic device, standard means of individual prosthetic socket fit

cannot be used. As described in section 2.2, a variation of the ratcheting system was

utilized for securement of the prosthetic device to the individual. An image of the

prosthetic socket design can be seen in Figure 45. Due to the uneven levels of

amputation, a spacer is included in the left prosthetic socket to make sure that the height

from floor to shoulder is even on both sides. A prosthetic alignment pyramid was

incorporated into the proximal end of the prosthetic foot, so an adapter was designed into

the distal end of the prosthetic socket to allow for dynamic alignment of the prosthetic

foot.

4.3.3 Prosthetic Foot Development

The final design for the prosthetic foot was inspired by several prosthetic feet currently used for the more active human amputees, as well as running shoe technology.
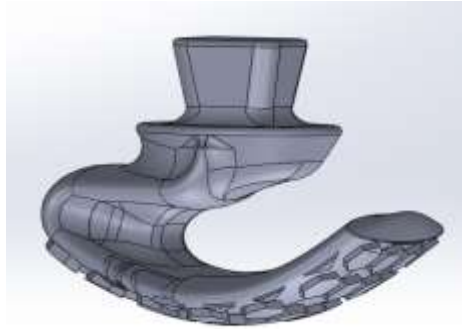
FIGURE 46- Prosthetic Foot 3-D CAD Model.

The curved areas of this design were bolstered to attain a reasonable lifespan. The tread on the distal face of the foot provided traction during ambulation. The curved face also shifts the users momentum forward following heel strike, and assists in the transition to toe-off. The tread and curvature on the bottom of the foot is modeled after running shoe technology. Creating a smooth transition from heel strike to toe-off is essential for emulating a normal gait. The factor of safety was calculated using SolidWorks (Dassault Systèmes, Waltham, Massachusetts) static loading simulation, and was determined to be 69.

4.4 Device Fabrication

The devices for this project were created using a 3D Systems (Rock Hill, SC)

CubePro printer (Figure 47)

FIGURE 47- Prosthetic Devices After 3D Printing.

The 3D printer software added support structures to support overhanging portions of the

device (Figure 48), and prints these structures and the actual device out simultaneously.

FIGURE 48- Prosthetic Devices After 3d Printing.

After the print job is complete, these support structures are removed. Once the supports

are removed, the residual structure was sanded smooth (Figure 49). In order to achieve a

FIGURE 49- Prosthetic Devices After Supports Are Removed, And Surfaces Sanded Down.

smooth and uniform finish, the designed parts placed into an acetone vapor bath for 3

hours (Figure 50). After three hours have passed, the designed parts are removed and

rinsed with water to remove any residual acetone vapor that still clings to the part.

FIGURE 50- Acetone Vapor Bath Setup.

Following the smoothing process, four holes are drilled and tapped on the prosthetic

socket to hold the set screws that interact with the alignment pyramid on the prosthetic

foot. Velcro and a silicone liner was installed for device retention purposes (Figure 51).

FIGURE 51- Prosthetic Devices After The Acetone Vapor Bath And Modifications.

Material cost and weight for the prosthetic devices and modifications came to $45 and

113 grams.

4.5 Device Testing

4.5.1 Computer Modeling

Computer simulation was performed on the beta prototype and final prototype 3D CAD designs of the prosthetic feet to determine the durability of the design when loads are applied in various locations. A static analysis and fatigue analysis were applied to each model, with loading conditions that emulate the heel strike, stance, and toe-off phase of a gait cycle.

4.5.1.1 Static Analysis
4.5.1.1.1 Beta Prototype Design

4.5.1.1.1.1 Heel Strike

Computer simulation for the heel strike phase of a gait cycle was conducted on the beta prototype design. The max stress in this simulation was $1.836e^6 \frac{N}{m^2}$. The maximum displacement was $1.418e^{-1}$mm. The maximum strain was $7.0e^{-4}$. The Factor of Safety was 127. Graphical representation of these values can be seen in Figure 52. The areas associated with max stress, strain, and factor of safety are located in the inner curve of the prosthetic foot, with the maximum displacement located in the toe of the prosthetic foot.

FIGURE 52- Heel Strike Static Analysis Of Beta Prototype. Max Stress (A), Strain (B), Displacement (C) And Factor Of Safety (D).

4.5.1.1.1.2 Stance Phase

Computer simulation for the stance phase of a gait cycle was conducted on the beta prototype design. The max stress in this simulation was $3.413e^6 \frac{N}{m^2}$. The maximum displacement was $4.351e^{-1}$mm. The maximum strain was $1.286e^{-3}$. The Factor of Safety was 68. Graphical representation of these values can be seen below in Figure 53. The areas associated with max stress, strain, and factor of safety are located in the inner curve of the prosthetic foot, with the maximum displacement located in the toe of the prosthetic foot.

FIGURE 53- Stance Phase Static Analysis Of Beta Prototype. Max Stress (A), Strain (B), Displacement (C) And Factor Of Safety (D).

4.5.1.1.1.3 Toe-Off

Computer simulation for the toe-off phase of a gait cycle was conducted on the beta prototype design. The max stress in this simulation was $4.41e^6\frac{N}{m^2}$. The maximum displacement was $6.479e^{-1}$mm. The maximum strain was $1.7e^{-3}$. The Factor of Safety was 531. Graphical representation of these values can be seen below in Figure 54. The areas associated with max stress, strain, and factor of safety are located in the midfoot area of the prosthetic foot, with the maximum displacement located in the toe of the prosthetic foot.
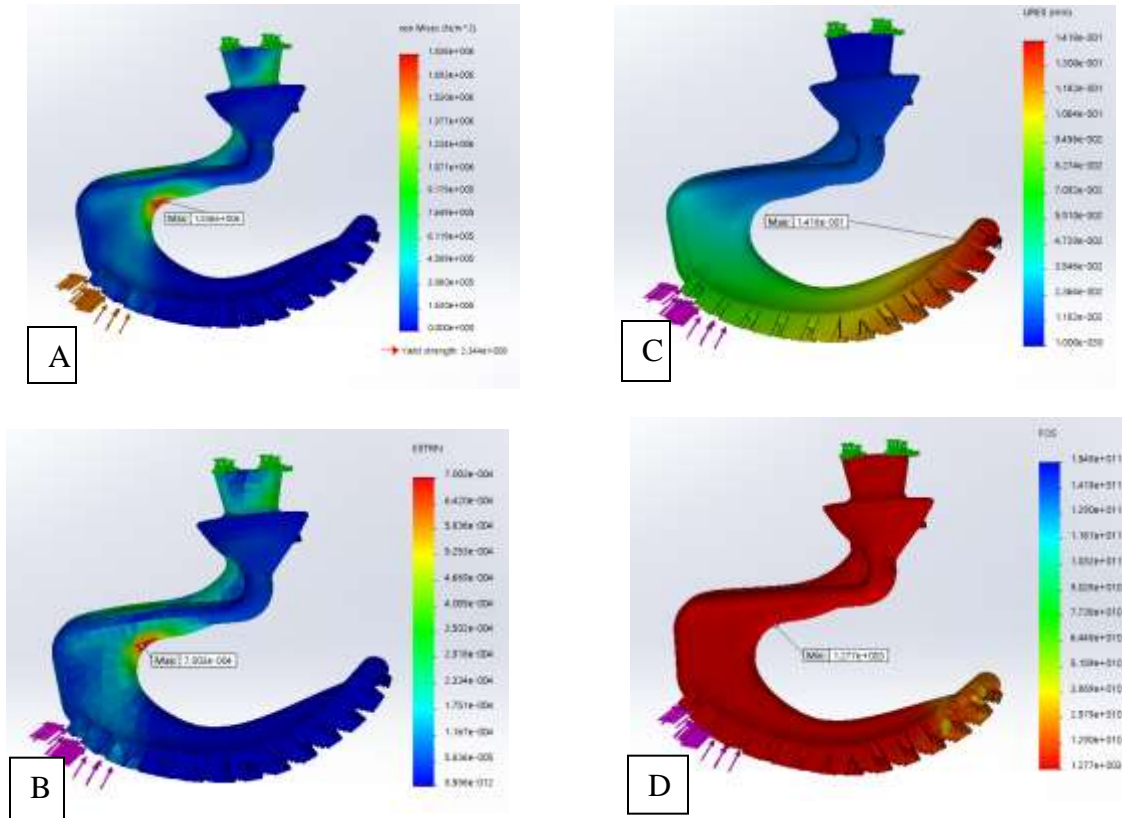
FIGURE 54- Toe-Off Phase Static Analysis Of Beta Prototype. Max Stress
(A), Strain (B), Displacement (C) And Factor Of Safety (D).

4.5.1.1.2 Final Prototype Design

4.5.1.1.2.1 Heel Strike

Computer simulation for the heel strike phase of a gait cycle was conducted on the final design. The max stress in this simulation was $1.272e^6 \frac{N}{m^2}$. The maximum displacement was $9.876e^{-3}$mm. The maximum strain was $3.97e^{-4}$. The Factor of Safety was 184. Graphical representation of these values can be seen below in Figure 55. The areas associated with max stress, strain, and factor of safety are located on the base of the alignment pyramid, with the maximum displacement located on the heel of the prosthetic foot.

FIGURE 55- Heel Strike Phase Static Analysis Of Final Prototype. Max
Stress (A), Strain (B), Displacement (C) And Factor Of Safety (D).

4.5.1.1.2.2 Stance Phase

Computer simulation for the stance phase of a gait cycle was conducted on the final

design. The max stress in this simulation was $3.381e^6 \frac{N}{m^2}$. The maximum displacement

was $1.76e^{-1}$mm. The maximum strain was $1.24e^{-3}$. The Factor of Safety was 69.

Graphical representation of these values can be seen below in Figure 56. The areas

associated with max stress, strain, and factor of safety are located on the base of the

alignment pyramid, with the maximum displacement located on the heel of the prosthetic
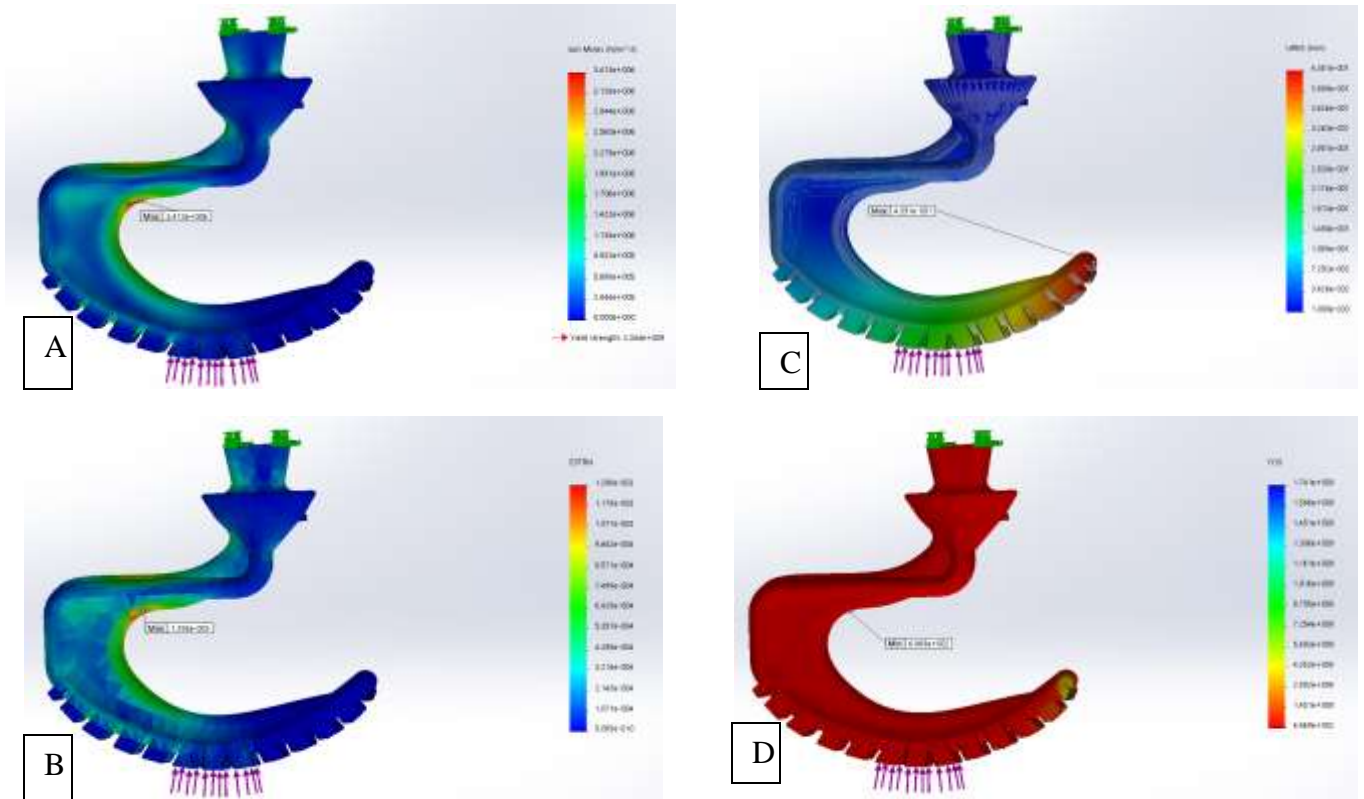
foot.
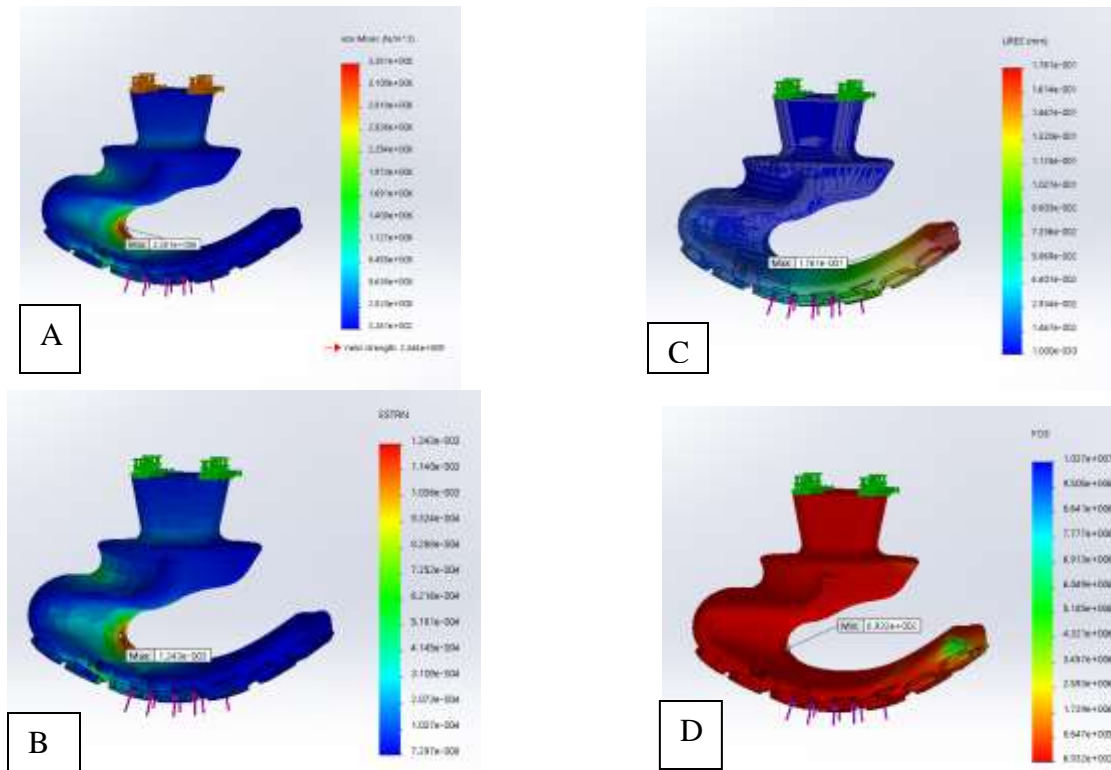
FIGURE 56- Stance Phase Static Analysis Of Final Prototype. Max Stress
(A), Strain (B), Displacement (C) And Factor Of Safety (D).

4.5.1.1.2.3 Toe-Off

Computer simulation for the toe-off phase of a gait cycle was conducted on the final

design. The max stress in this simulation was $9.506e^6 \frac{N}{m^2}$. The maximum displacement

was $5.843e^{-1}$mm. The maximum strain was $3.109e^{-3}$. The Factor of Safety was $1.442\ e^6$.

Graphical representation of these values can be seen below in Figure 57. The areas

associated with max stress, strain, and factor of safety are located on the inner curve of

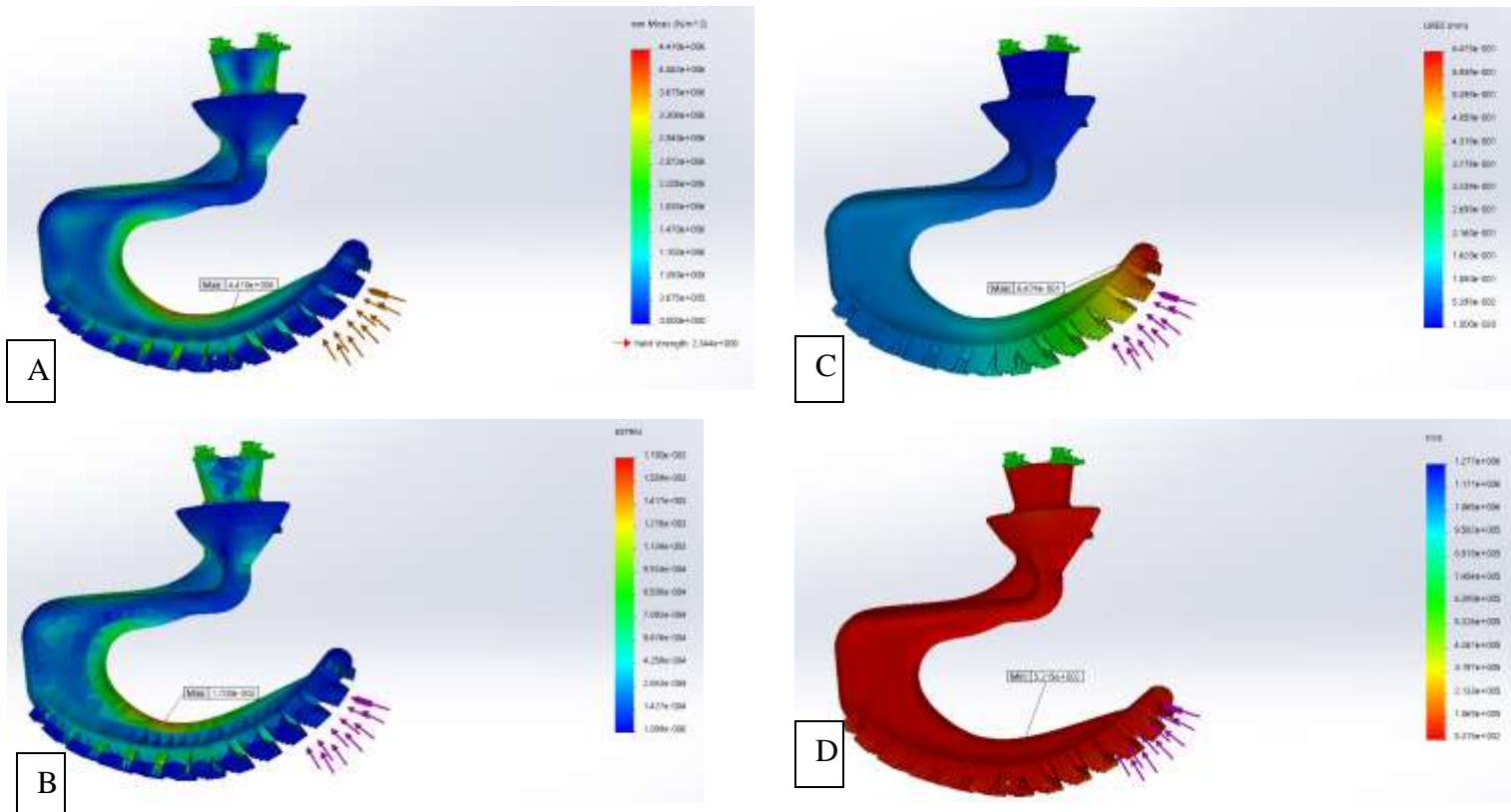the prosthetic foot, with the maximum displacement located on the toe of the prosthetic
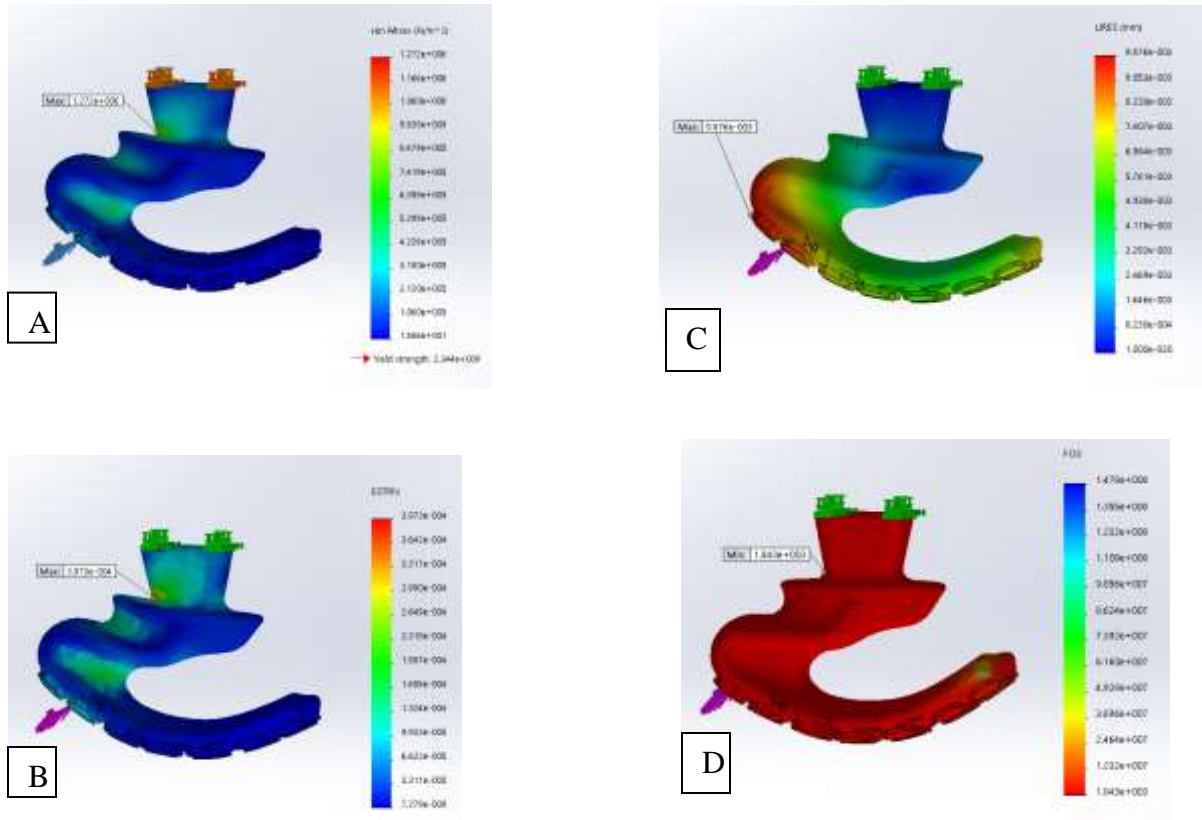
foot.
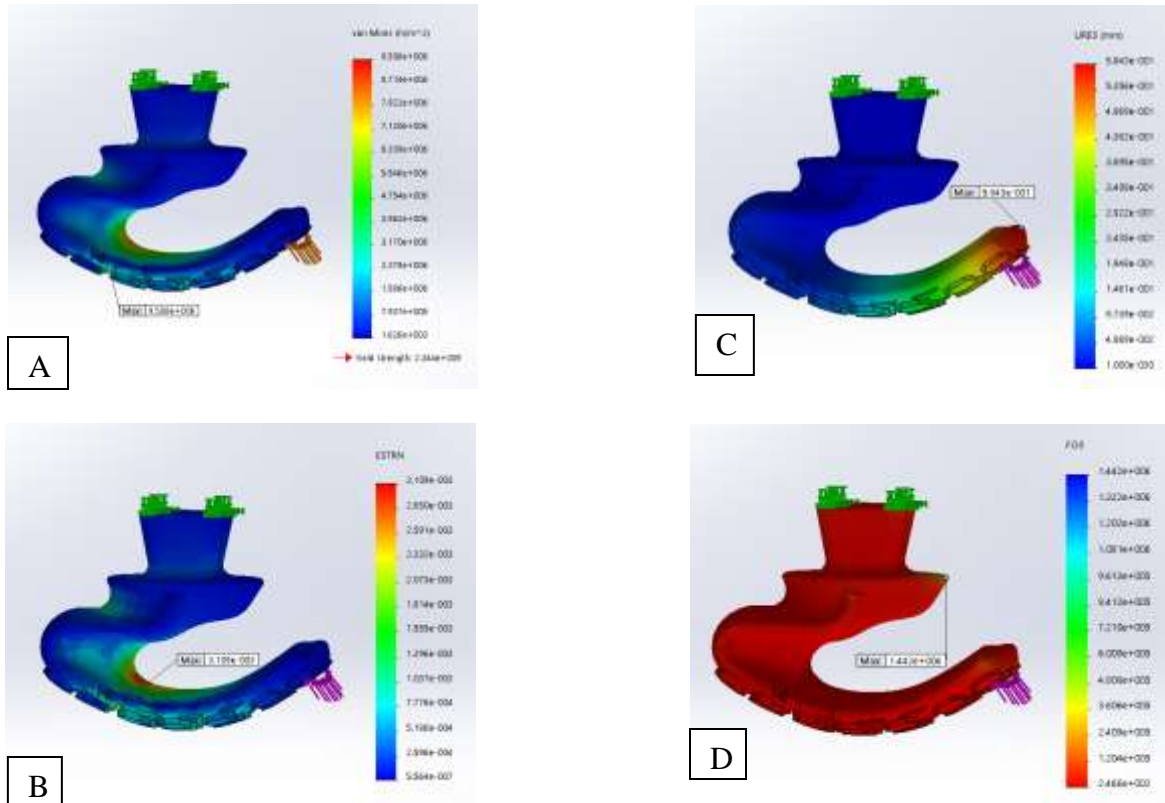
FIGURE 57- Toe-Off Phase Static Analysis Of Final Prototype. Max
Stress (A), Strain (B), Displacement (C) And Factor Of Safety (D) Are Shown.

4.5.1.2 Fatigue Analysis

4.5.1.2.1 Beta Prototype Design

4.5.1.2.1.1 Heel Strike

The beta prototype design was fatigue tested with the same constraints and loading areas as the static test for heel strike, with the only difference being the magnitude of the ground reaction force. In the fatigue test, the force applied to the prosthetic foot was 6 N (Demes 1994). The loading condition was 100 Hz zero based, meaning 6 N was loaded, unloaded to 0N, and loaded again. This analysis was performed until failure was reached. In this scenario, the fatigue life was predicted to be $1.001e^6$ cycles. A graphical representation can be seen below in Figure 58.
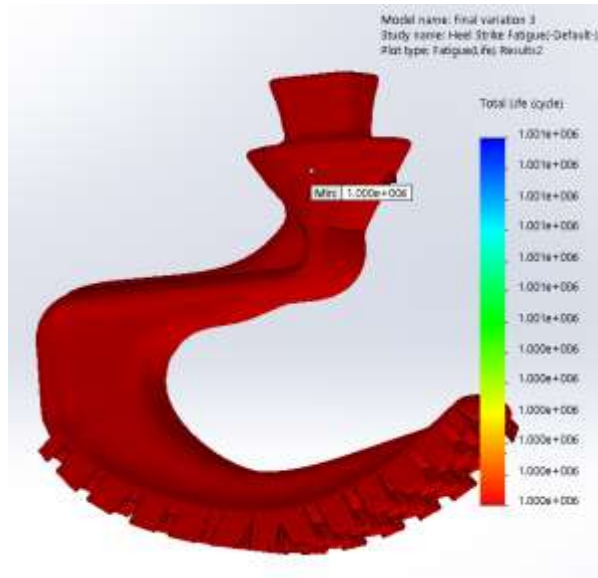
FIGURE 58- Heel Strike Phase Fatigue Analysis Of Beta Prototype.

4.5.1.2.1.2 Stance Phase

The beta design was fatigue tested with the same constraints and loading areas as the static test for the stance phase, with the only difference being the magnitude of the ground reaction force. This analysis proceeded until failure was reached. In this scenario, fatigue life was predicted to be $3.162e^5$ cycles. A graphical representation can be seen below in Figure 59.

FIGURE 59- Stance Phase Fatigue Analysis Of Beta Prototype.

4.5.1.2.1.3 Toe-Off

The beta design was fatigue tested with the same constraints and loading areas as the static test for the toe-off phase, with the only difference being the magnitude of the ground reaction force. In this scenario, the fatigue life was predicted to be $1.001e^6$ cycles. A graphical representation can be seen below in Figure 60.

FIGURE 60- Stance Phase Fatigue Analysis Of Beta Prototype.

4.5.1.2.2 Final Prototype Design

4.5.1.2.2.1 Heel Strike

The final design was fatigue tested with the same constraints and loading areas as the static test for the heel strike phase, with the only difference being the magnitude of the ground reaction force. In the fatigue test, the force that is applied to the prosthetic foot is 6 N. (Demes 1994) The loading condition was 100 Hz zero based, and proceeded until failure was reached. In this situation, the fatigue life was predicted to be $1.001e^6$ cycles. A graphical representation can be seen below in Figure 61.

FIGURE 61- Heel Strike Phase Fatigue Analysis Of Final Prototype.

4.5.1.2.2.2 Stance Phase

The final design was fatigue tested with the same constraints and loading areas as the static test for the stance phase, with the only difference being the magnitude of the ground reaction force. In this situation, the fatigue life was predicted to be $3.162e^5$ cycles. A graphical representation can be seen below in Figure 62.
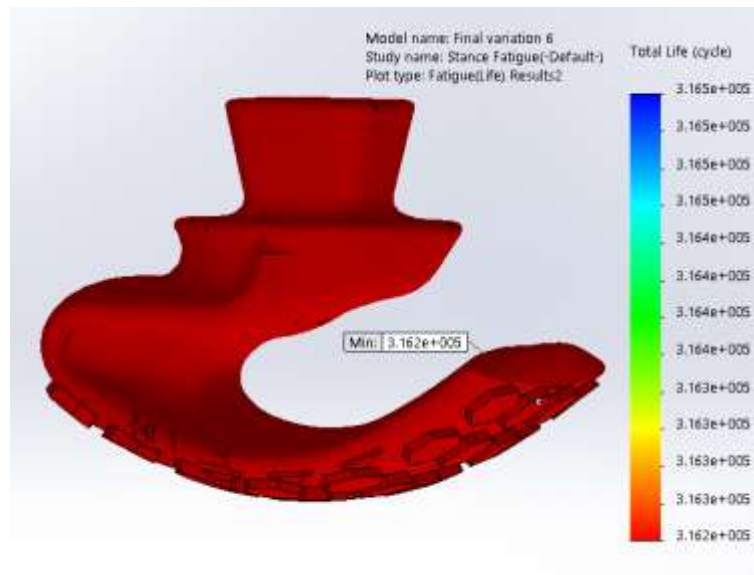
FIGURE 62- Stance Phase Fatigue Analysis Of Final Prototype.

4.5.1.2.2.3 Toe-Off

The final design was fatigue tested with the same constraints and loading areas as the static test for the toe-off phase, with the only difference being the magnitude of the ground reaction force. In this situation, the fatigue life was predicted to be $1.001e^{6}$ cycles. A graphical representation can be seen below in Figure 63.
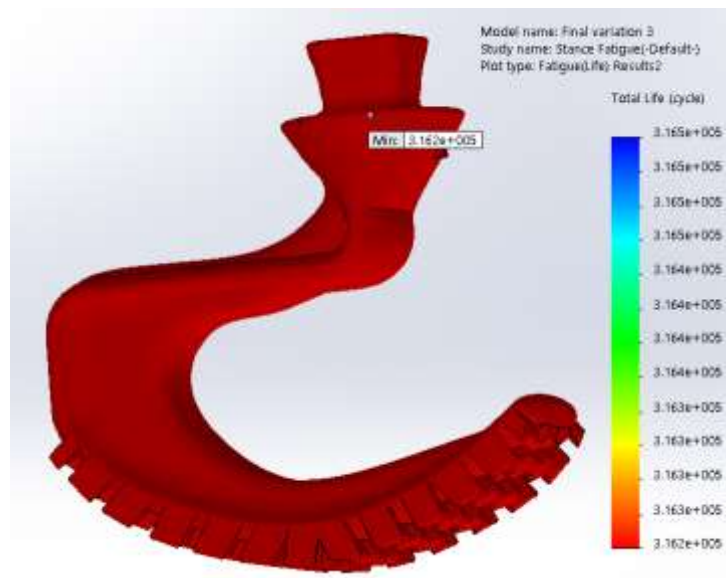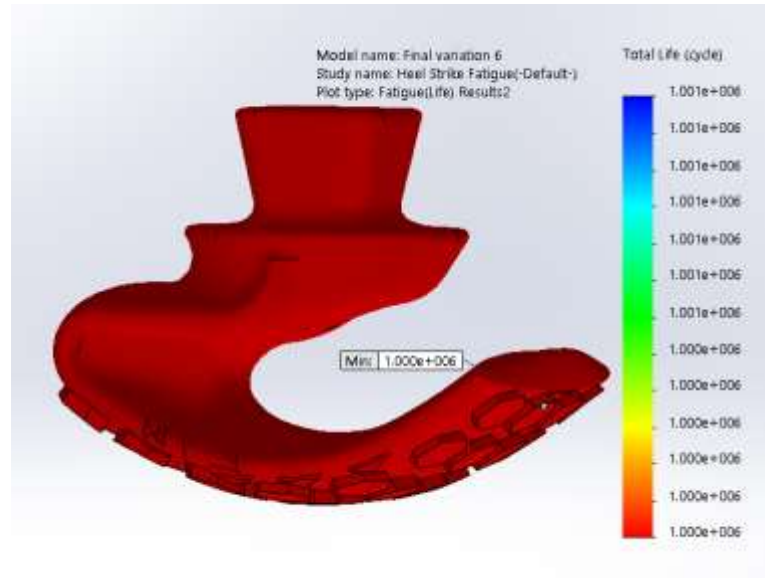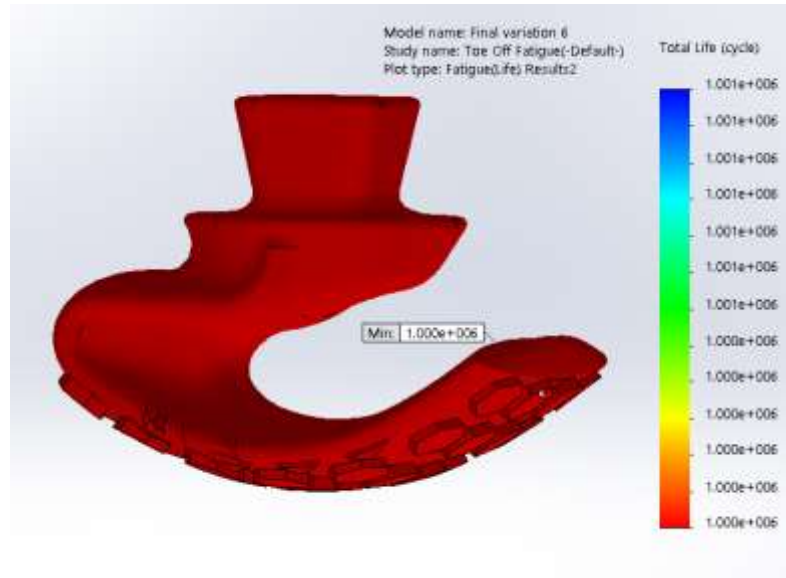

FIGURE 63- Toe-Off Phase Fatigue Analysis Of Final Prototype.

4.5.2 Mechanical Testing

The prosthetic foot was anchored to the mechanical testing machine using a stationary vice on the alignment pyramid, and force was applied to the mid-stance portion of the foot (Figure 65). A second vice, holding the aluminum block, applying the vertical force was attached to the mechanical press with a loose fitting pin. This resulted in minor vibration of the mobile portion of the mechanical press during testing. An overview of the system and the pin can be seen in Figure 64 below.
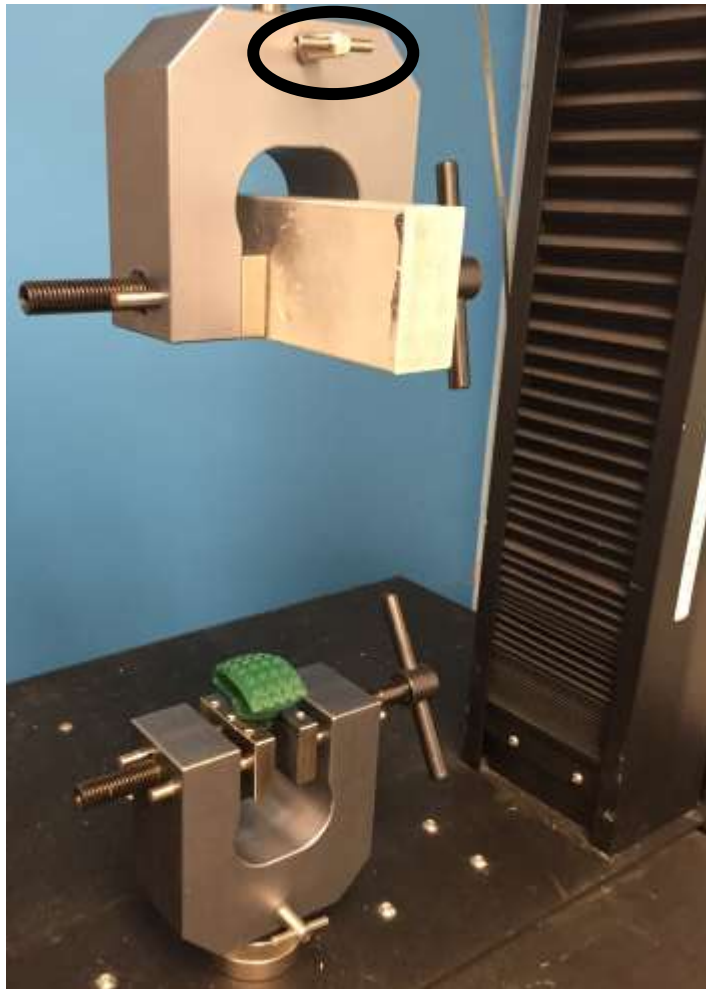
FIGURE 64- Overview Of Testing Setup. Loose Fitting Pin Is Circled In The Top Of The Image.

FIGURE 65- Mechanical Stress Testing Of The Prosthetic Foot.

The force-deformation from the fatigue test can be seen in Figure 66 below.

Although the software was set to a maximum of 25 N, initial testing resulted in loading
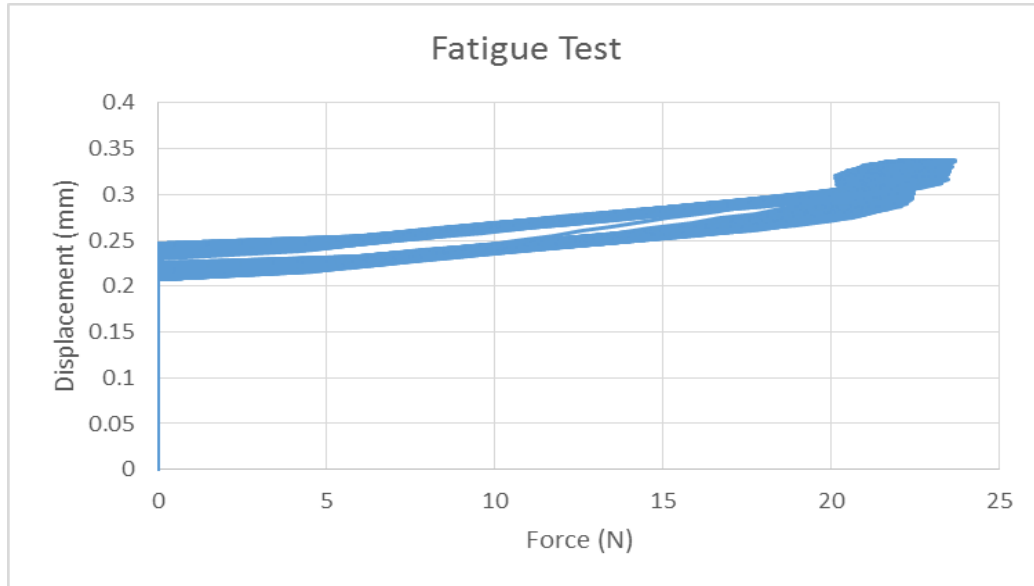
FIGURE 66- Deformation Curve Of The 25 N Fatigue Test.

forces to exceed 100N. To address this, a displacement limit was utilized in place of the

maximum force limit. This resulted in maximum forces around 25 N to be applied.

These forces were applied 50 times per test. The beginning of the force-deformation

curve indicates displacement increased with little to no increase in force. This test was

repeated five times, and all resulting deformation curves followed the same path.

Data from the fatigue test of 10,000 cycles can be seen in Figure 67. This test ran

for 10,000 cycles at 1 Hz due to machine limitations. The fatigue test concluded with no

evidence of wear visible on the prosthetic foot. During the fatigue test, the forces being
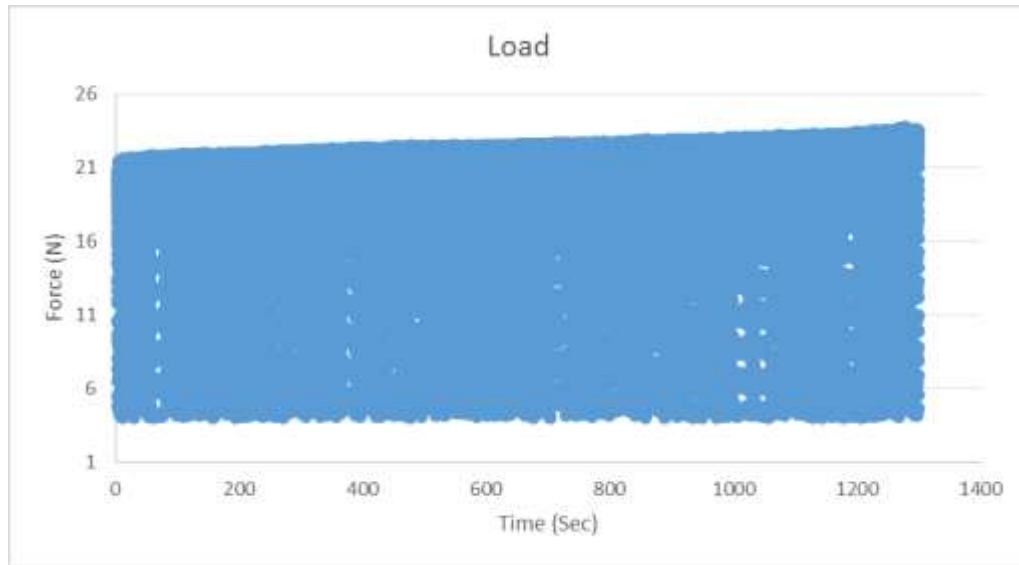
FIGURE 67- Force-Deformation Curve For Fatigue Test.

applied increased over time. This increase in applied force indicates a drift in the starting

position of the mechanical press. An example of this can be seen in Figure 63.

Since no visible sign of wear was present on the prosthetic foot, it was decided that a

loading until failure scenario should be performed to determine the maximum force the

prosthetic foot can withstand before failing. The ultimate failure of the prosthetic foot

occurred at approximately 3000 N which led to 5.4 mm of displacement A fracture

occurred when the toe region of the foot was bent in a manner that resulted in contact

with the vice securing the device (Figure 68). This induced a torque on the foot, and

FIGURE 68- Ultimate Failure Of The Prosthetic Device.

fractured the device on the caudal portion of the most distal aspect of the prosthetic foot.

This location does not match the simulated area of highest stress because the computer
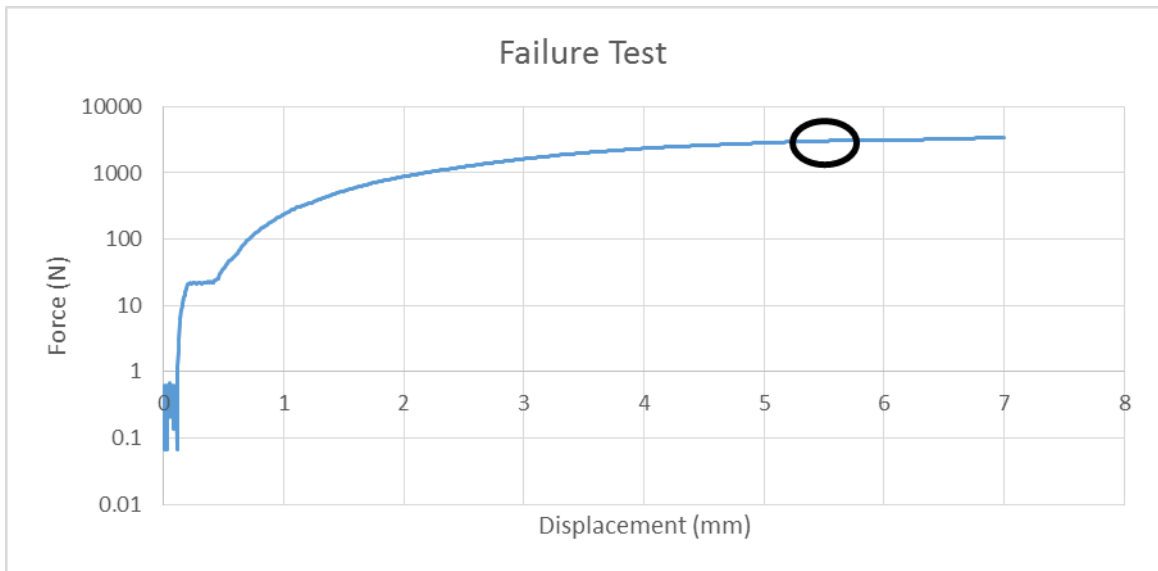
FIGURE 69- Force-Deformation Curve Of The Failure Test. Point Of Ultimate Failure
Circled.

simulation did have this induced torque in its analysis. The foot withstood 3000 N prior

to the failure mechanism described. Force-Deformation history was recorded during

failure testing in Figure 69. The curve goes beyond the point of fracture (5.4 mm of

displacement).

4.5.3 Evaluation of Prosthetic Fit and Usability

The acclimation period for the subject to become accustomed to using the prosthetic took longer than anticipated. The initial fittings caused subject confusion and anxiety, and she would attempt to get away from the researchers performing the fitting. Following the initial fitting, the goal was to place the subject in a weight bearing position while using the prosthetics. This allowed the subject to exhibit a more natural overall height. The visits with the companion animal subject were kept relatively short, approximately 40 minutes in duration, so as not to induce fear or stress in association with the researchers or the prosthetic devices. After three visits comprised of maintaining the subject in a weight bearing stance, initial walking steps were taken. These steps were awkward and clumsy, but were interpreted as the animal becoming accustomed to her new prosthetic devices, and beginning to explore the potential these devices offered. Several more visits followed after the initial steps were taken, and the animal's confidence in using the prosthetic devices increased with every visit. To further test the capability of the prosthetic feet, the cat was able to jump from a counter top height to the floor, with the prosthetic devices remaining attached and intact. Similar to the use of human prosthetic devices, the fit of the prosthetic sockets needed constant adjustment. Various durometers and thicknesses of padding were implemented to increase comfort and retention of the device during use. The initial steps using the prosthetic devices suggested that the subject was adapting to the use of these devices, and using 3D printed prosthetic devices for companion animals is a feasible endeavor. However, in the final visits with the companion animal, the subject learned how to remove the prosthetic devices and refused to cooperate with the rehabilitation process.

4.6 Preliminary Gait Analysis

4.6.1 Marker Set

Due to the lack of subject willingness, not all planned markers were able to be
implemented (Figure 70). An updated list of markers that were used is shown in Table
III.

FIGURE 70- Reflective Marker Placement.

TABLE III:

POSITION OF REFLECTIVE MARKERS USED DURING GAIT ASSESSMENT.

A: Distal Forelimb	F: L1 Vertebrae
B: Elbow Joint	G: Ischium
C: Shoulder Joint	H: Stifle Joint
D: C1 Vertebrae	I: Pelvic Limb Ankle
E: T1 Vertebrae	J: Pelvic Limb Paw

4.6.2 Data Collection

The owner of the feline subject trained the cat to walk in a straight line parallel to a
white backdrop by using treats for enticement. This setup was incorporated into the gait
analysis volume, and replicated once reflective markers were adhered to the cat.
Cameras were positioned to provide the subject a wider lane to walk and increasing the

likelihood of capturing gait trials with both cameras. Although a number of trials were performed, in most trials the cat failed to walk within the designated area, cutting several markers out of the field of view. Two trials were viable for the right side, while six trials were viable for the left. The average speed at which the companion animal ambulated through the designated capture area was 50 cm/sec.

4.6.3 Non-Prosthetic Gait Interpretation and Analysis

Tarsus angles ranged from 122-7° for the left and 177-43° for the right (Figure 71).

FIGURE 71- Tarsus Joint Angles During Gait Cycle and Reference Image. Grey Shade Indicates Swing Phase.

The peak right tarsus angle is substantially higher (177°) than the peak left tarsus angle (122°) with a standard deviation of 15°. The swing phase of the gait cycle (shaded grey) was initiated around 40% of the cycle in the right limb, whereas the swing phase was initiated much earlier, around 30% of the gait cycle in the left limb.

Stifle angles ranged from 109-52° for the left and 145-67° for the right (Figure 72).

The peak angles of this joint for the left stifle joint is 109° with a standard deviation of
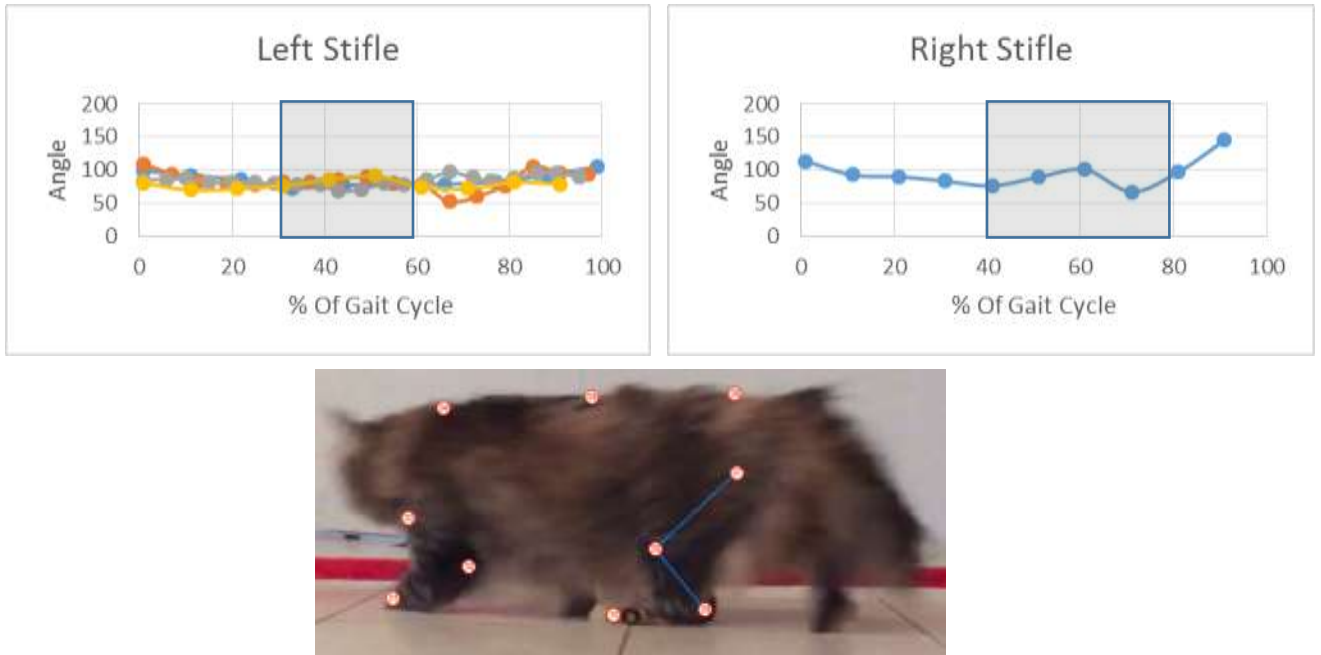
FIGURE 72- Stifle Joint Angles During Gait Cycle and Reference Image. Grey Shade Indicates Swing Phase.

7°, with the peak joint angle in the right residual limb is 145°.

The endpoints of this angle are represented by the first lumbar vertebrae, and the

stifle joint with the angle centered on the greater trochanter. Hip joint angles and their
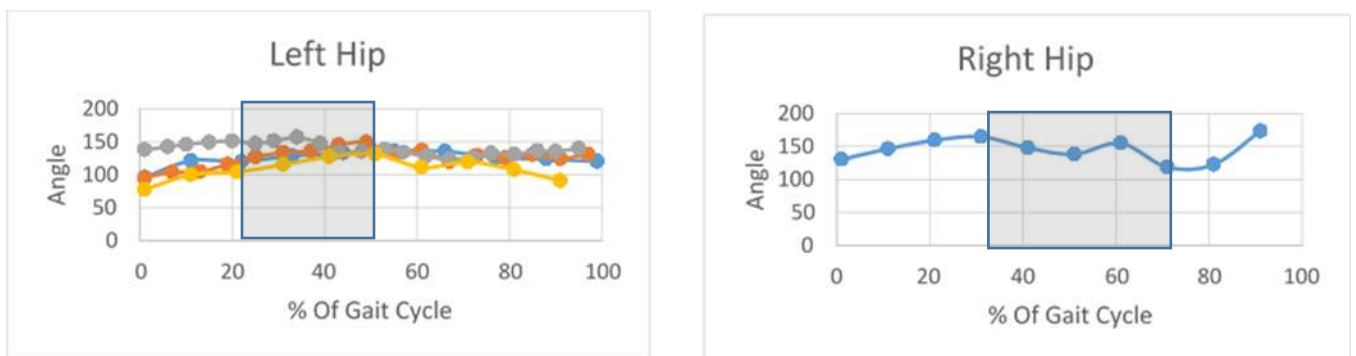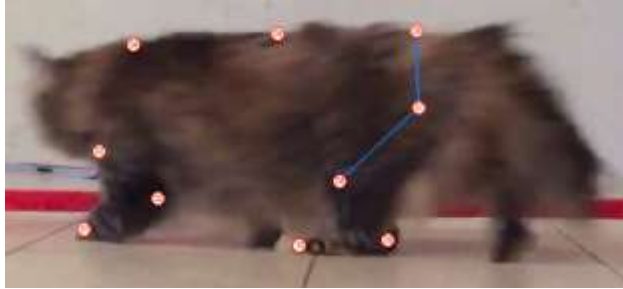
FIGURE 73- Hip Joint Angles During Gait Cycle. Grey Shade Indicates Swing Phase.

histories are similar in both scenarios. The peak joint angle for the left hip was to be

156° with a standard deviation of 10° and the peak joint angle for the right hip was 140°.

The spinal curvature at the first lumbar vertebrae is represented in Figure 74. This
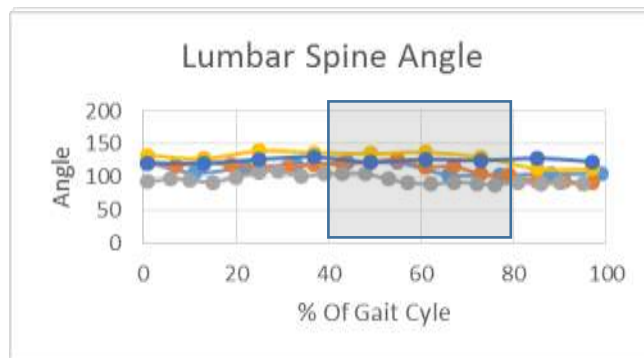
FIGURE 74- Lumbar Spine Angle Gait Data and Reference Image. Grey Shade Indicates Swing Phase.

data set establishes a baseline for the comparison between the final gait analysis with use

of the prosthetic devices.

Thoracic spine curvature was determined using markers positioned at the bony

prominences corresponding with the T1 vertebrae and Sacrum, centered at the L1

vertebrae (Figure 75). There was little difference between the angles captured by the two

cameras; thus the data was consolidated into one graph. Thoracic spine angles ranged
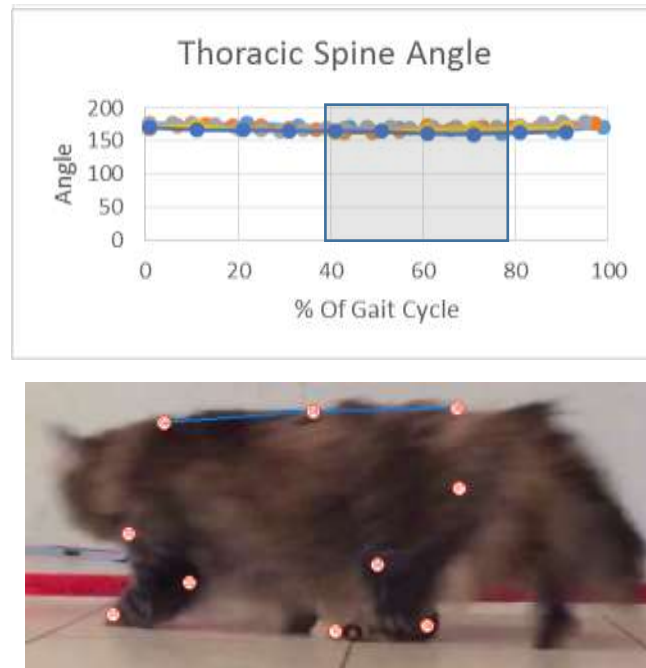
FIGURE 75- Thoracic Angle Gait Data and Reference Image. Grey Shade Indicates Swing Phase.

from 179-160° during the gait cycle.

Figure 76 depicts the shoulder joint angles found during the gait cycle.   When

comparing the left and right shoulder joint angles, some differences become apparent.

The peak joint angle for the left shoulder was found to be 158° with a standard deviation

of 6, and the peak right shoulder joint was 145° with a standard deviation of 16°. In
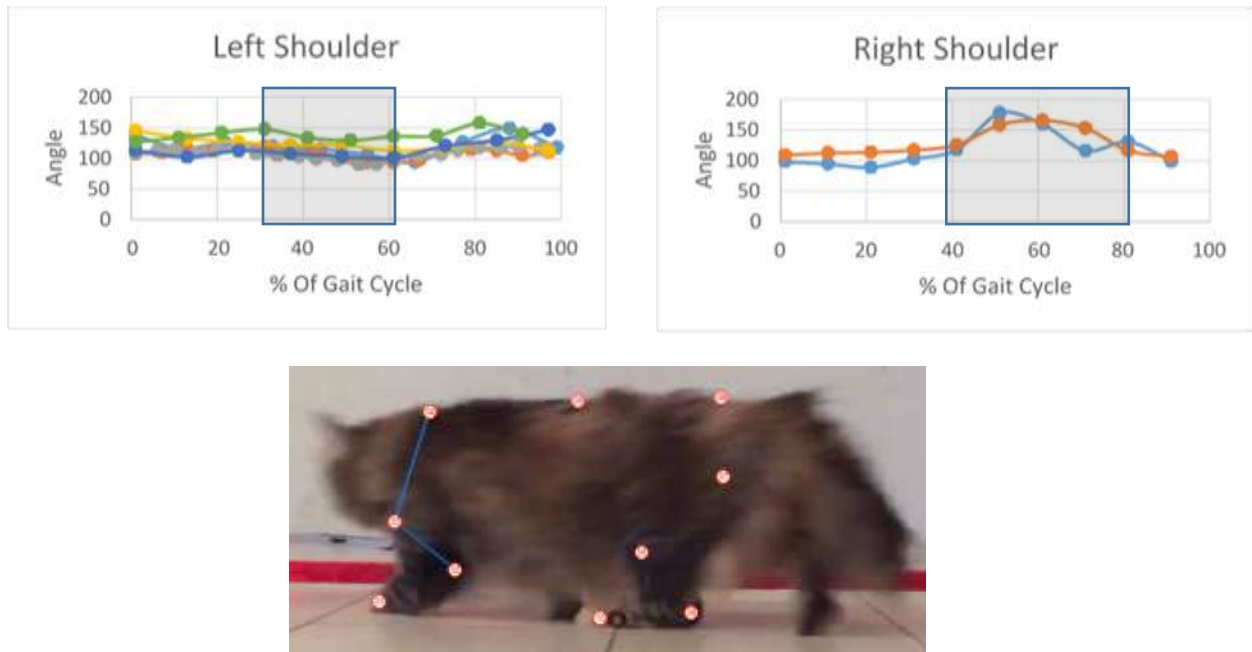
FIGURE 76- Shoulder Joint Angles During Gait Cycle and Reference Image. Grey Shade Indicates Swing Phase.

addition to differences in the magnitude of angle, differences in onset of swing phase were found for the left and right thoracic limb. Right thoracic limb swing phase was initialized at ~40% of a full gait cycle, while the swing phase was initialized at ~70% of a full gait cycle in the left limb.

The most cranial and proximal joint angle evaluated during this gait analysis is the elbow joint of the thoracic limbs. Differences were found between left and right elbow joint angles across the gait cycle. The peak joint angles for the shoulder of the left limb was 143° with a standard deviation of 5, and the peak value for the shoulder of the right limb was 177° with a standard deviation of 24° (Figure 77). Shoulder joint angle profiles were unique when comparing left and right. The onset of the swing and stance phases of

the right thoracic limb is shifted nearly 20% earlier when compared to the left thoracic

limb.
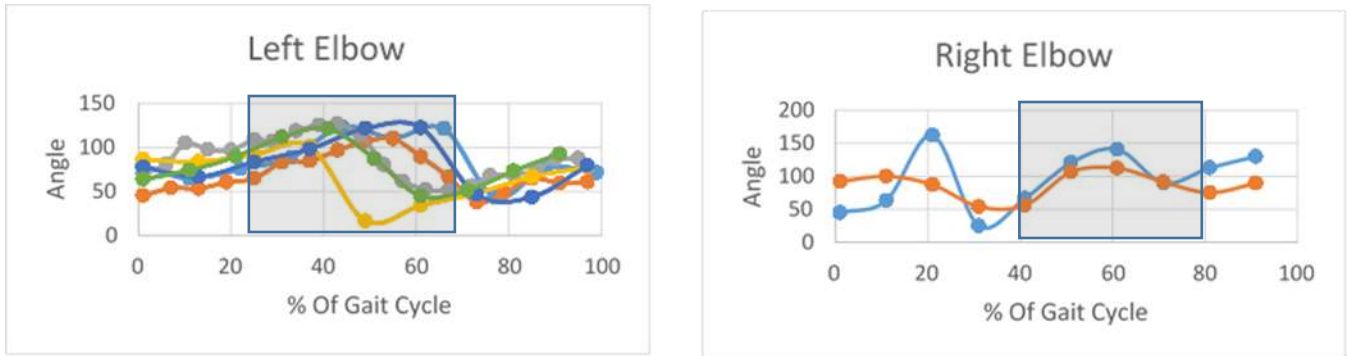
FIGURE 77- Elbow Joint Angles During Gait Cycle and Reference Image. Grey Shade Indicates Swing Phase.

4.6.4 Prosthetic Gait Analysis

Due to a change in filming location, only the left side was able to be captured for the

gait analysis with the prosthetic device.

Tarsus angles during use of the prosthetic devices ranged from 115-39° for the left

limb (Figure 78). The swing phase of the gait cycle was initiated around 20% of the
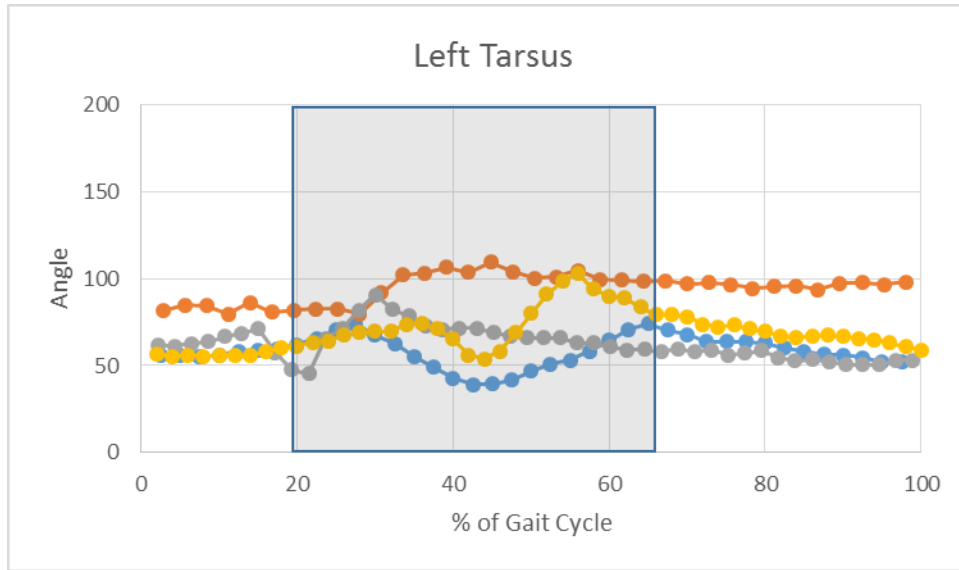
FIGURE 78- Tarsus Joint Angles During Use of The Prosthetic Devices. Grey Shade Indicates Swing Phase.

cycle and completed around 65% of the cycle. There is little change in angle during the

stance phase, as the angle of the ankle stays relatively close to 50° for three of the cycles.

The peak joint angle found in these instances is 115° with a standard deviation of 45°.

Stifle angles during use of the prosthetics ranged from 109-57° for the left limb (Figure 79). There is little change when comparing one gait cycle to the others. A
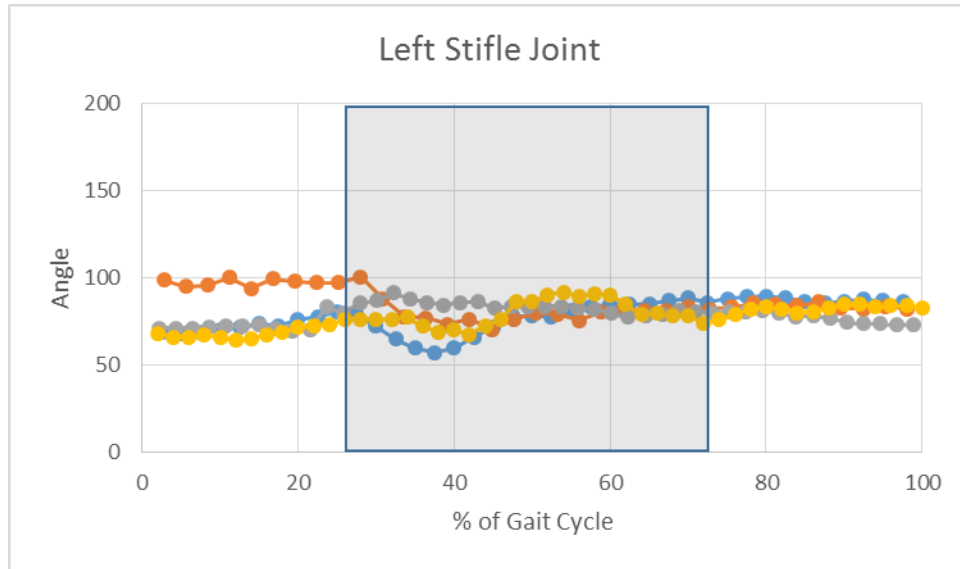
FIGURE 79- Stifle Joint Angle Gait Data Using The Prosthetic Devices. Grey Shade Indicates Swing Phase.

contraction of about 20° initiating at 25% of the gait cycle occurs in all four gait cycles. The joint remains flexed until 45% of the gait cycle when the joint angle returns to a steady state of around 75°. The peak angle seen in this joint is 100° with a standard deviation of 44°.

The data set presented in Figure 80 represents the angle found at the left hip. The endpoints of this angle are represented by the first lumbar vertebrae, and the stifle joint with the angle centered on the greater trochanter. The angles at the hip during the entire gait cycle fluctuate within a range of 10°, with a peak value of 167° and standard deviation of 59°. This indicates that the movement of the pelvic limbs is due to movement about the stifle joint, and not the hip since the angels of the hip hardly fluctuate.
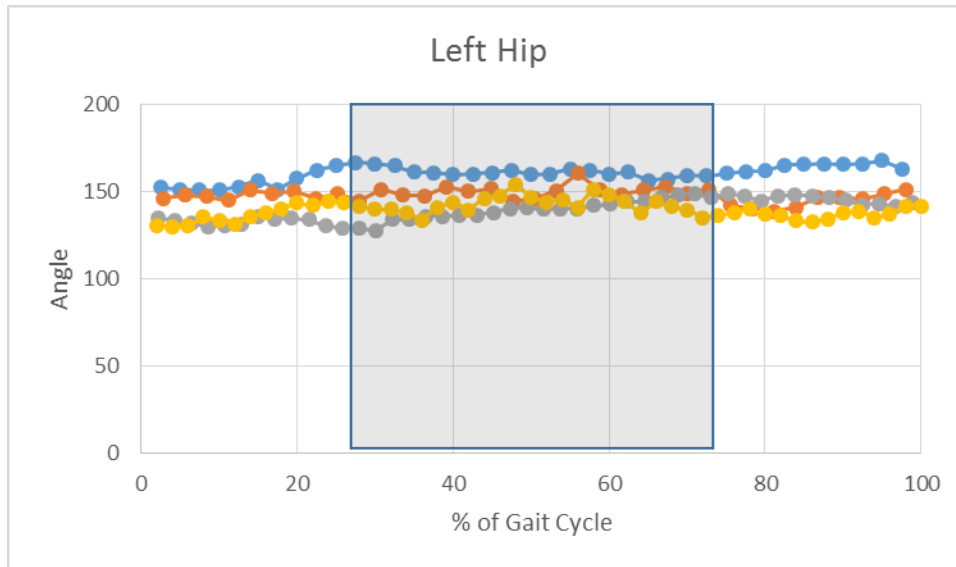
FIGURE 80- Hip Joint Angle Gait Data Using The Prosthetic Devices. Grey Shade Indicates Swing Phase.

The spinal curvature at the first lumbar vertebrae is represented in Figure 81. The

angles for the spinal curvature at the first lumbar vertebrae were created by using the first
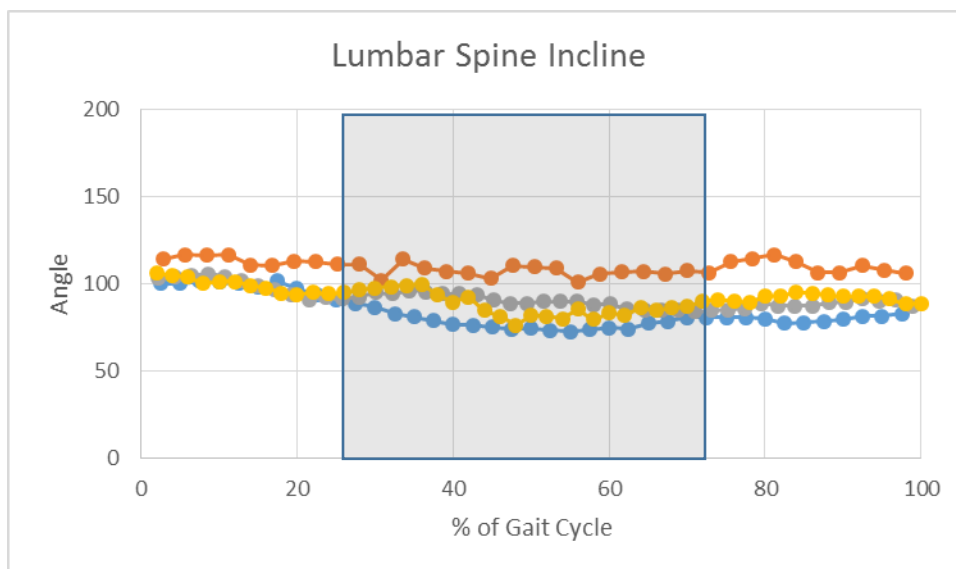
FIGURE 81- Lumbar Spine Angle Data Using The Prosthetic Devices. Grey Shade Indicates Swing Phase.

thoracic vertebrae and the ischium markers as endpoints of the angle centered on the first

lumbar vertebrae. The peak angle seen during the gait trials is 116° with a standard

deviation of 48°.

Thoracic spine curvature was determined using markers positioned at the bony

prominences corresponding with the T1 vertebrae and Sacrum, centered at the L1
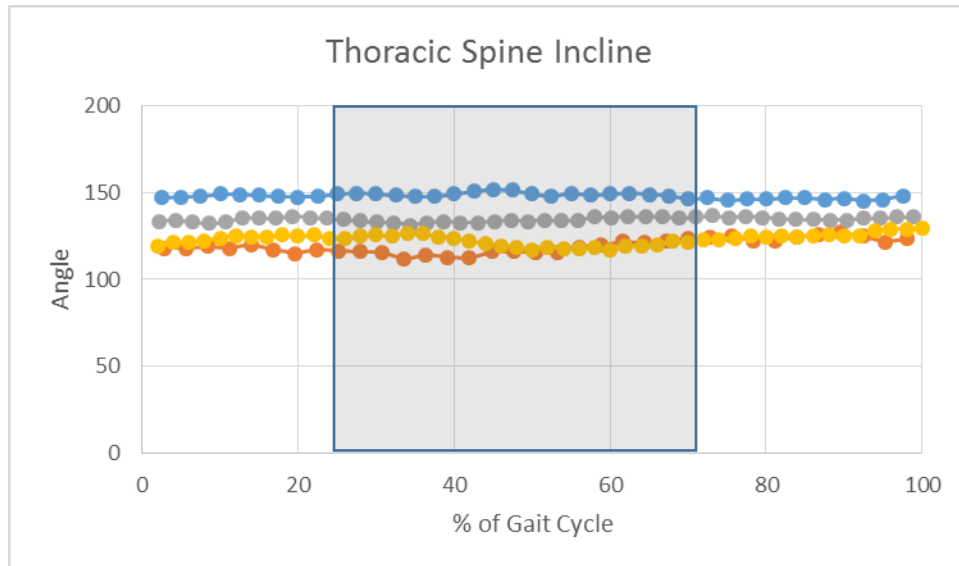
FIGURE 82- Thoracic Spine Angle Data Using The Prosthetic Devices. Grey Shade Indicates Swing Phase.

vertebrae (Figure 82). Thoracic spine angles ranged from 152- 111° during the gait cycle

with the prosthetic devices in use.
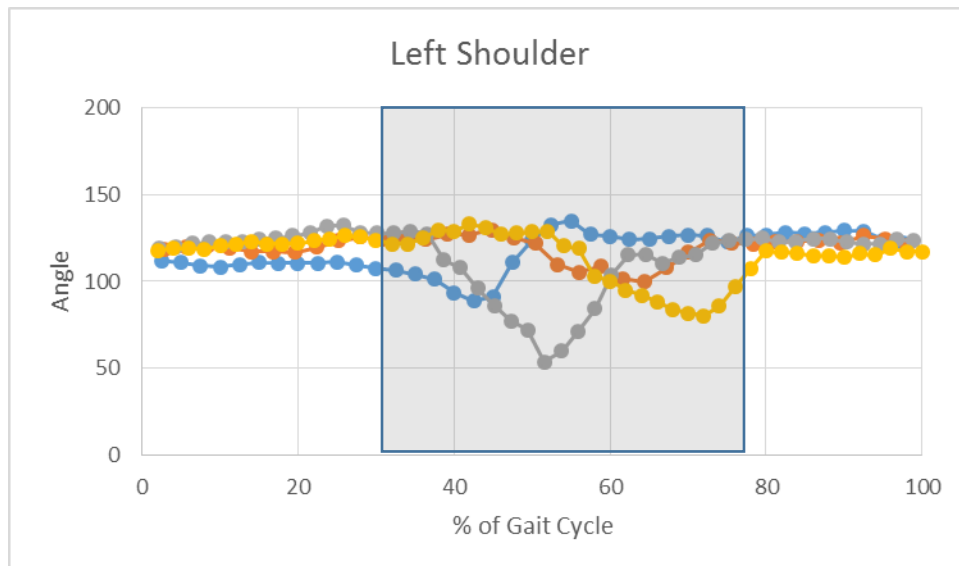
FIGURE 83- Shoulder Angle Data Using The Prosthetic Devices. Grey Shade Indicates Swing Phase.

Figure 83 depicts the angles found during the gait cycle of the shoulder joint in the

left limb of a feline subject. The shoulder joint in the thoracic limb was initialized at

roughly 30% of a full gait cycle. The peak values recorded at the shoulder are 134° with

a standard deviation of 49°.

The most cranial and proximal joint angle in question during this gait analysis is the

elbow joint of the left thoracic limb. This joint is the closest joint to the amputation site
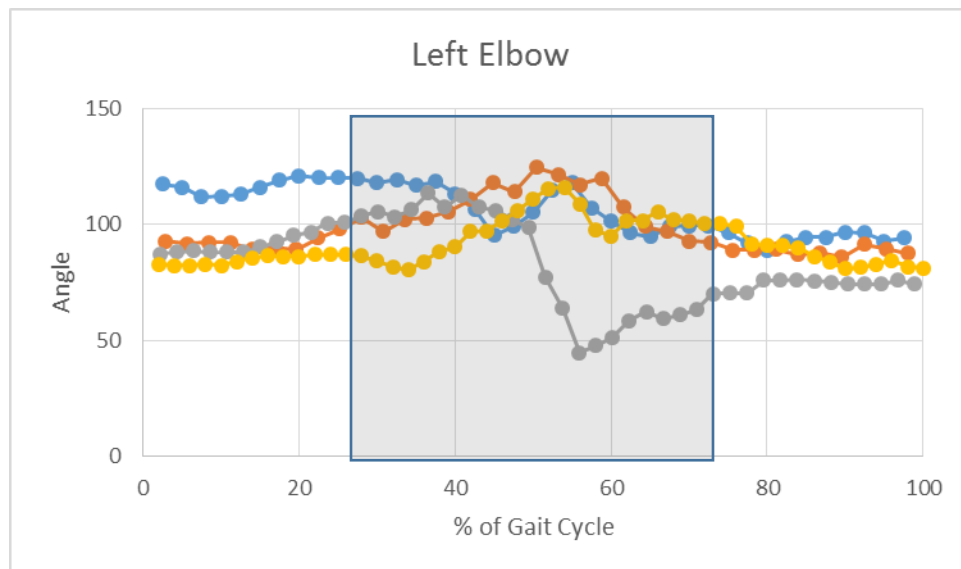
FIGURE 84- Elbow Angle Data Using The Prosthetic Devices. Grey Shade Indicates Swing Phase.

of the feline subject. Analysis of these graphs, seen in Figure 84, shows an interesting

gait pattern. The overall result of the gait cycle shows a gradual decline in joint angle,

with a peak value of 124° and standard deviation of 45°.

Discussion

5.1 Prosthetic Device Testing

The developed prosthetic device was subjected to a static mechanical test and performed to the designer's expectations by surviving the static test. The static test indicated that the prosthetic foot could withstand greater forces than the 25N, so a test to failure was performed. The test to failure increased confidence in the durability of the prosthetic foot given that the force required to achieve ultimate failure was over 3000 N. This high level of durability corresponds to the exceptionally high factor of safety built into the design of the prosthetic foot. A factor of safety of 69 was achieved after multiple design iterations. Having such a high factor of safety is an overdesign, which leads to increased weight and less deformation than what is desired. A factor of safety closer to, but not less than 4 would be comparable to industry standard for prosthetic devices. This lowered factor of safety will allow the prosthetic device to exhibit more energy absorption attributes and be lighter in weight. Factor of safety, as determined in SolidWorks, used solid ABS material properties in the calculation, which does not fully represent the material properties of printed ABS plastic. Printed and solid ABS vary in overall strength, with printed ABS plastic being weaker. The difference in strength comes from the voids found in printed ABS plastic, where solid ABS plastic is uniform throughout. The inherent weakness found in printed ABS plastic was the main reason for maintaining a higher factor of safety in the design.

The fatigue testing performed through computer simulation estimated that the life cycle of the prosthetic foot would be 316,200 cycles of loading and unloading of a 6 N vertical force that would occur during normal gait. Mechanical testing to evaluate fatigue was also performed. The mechanical testing machine used to perform the fatigue test

lacked the control necessary to accurately apply such a small force, so the maximum

force that occurs during a feline jumping from a height of 1 m (25N) was used. The

mechanical testing was also limited to the frequency at which the load could be applied.

The machine could not sense, register, and reverse the loading of the foot if the press was

moving faster than 1 Hz. This test was run for a full day (8 hours), and 10,000 cycles of

25N were achieved. The prosthetic foot showed no signs of yielding or fracturing post

fatigue testing. The success of this indicates that the prosthetic foot has the ability to

withstand daily use. The results from the static and dynamic fatigue testing performed on

the prosthetic devices indicate that prosthetic devices fabricated using additive

manufacturing are a viable option for use in companion animals. This is yet another

application for which additive manufacturing can be used (Gibson 2006).

The testing performed with the companion animal using the prosthetic devices was

challenging. The acclimation period was longer and more difficult than initially

anticipated. In order to have more control over the experiment, a smaller enclosed room

was used for donning, acclimation, and use of the prosthetic devices. For the first 2 visits

with the companion animal, the subject was reluctant to don the prosthetic devices.

These visits also consisted of physically placing the companion animal into a weight

bearing stance, and attempting to encourage the feline into taking steps using various

bating techniques. The companion animal would occasionally sit and attempt to retreat

away from the prosthetic devices dragging them on the floor, thereby indicating

reluctance to continue using the prosthetic devices. After the second visit, the companion

animal was much more accommodating. The first step with full weight bearing was

accomplished during the third visit. The amount of retreating from the prosthetic

devices was reduced as the companion animal became more accustomed to wearing the

prosthetic devices. During the fourth and fifth visits, the companion animal took a series

of steps, which were videotaped. The location of the prosthetic testing varied from the

location that the initial gait analysis, so the videos of pre- and post-prosthetic device use

were not performed under the same conditions. The change in location occurred to allow

the researchers more control of the environment. There was no furniture in this room for

the companion animal to hide under, which made working with the companion animal

easier. The videos containing the perpendicular view of the sagittal plane capturing the

left side of the body was used for analysis.

The results from the mechanical testing and patient use protocols were compared to

the five highest priorities determined from the QFD. These priorities include shock

absorption, device material, pressure reduction, retention of the device during use, and

cost. There was minimal shock absorption from the prosthetic foot as evidenced from the

mechanical testing, so a padded lining was implemented to aid in mitigate shock to the

residual limb during prosthetic contact with the ground. The device was created

fabricated using ABS plastic, which resulted in durable, lightweight, and cost effective

prosthetic devices. The devices weighed roughly 113 grams each, and cost $45 in

materials to make each prosthetic device. The pressure applied to the residual limb was

mitigated through the design of the prosthetic socket. The prosthetic socket was design

so that areas tolerant to pressure (soft tissue) would be loaded, and areas of intolerance

(boney prominences) would be relieved of pressure. The padded lining used on the

inside of the prosthetic socket also increased the retention of the device during use given

its friction properties. Even with the lining, the companion animal was able to actively

remove the prosthetic device. However, during ambulation the prosthetic devices

remained in place. A goal of the prosthetic development was to provide a low cost,

affordable option to owners. The material cost of each device was $45 and required

approximately 12 hours to print.

5.2 Gait Analysis

Gait data for healthy feline walking has been published describing elbow, carpus,

stifle, and tarsus joint kinematics. (Day 2006) Pre- and post-prosthetic use gait data was

compared to these published data.

During the pre-prosthetic device gait analysis, flexion of the elbow was initiated at

roughly 60% of the gait cycle. The gait data from this experiment shows the elbow

begins flexion at 60% of the gait cycle. The joint angles throughout the entire gait cycle

without the prosthetic devices are flexed an additional 30° (Figure 85). This is explained
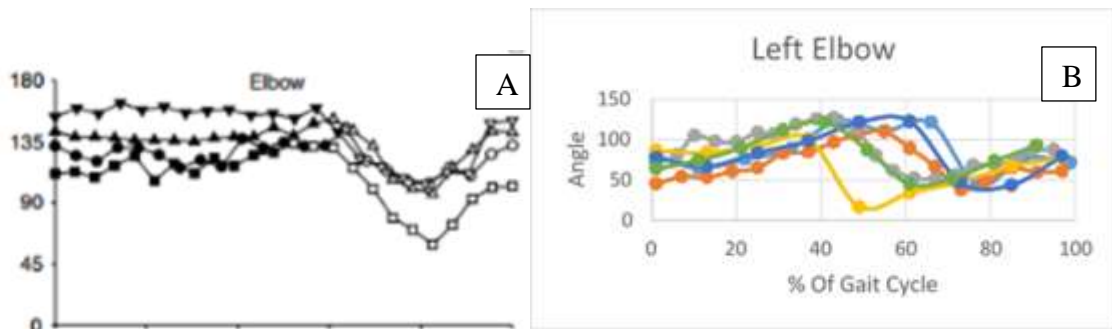
FIGURE 85- Elbow Joint Gait Data Comparison Between Pre-Prosthetic Gait Analysis (B) (n=1; 6 trials) And Day et al. (A).

due to the fact that the companion animal's shoulders are closer to the ground than a

healthy feline, thus flexing the elbows during the entire gait cycle.

The stifle joint kinematics captured during the gait analysis without use of the prosthetic devices follows a similar profile to the joint angle data described by Day et al.
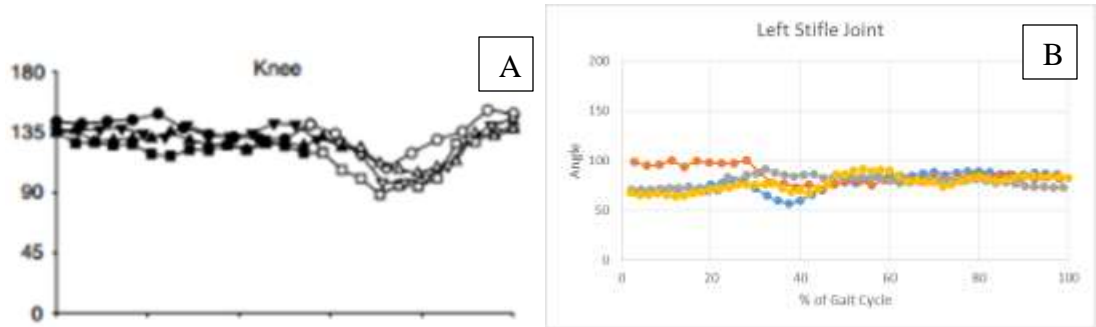
FIGURE 86- Stifle Joint Angles Comparison Between Pre-Prosthetic Gait Analysis (B) (n=1; 4 trials) And Day et al. (A)

The difference between these data sets is additional stifle joint flexion of ~30° throughout the entire gait cycle (Figure 86).   This flexion of the pelvic limb is attributed to the limb length discrepancy between the pelvic and thoracic limbs caused by the amputation.

The profile of the tarsus joint angles throughout the gait cycle without the use of prosthetic devices is similar to the profile of the joint angles documented by the Day et al. The initiation of flexion and extension occurred during the same percentage of the gait cycle-for our subject and felines evaluated by Day et al. The difference between the two gait profiles is the 30° flexion for our subject over the entire gait cycle.   This flexion
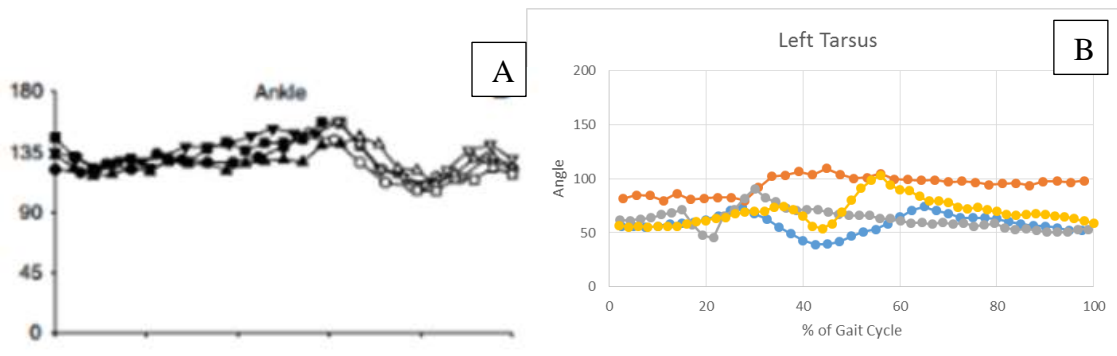

Figure 87 - Tarsus Joint Angles Comparison Between Pre-Prosthetic Gait Analysis (B) (n=1; 4 Trials) And Day et al. (A).

appears in every joint angle of the pre-prosthetic gait analysis to the joint angle data from

the Day et al. The consistency of this shift suggests that the amputations at the thoracic limbs are the cause. A decrease in the shoulder height associated with the amputation lowers the cervical spine, thoracic spine and shoulder height. To compensate for this adjusted shoulder height, the companion animal must also shorten the pelvic limbs, resulting in the extra 30° flexion and a crouched gait.

The joint angle data collected during the gait analysis with the prosthetic devices in use was compared to both the joint angle data provided by Day et al., and the joint angle data collected during the gait analysis without the use of the prosthetic devices. The elbow, stifle, and tarsus joint angles were compared, while the shoulder, thoracic spine angle, lumbar spine angle, and hip joint angles with and without the prostheses were compared.

The joint angles for the elbow during use of the prosthetic devices has a similar profile to the non-prosthetic kinematics, as well as the kinematics reported by Day et al. The 30° of extra flexion that occurred without the use of the prosthetic devices was not present in the gait when using the prosthetic devices. This increased flexion was due to the shortened thoracic limbs, but use of the prosthetic devices provides for a more normal gait, eliminating this 30° difference in flexion.

Shoulder joint angles remained consistent without use of the prosthetic devices. During the gait with the prosthetic devices, there was an increase in joint angle at ~50% of the gait cycle, during the swing phase. This sudden extension of the shoulder suggests that the companion animal uses its shoulders to swing the prosthetic foot forward during a step.

The next feature evaluated between the two scenarios is the thoracic spine angle (formed by cervical, thoracic, and lumbar markers with the thoracic marker serving as the vertex). During the non-prosthetic gait, the thoracic spine was angled at approximately 168° during the entire cycle. Use of the prosthetic devices increased this angle to 133°. During subject testing with the use of prosthetic devices, the companion animal's stance was similar to a feline without thoracic limb amputation. Unfortunately, thoracic spine angle was not reported by Day et al., so comparisons cannot be made.

The lumbar spine joint angles remained constant throughout the gait cycles of both scenarios. The lumbar angle for the data set gathered from the gait analysis prior to use of the prosthetic device show a relatively flat profile, centered at 94°. The angle for the data set gathered from the gait analysis that utilized the prosthetic devices shows a similar profile, centered at 100°.

Hip joint angle during gait with the prosthetic devices showed a uniform profile, centered at 143°. Hip joint angle during gait without the use of the prosthetic devices had a similar profile, with averages ranging from 150° to 120°. Comparing this data to kinematic data gathered from Suter et al. and Guillot et al. indicates that the hip joint angle for this particular companion animal does not represent hip joint kinematic data from a normal feline gait cycle. This result further suggests that the adaptive behavior of the pelvic limbs were not influenced by the prosthetic devices.

Instead of the prosthetic devices correcting for the additional 30° flexion seen in the gait analysis without the prosthetic device (as compared to Day et al.), no change in stifle joint angle between the prosthetic and no prosthetic scenarios occurred. Stifle joint angle profiles (prosthetic vs. no prosthetic) were similar, with an average joint angle of 86°.

This suggests that the presence of the prosthetic devices did not impact the kinematics of the pelvic limbs, which have accommodated the loss of thoracic limbs by being flexed for the past two years. This characteristic may be mitigated after further acclimation to the prosthetic devices.

Tarsus joint angle profiles during walking with and without the prosthetic devices were similar with a mean angle of approximately 60°. This further suggests that the presence of the additional 30° flexion compared to the reported gait data (Day 2006) is a compensatory behavior for the missing thoracic limbs. This kinematic behavior may be corrected after acclimation and sufficient rehabilitation.

5.3 Limitations

Limitations were encountered during the mechanical testing and subject testing. The materials testing machine used in the static and fatigue mechanical testing was a belt driven machine. Any slack in this belt results in a response delay. This caused the accuracy of the machine to decrease when using a force control parameter. This limitation was corrected by setting the control parameter to a finite distance the machine can travel. The connection pin between the mounting hardware and the materials testing machine was a loose fitting pin. This resulted in unwanted movement of the mounting hardware during testing. The experimental factor of safety was unable to be calculated due to an errant torque introduced during the mechanical testing. This torque was introduced when the distal end of the prosthetic foot came into contact with the mounting fixture.

During subject testing, cooperation of the companion animal was essential for successful gait trials. During the gait trials without the use of prosthetic devices,

110

reflective markers were placed over bony prominences to identify anatomical landmarks. After a handling of the subject and multiple trials several markers dropped off of the subject. To minimize stress to the subject, the trials were not paused to make corrections to the missing markers. Therefore, the post-processing was labor intensive with virtual markers were manually defined as bony prominences. This process was aided since the fur in the areas of interest were trimmed, thereby creating clear contrast. The companion animal did not ambulate perpendicular to the stationary cameras. This may decrease the accuracy of the calculations performed to determine the kinematics. The speed during these trials also varied, averaging to 50 cm/sec, also has the potential of varying the results between trials.

Acceptance of the prosthetic devices took several weeks before initial steps were made. Confidence using the prosthetic devices increased following each visit, and several gait cycles were recorded for analysis. After 13 visits, the companion animal became aware of the ability to actively remove the prosthetic devices. Once this behavior was learned, the subject refused to ambulate with the prosthetic devices and would remove the prosthetic devices.

The computer analysis performed on the 3D prosthetic devices used material properties for solid ABS plastic in the mechanical loading simulations. The material properties for solid ABS plastic and 3D printed ABS plastic differ. Because the factor at which these two properties differ is unknown, a higher factor of safety was accepted to ensure the prosthetic devices were durable enough for use.

5.3 Future Work

A new iteration of design for these prosthetic devices should be completed. This new design should be optimized to reduce the factor of safety. The reduced factor of safety will come from reducing material in the webbing of the prosthetic foot. This should allow for more energy absorption of the prosthetic foot, as well as reduce the overall weight of the prosthetic device. The infill settings on the 3D printer will also need to be adjusted, decreasing the amount of material used in the creation of the prosthetic devices. Further analysis will be required to determine how much material can be removed while still providing a durable and safe device for use. This newly optimized design should facilitate in the ambulation of the companion animals using the devices. A more traditional motion analysis study should be performed with multiple motion capturing cameras set up to capture a designated volume and accurately trace, and calculate the kinematics of a companion animal's gait throughout the volume. This will remove any limitations imposed by having a single pathway for the companion animal to ambulate down and stationary cameras fixed along one plane.

An alternative rehabilitation process should be adopted for any future studies. Initial exposure to the prosthetic devices should begin with donning the prosthetic sockets. This should be done to slowly introduce to the companion animal the feeling of having foreign objects attached to their bodies. This should be done for several visits, and transitioning into weight bearing training on the prosthetic sockets. Following several visits of placing the companion animal into a weight bearing stance, then the prosthetic feet can be attached to the prosthetic sockets. Once the entire prosthetic device is donned by the companion animal, weight bearing with the prosthetic feet can begin. Once the companion animal is comfortable with the weight bearing stance using the prosthetic

devices, attempts at walking can begin. This slow introduction to the prosthetic devices should allow for the acclimation period to have more success.

The rehabilitation process for this particular companion animal will encompass its entire life. The caregiver will be required to don and doff the prosthetic devices every day, and continue to work with the companion animal until the companion animal prefers to ambulate with the prosthetic devices rather than without. Should the companion animal continue to grow, new prosthetic sockets will need to be fabricated. Attention must be paid to the distal aspects of the residual limbs to ensure that no skin breakdown or irritation develops. Should these develop, full recovery from these injuries must take place before using the prosthetic devices.

The results of this project prove the feasibility of using prosthetic devices as viable alternatives for traditional load bearing prosthetic devices for companion animals. Further studies may take the results of this project and apply similar ideas and concepts to the human market. With the proper design and materials, 3D printed prosthetic devices may be a viable options for human amputees.

A goal of this project is to lay the foundation for an e-Nable style community for companion animals to develop. The final prosthetic device design will be made available to the public as an open source design to support the companion animal prosthetic community and to address the large population of companion animals with amputations.

Conclusion

This study successfully demonstrated the feasibility of designing, developing and fabricating a custom subject-specific feline thoracic limb prosthetic devices using 3D printing. This project showcases the feasibility of using additive manufacturing to create cost effective, and durable prosthetic devices for use in companion animals. Each prosthetic device cost $45 in materials, not including labor and processing time, and weighed an average of 113 grams. The design for the prosthetic device and socket will be placed on an open source, cloud based CAD server for use in community projects that aid in the rehabilitation of companion animals in similar situations.

The testing protocol used to demonstrate the performance of this prosthetic device designed for a companion animal was on criteria used for human prosthetic devices. Additive manufacturing techniques were utilized to minimize costs of traditional production techniques while still allowing for customization. Computer simulation and mechanical testing was performed to ensure the prosthetic devices were able to withstand daily use. The prosthetic foot was able to withstand over 3000 N before failure occurred. This is well above the forces expected in daily use of a feline companion animal and future designs should optimize the design to withstand daily loading and improve energy absorbing characteristics.

Gait analysis demonstrated benefits of prosthetic device use. The comparison to the initial gait analysis to the documented feline joint angles (Day et al.) resulted in an additional 30° flexion in all limbs. The gait analysis performed with the use of the prosthetic devices removed this flexion for the thoracic limbs. Since these are the limbs
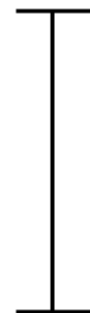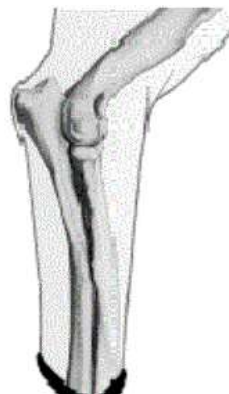
114

with the amputations, the correction of this extra joint flexion is the result of the use of

the prosthetic devices.

Right Limb Measurement Form

CIRCUMFERENCE MEASUREMENT (in) AT VARIOUS DISTANCES FROM RIGHT DISTAL END (in)

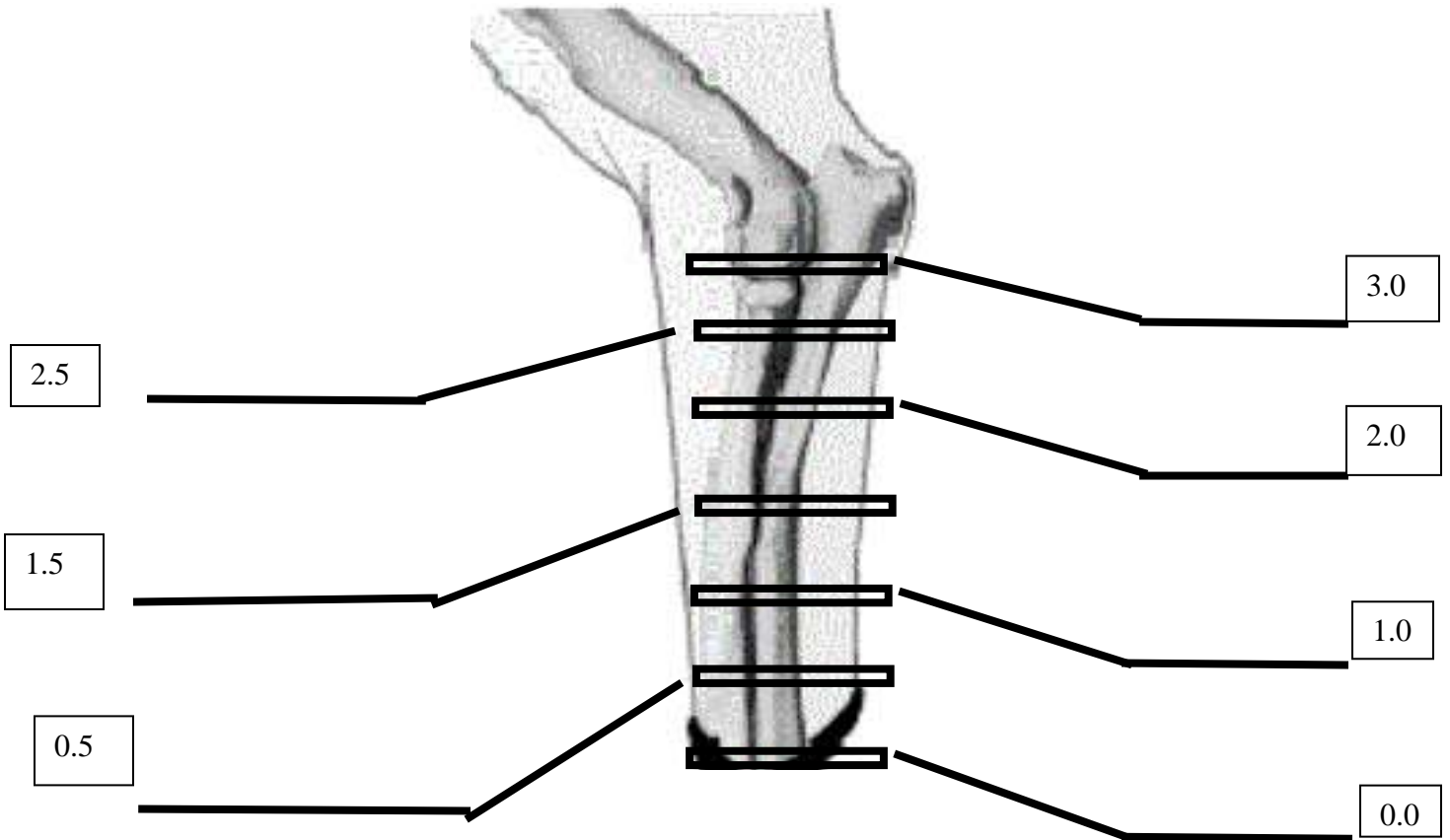

3.0

2.5

2.0

1.5

1.0

0.5

0.0
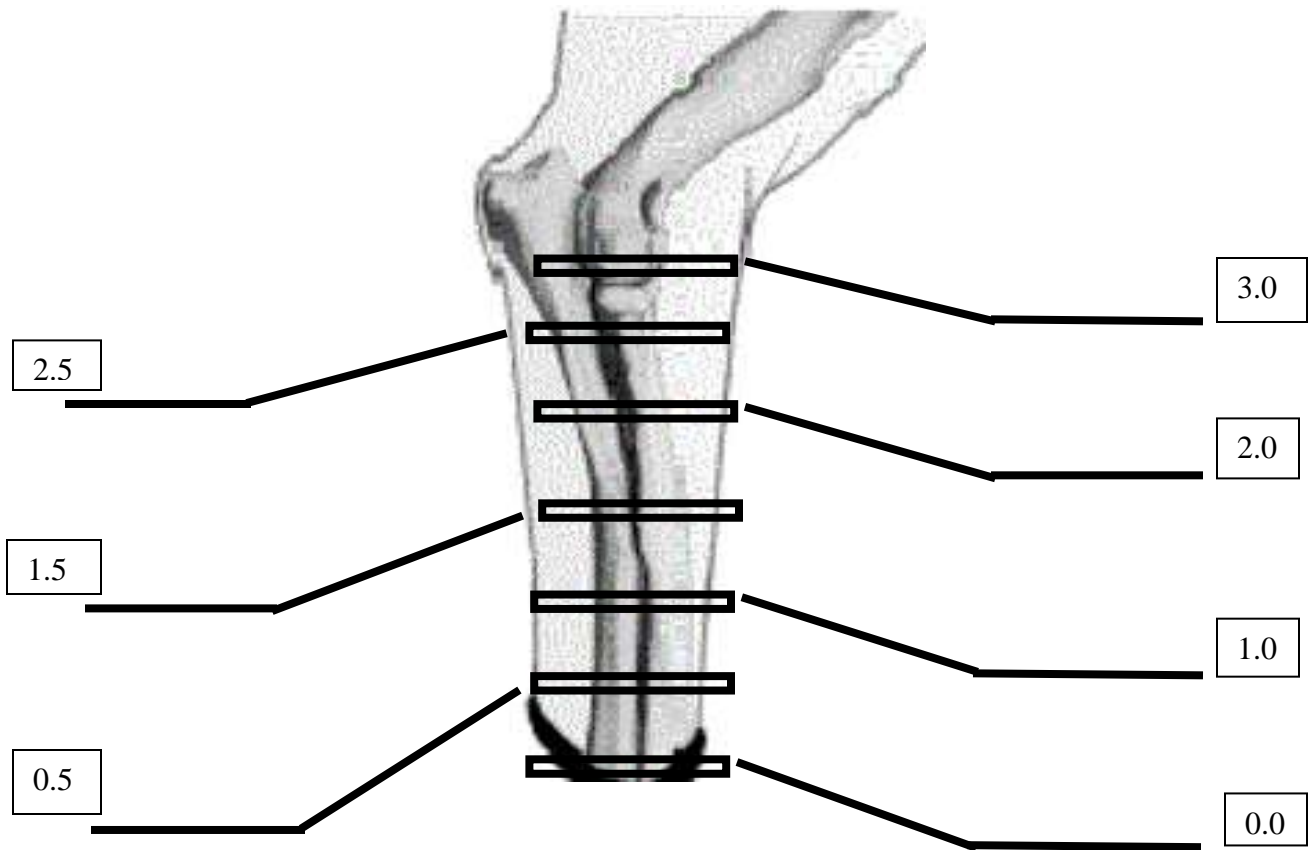
Femur Length (in.):

Measurement from elbow to distal end of the limb (in)

Left Limb Measurement Form

CIRCUMFERENCE MEASUREMENT (in) AT
VARIOUS DISTANCES FROM LEFT DISTAL END (in)

3.0

2.5

2.0

1.5

1.0

0.5

0.0

Femur Length (in.):

Measurement from elbow to distal end of the limb (in)

Feline Gait Analysis Protocol

Marker Placement:

1) Reflective markers (1 mm diameter) will be placed on bony prominences of anatomical features. The distal ends of the residual thoracic limbs will also be locations for reflective markers.
2) Markers will be attached using toupee tape, and scissors may be required to trim fur to minimize motion artifact.
3) Marker locations will include (on both sides of the body except for the markers on the spine):

    a. Dorsal aspect of thoracic paw.
    b. Styloid Process of the Radius.
    c. Olecranon.
    d. Lateral Epicondyle.
    e. Greater Tuberosity.
    f. T1 vertebrae (palpate the neck of the subject, the vertebrae of the neck will feel smooth, and the first bony prominence felt is T1.)
    g. L1 vertebrae. (Palpate the spine, the protruding characteristic of the thoracic vertebrae will give way to a more robust protrusion. This first robust protrusion is the start of the lumbar vertebrae.)
    h. Sacrum. (Placed immediately following the seventh palpable lumbar vertebrae.)
    i. Greater Trochanter of the femur.
    j. Lateral Femoral Condyle.
    k. Lateral Tibial Condyle.
    l. Lateral Malleolus of the Fibula.
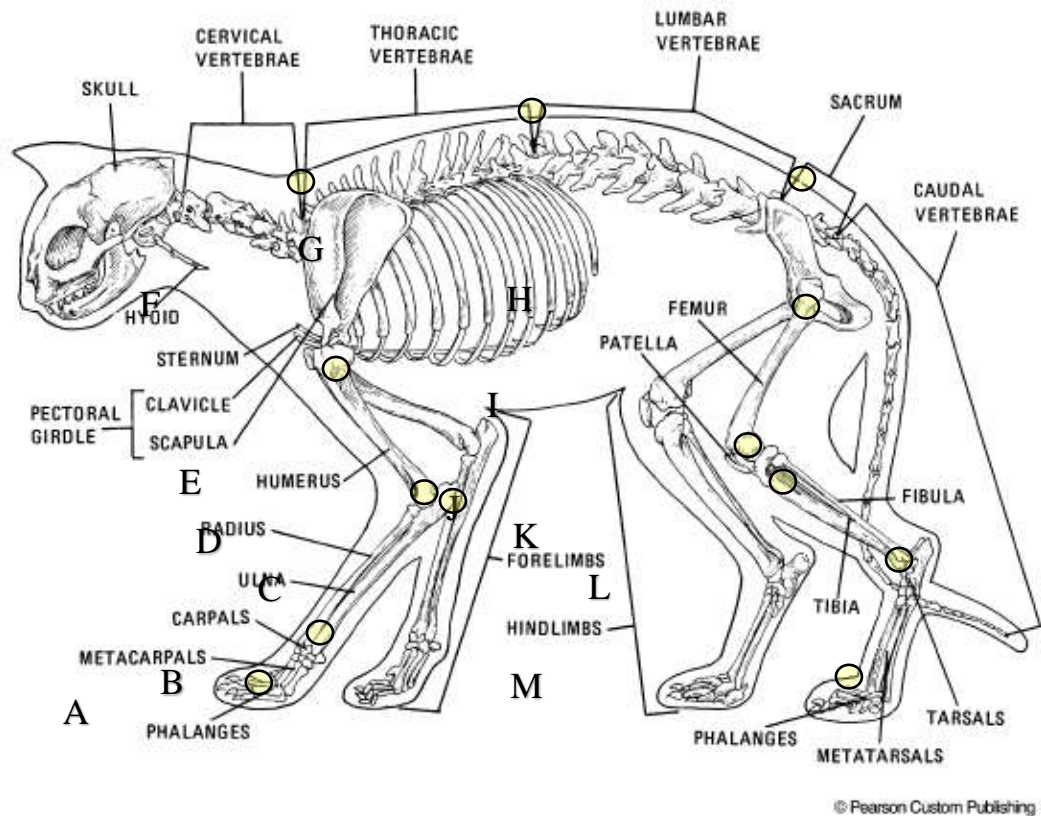   m. Dorsal aspect of the pelvic paw.

Figure 2: Marker Placement

Procedure Setup:

1) Set the tripods 3 feet away, perpendicular, and centered in relation to the targeted walkway (Visual reference in Figure 2).
2) Record the heights of each cell phone's camera on each tripod relative to the floor.
3) Ensure portrait orientation lock is off.
4) Use a leveling tool on each iPhone to ensure the cameras are level.
5) Place two yard sticks parallel to and on either side of the walking path.
6) Attach the markers to the subject according to Figure 1.
7) Allow the subject to ambulate for 5 minutes with the reflective markers to become acclimated to their presence.
8) Place the subject at one end of the targeted walkway, and initiate video recording prior to subject walking.
9) Flip on and off a timing light to sync the videos.
10) Use a treat on the opposite end of the targeted walkway to coax the subject to walk in a straight line, perpendicular to the cameras. Speed of the subject will not be controlled, so additional trials will be captured if needed to obtain trials with similar speed.

11) The procedure will be repeated for seven successful trials to gather sufficient data to analyze the gait of the subject.
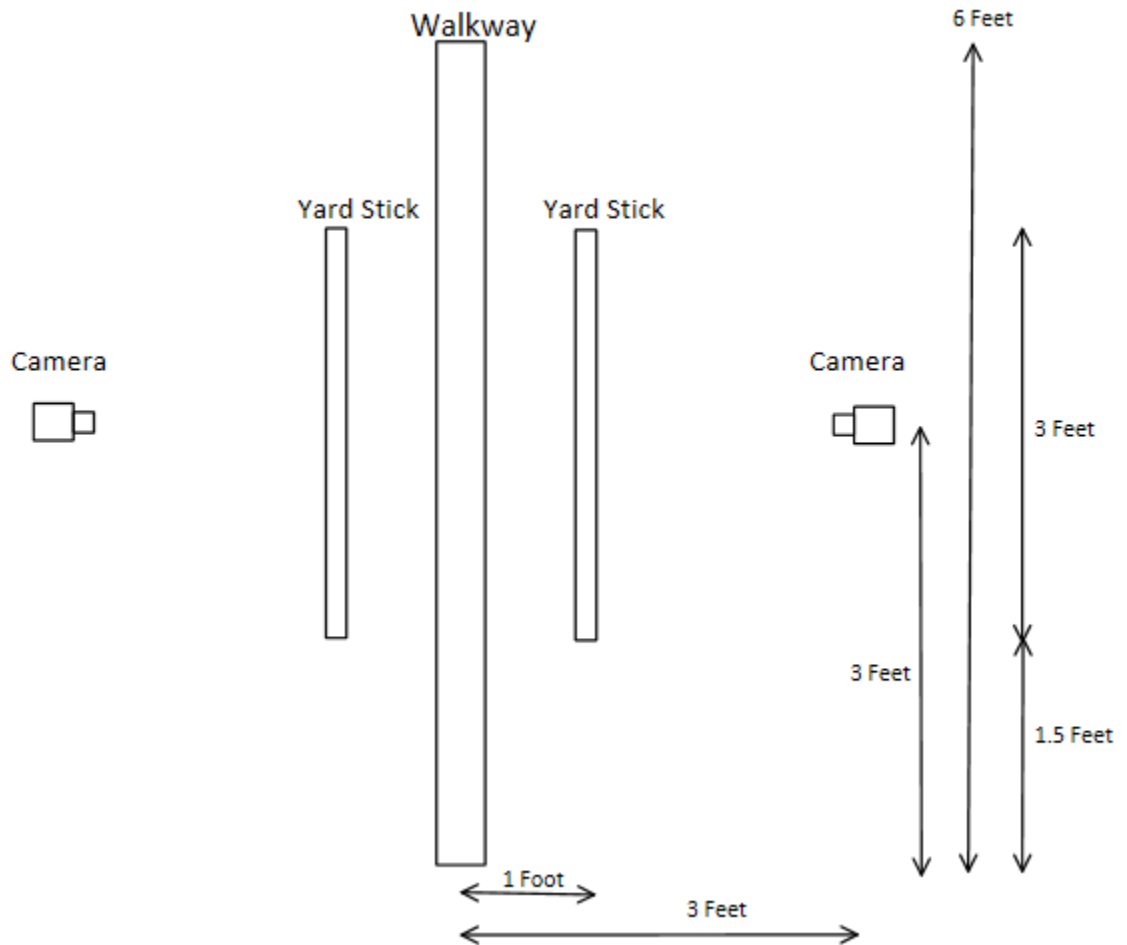   a.   A successful trial will include a minimum of 3 captured gait cycles.

Figure 3: Walkway Layout for Sagittal Plane Kinematic Analysis

Bibliography

Adamson, C., Kaufmann, M., Levine, D., Millis, D., Marcelling-Little, D.J. 2005. Assistive devices, orthotics, and prosthetics. *The Veterinary Clinics of North America. Small Animal Practice.* 35(6): 1441-1451.

Agrawal, V., Gailey, R., Gaunaurd, I., O'Toole, C., Finnieston, A., Tolchin, R. 2014. Comparison of four different categories of prosthetic feet during ramp ambulation in unilateral transtibial amputees. *Prosthetics and Orthotics Internations.* 1-10.

Babuška, I., Szabó, B. 1991. *Finite Element Analysis.* New York: John WIley & Sons, Inc.

Brauer, John. 1993. *What Every Engineer Should Know About Finite Element Analysis.* Milwaukee: Marcel Dekker, Inc.

Campbell, I., Bourell, D., Gibson, I. 2012. Additive Manufacturing: Rapid Prototpying Comes of Age. *Rapid Prototyping Journal* 18(4): 255-258.

Cohen, Lou. 1995. *Quality function deployment: how to make QFD work for you.* Reading: Addison-Wesley.

Corbee, R., Maas, H., Doornenbal, A., Hazewinkel, H. 2014. Forelimb and hindlimb ground reaction forces of walking cats: Assessment and comparison with walking dogs. *The Veterinary Journal.* 202:116-127.

Day, L., Jayne, B. 2006. Interspecific scaling of the morphology and posture of the limbs during the locomotion of cats (Felidae) *The Jounral of Experimental Biology.* 210: 642-654.

Demes, B., Larson, S., Stern, J., Jungers, W., Biknevicius, A., Schmitt, D. 1994. The Kinetics of Primate Quadrupedalism: "Hindlimb Drive" Reconsidered. *Journal of Human Evolution.* 26(5-6): 353-374.

Edelstein, J. 1988. Prosthetic feet. State of the Art. *Physical Therapy* 68(12): 1874-1881.

Farrell, B., Prilutsky, B., Kistenberg, R., Dalton, J., Pitkin, M. 2014. An animal model to evaluate skin-implant-bone integration and gait with a prosthesis directly attached to the residual limb. *Clinical Biomechanics.* 29(3):336-349

Fuchs A., Goldner, B., Nolte, I., Schilling, N. 2014. Ground reaction force adaptations to tripedal locomotion in dogs. *The Veterinary Journal* 201(3):307-315.

Gibson, I. Rosen, D. Stucker, B. 2015.*Additivue Manufacturing Technologies.* New York: Springer.

Gilbert, S. G. (2000). Outline of Cat Anatomy with Reference to the Human. Toronto: University of Toronto Press.

Gillinov, S., Laux, S., Kuivila, T., Hass, D., Joy, S. 2015 Effect of Minimalist Footwear on Running Efficiency: A Randomized Crossover Trial. *Sports Health.* 7(3):256-260.

Gibson, I., Cheung, L., Chow, S., Cheung, W., Beh, S., Savalani, M., Lee, S. 2006. The Use of Rapid Prototyping to Assist Medical Applications. *Rapid Prototyping Journal* 12(1): 53-58.

Goldner B., Fuchs, A., Nolte, I., Schilling, N. 2015. Kinematic adaptations to tripedal locomotion in dogs. *The Veterniary Journal.* 204(2):192-200.

Guillot, M., Gravel, P., Gauthier, M., Leblond, H., Tremblay, M., Rossignol, S., Martel-Pelletier, J., Pelletier, J., A de Guise, J., Troncy, E. 2015. Coxofemoral Joint Kinematics Using Video Fluoroscopic Images of Treamill-Walking Cats: Development of a Technique to Assess Osteoarthritis-Associated Disability. *Journal of Feline Medicine and Surgery.* 17(2): 134-143.

Hayden, M. 2015. Private Communication.

Hsu, L., Huang, G., Lu, C., Hong, D., Liu, S. 2010. The development of a rapid prototyping prosthetic socket coated with a resin layer for transtibial amputees. *Prosthetics and Orthotics Internationsl* 34(1): 37-45.

Lacquaniti F., Grasso, R., Zago, M. 1999. Motor Patterns in Walking. *News in Physiological Science.* 14:168-174.

Marcellin-Little, D. J., Drum, M., Levine, D., McDonald, S. 2015. Orthoses and exoprostheses for companion animals. *The Veterinary Clinics of North America. Small Animal Practice.* 45(1): 167-183.

Negi S., Dhiman, S., Sharma, R. 2014. Basics and Applications of Rapid Prototyping Medical Models. *Rapid Prototyping Journal* 20(3): 256-267.

Ng P., Lee, P., Goh, J. 2002. Prosthetic Sockets Fabrication Using Rapid Prototyping Technology. *Rapid Prototyping Journal* 8(1): 53-59.

Rogers B., Gitter. A., Bosker G., Faustin M., Lokhande M., Crawford R., (2001). Clinical evaluation of prosthetic sockets manufactured by selective laser sintering. The Universyt of Texas Health Science Center at San Antonio, The University of Texas at Austin.

Shurr, D., Cook, T. 2001). *Prosthetics & Orthotics*, Norwalk, Appleton & Lange.

Stadig, S., Bergh, A. 2014. Gait and jump analysis in healthy cats using a pressure mat system. *Jounral of Feline Medicine and Surgery.* 17(6):523-529.

Suter, E., Herzog, W., Leonard, T.R., Nguyen, H. 1998. One-year changes in hind limb kinematics, ground reaction forces and knee stability in an experimental model of osteoarthritis. *Journal of Biomechanics.* 31: 511-517.

Thrall, D. 2007. Textbook of Veterinary Diagnostic Radiology, St. Louis, Saunders Elsevier.

Wong, K., Hernandex, A. 2012. A Review of Additive Manufacturing. *International Scholarly Research Network*: 2012:1-10.

Wright, M., Walters, S. 1980. *The Book of the Cat*, New York: Summit Books.